JACOBS UNIVERSITY

Development of Two Novel Fluorescent Enzyme Assays: Nano-TRF and Supramolecular Tandem Assays

by

Andreas Hennig

A thesis submitted in partial fulfillment
of the requirements for the degree of

Doctor of Philosophy
in Chemistry

Approved, Thesis Committee

Prof. Werner M. Nau, internal member

Prof. Nikolai Kuhnert, internal member

Prof. Ulrich Schwaneberg, internal member

Dr. Thilo Enderle, external member

Prof. Franz-Josef Meyer-Almes, external member

Date of Defense: July, 11th 2007

School of Engineering and Science
Jacobs University Bremen, Germany

To my beloved parents

There is a theory which states that if ever anybody discovers exactly what the universe is for and why it is here, it will instantly disappear and be replaced by something even more bizarre and inexplicable. There is another theory which states that this has already happened.

(Douglas Adams)

Table of Contents

Acknowledgements

I would like to express my deepest gratitude to my supervisor Prof. Dr. Werner M. Nau, who allowed me to conduct my thesis in this fascinating scientific field. Many achievements would not have been possible without his constant guidance, encouragement, motivation and fruitful support throughout the thesis. The numerous discussions with him were a never-ending source of inspiration.

I would like to thank Dr. Thilo Enderle, Prof. Kuhnert, Prof. Meyer-Almes, and Prof. Schwaneberg in their function as co-referees.

I am indebted to the kind support of Dr. Thilo Enderle and Dr. Doris Roth from Fa. Hoffmann-La Roche who introduced into the field of drug discovery and high-throughput screening.

I am grateful to the present and former members of Prof. Nau's research group for their kind affiliation, the friendly atmosphere and many fruitful discussions. In particular, I would like to thank Dr. Fang Huang for introducing me into the peptide projects, Dr. Hüseyin Bakirci for sharing his "kitchen tricks" in supramolecular chemistry and Dr. Gabriela Gramlich for teaching me the synthesis of Fmoc-DBO. In addition, I am indebted to Mara Florea, who has significantly contributed to the protease and phosphatase assays, to Garima Ghale, who contributed to the CB7 protease project, and to Roy D'Souza, who wrote all the codes for the tandem assay simulations. Finally, I am thankful to Apurba L. Koner for discovering the CB7-dapoxyl system, which provided an excellent starting point for the tandem assay project.

I would like to thank Prof. Schwaneberg and his group for their kind supply of "bio"-related chemicals and buffer "ingredients", whenever I needed some for immediate testing.

I want to thank Fa. Hoffmann-La Roche for financial support within the joint Nano-TRF project and the graduate program "Nanomolecular Science" at Jacobs University.

Finally, I want to thank my parents for their constant support in every aspect of my life and my girlfriend Anne for her patience and support during times of hard work.

List of Publications

The present thesis was carried out during the period of 03/2004-05/2007 in the School of Engineering and Science/Department of Chemistry at Jacobs University Bremen. The scientific achievements obtained during the doctoral research are reflected in the following publications and manuscripts in preparation.

Manuscripts in print and in press

1. A. Hennig, D. Roth, T. Enderle, W. M. Nau, Nanosecond Time-Resolved Fluorescence Protease Assays, *ChemBioChem*, **2006**, *7*, 733-737.
2. H. Sahoo, A. Hennig, W. M. Nau, Temperature-Dependent Loop Formation Kinetics in Flexible Peptides Studied by Time-Resolved Fluorescence Spectroscopy, *Int. J. Photoenergy*, **2006**, Article ID 89638, 9 pages.
3. A. Hennig, M. Florea, D. Roth, T. Enderle, W. M. Nau, Design of Peptide Substrates for Nanosecond Time-Resolved Fluorescence Assays of Proteases: 2,3-Diazabicyclo[2.2.2]oct-2-ene as a Noninvasive Fluorophore, *Anal. Biochem.*, **2007**, *360*, 255-265.
4. A. Hennig, G. Ghale, W. M. Nau, Effects of Cucurbit[7]uril on Enyzme Activity, *Chem. Commun.*, **2007**, 1614-1616.
5. A. Hennig, T. Schwarzlose, W. M. Nau, Bridgehead Carboxy-Substituted 2,3-Diazabicyclo[2.2.2]oct-2-enes: Synthesis, Fluorescent Properties and Host-Guest Complexation Behavior, *Arkivoc*, **2007**, *8*, 341-357.
6. A. Hennig, H. Bakirci, W. M. Nau, Label-Free Continuous Enzyme Assays with Macrocycle-Fluorescent Dye Complexes, *Nature Methods*, **2007**, *4*, 629-632.
7. H. Sahoo, D. Roccatano, A. Hennig, W. M. Nau, A 10-Å Spectroscopic Ruler Applied to Short Polyprolines, *J. Am. Chem. Soc.*, **2007**, *129*, 9762-9772.
8. W. M. Nau, A. Hennig, A. L. Koner, Squeezing Fluorescent Dyes into Nanoscale Containers - The Supramolecular Approach to Radiative Decay Engineering, *Springer Series On Fluorescence*, Vol. 4, **2007**, 185-211.
9. H. Sahoo, A. Hennig, M. Florea, D. Roth, T. Enderle, W. M. Nau, Single-Label Kinase and Phosphatase Assays for Tyrosine Phosphorylation Using Nanosecond Time-Resolved Fluorescence Detection, *J. Am. Chem. Soc.*, **2007**, *51*, 15927-15934.

Manuscripts in preparation

10. A. Hennig, D. Roth, T. Enderle, W. M. Nau, Interaction of Cucurbit[7]uril with Protease Substrates: Application to Nanosecond Time-Resolved Fluorescence Assays.
11. A. Hennig, H. Bakirci, W. M. Nau, A Supramolecular Sensor System for Nanosecond Time-Resolved Fluorescent Detection.
12. A. Hennig, R. D'Souza, W. M. Nau, Supramolecular Tandem Assays.
13. A. Hennig, W. M. Nau, Determination of Arginase Inhibition by a Substrate-Coupled Supramolecular Tandem Assay.

Patents

One of my projects has lead to the following patent application.

W. M. Nau, A. Hennig, H. Bakirci, Bestimmung von Konzentrationsänderungen mit Hilfe von supra-biomolekularen Tandem-Assays, PCT Patent Application.

List of Attended Conferences

I have attended the following conferences during my PhD studies.

1. 2nd European Short Course on Principles & Applications of Time-Resolved Fluorescence Spectroscopy, 01.11.-05.11.2004, Berlin (D).
2. Meeting of the photochemistry branch of the GDCh, 29.03.-31.05.2005, Jena (D), Poster: “Fast Time-Resolved Fluorescent (Fast-TRF) Protease Assays“.
3. NRP Spring School: Supramolecular Functional Materials, 11.04.-15.04.2005, Murten (CH), Poster: “Supramolecular Radiative Decay Engineering (SRDE) with Cucurbituril“.
4. NRP Final Symposium: Supramolecular Functional Materials, 16.06.-18.06.2005, Murten (CH), Short presentation: “Enhancement on time-resolved energy transfer assays by supramolecular complex formation“.
5. Central European Conference on Photochemistry (CECP), 05.03.-09.03.2006, Bad Hofgastein (A), Poster: “Fluorescence Lifetime-Based Sensor Applications: Nano-TRF Assays & Lifetime Enhancers“, Poster: “Nanosecond Time-Resolved Fluorescence (Nano-TRF) Assays – Application to Proteases“.
6. Joint International Symposium on Macrocyclic & Supramolecular Supramolecular Chemistry, 25.06.-30.06.2006, Victoria, BC (CDN), Poster: “Interactions of Cucurbituril with Peptide Substrates in Enzyme Assays: Potential Applications“.
7. ChemieContact – Innovation sucht Partner des VCI (Verband der Chemischen Industrie e.V.), 10.10.2006, Hamburg (D), Poster: “Enzym- und Katalysatorscreening mit Hilfe von suprabiomolekularen Tandem Assays”.
8. Bremen Molecular and Marine Biology (BMMB) meeting, 26.01.-27.01.2007, Etelsen (D), Poster: “Supra-Biomolecular Tandem Assays“.
9. II. International Symposium on Macrocyclic & Supramolecular Supramolecular Chemistry, 24.06.-28.06.2007, Salice Terme (IT), Poster: “Supramolecular Tandem Assays – Application Examples”.

List of Acronyms

ADP	adenosine 5′-diphosphate
AMC	7-amino-methyl-coumarin
AMP	adenosine 5′-monophosphate
ATP	adenosine 5′-triphosphate
βNA	*β*-naphthylamine
cAMP	adenosine 3′,5′-cyclic monophosphate
CB7	cucurbit[7]uril
CE	capillary electrophoresis
CX4	*p*-sulfonato-calix[4]arene
DBO	2,3-diazabicyclo[2.2.2]oct-2-ene
Dbo	asparagine derivative of DBO
DBO-A	aminomethyl derivative of DBO
DMF	dimethylformamide
DMSO	dimethylsulfoxide
EC	enzyme class
EEDQ	*N*-ethoxycarbonyl-2-ethoxy-1,2-dihydroquinoline
EET	electronic energy transfer
ELISA	enzyme-linked immunosorbent assay
FLARe	fluorescence lifetime assay repertoire
Fmoc	fluorenylmethoxycarbonyl
FRET	fluorescence resonance energy transfer
GTP	guanosine 5′-triphosphate
HMPA	hexamethylphosphoramide
HPLC	high-performance liquid chromatography
HTS	high-throughput screening
MS	mass spectrometry
MTAD	4-*N*-methyl-1,2,4-triazolin-3,5-dione
NMR	nuclear magnetic resonance
PET	photoinduced electron transfer
pNA	*p*-nitroaniline
Suc	succinyl
TCSPC	time-correlated single photon counting
TFA	trifluoroacetic acid
TLC	thin layer chromatography
TRF	time-resolved fluorescence

List of Mathematical Symbols

χ^2	goodness-of-fit parameter, chi-squared
$[D]$	concentration of an uncomplexed fluorescent dye
$[D]_0$	total concentration of a fluorescent dye
ε	extinction coefficient
E	efficiency of energy transfer
$[E]$	enzyme concentration
$[H]$	concentration of an uncomplexed macrocyclic host
$[H]_0$	total concentration of a macrocyclic host
$[HD]$	concentration of a host-dye complex
$[HG]$	concentration of a host-guest complex
$[HP]$	concentration of a host-product complex
I	fluorescence intensity
I_D	fluorescence intensity of a FRET donor in absence of acceptor
I_{DA}	fluorescence intensity of a FRET donor in presence of acceptor
$I(t)$	intensity decay
$J(\lambda)$	spectral overlap between donor emission and acceptor absorbance
κ^2	orientation factor in resonance energy transfer
k_a	association rate constant
k_{cat}	catalytic turnover number
k_q	quenching rate constant
K_{HD}	binding constant of a fluorescent dye to a macrocyclic host
K_{HS}	binding constant of a substrate to a macrocyclic host
K_{HP}	binding constant of a product to a macrocyclic host
K_a	association constant
K_i	inhibition constant
K_M	Michaelis-Menten constant
λ_{exc}	maximum excitation wavelength
λ_{em}	maximum emission wavelength
n	refractive index or number of amino acids
ϕ	fluorescence quantum yield
pK_a	acid dissociation constant, negative decadic logarithm
$[P]$	concentration of an uncomplexed product
$[P]'$	concentration of a product in an enzymatic reaction
$[P]_0$	total concentration of a product
R_0	Förster distance in resonance energy transfer
R_{avg}	average distance
R_{eff}	effective average distance
$[S]$	concentration of an uncomplexed substrate
$[S]'$	concentration of a substrate in an enzymatic reaction
$[S]_0$	total concentration of a substrate
τ	fluorescence decay time or fluorescence lifetime
x	molar fraction

Abstract

This doctoral thesis describes two novel fluorescent methods for assaying enzymatic activity, which are referred to as nanosecond time-resolved fluorescence (Nano-TRF) assays and supramolecular tandem assays. The first method, developed in collaboration with Fa. Hoffmann-La Roche, introduces a novel fluorescent probe (Dbo) for enzyme assays, which combines several desirable properties. First, Dbo has an exceedingly long fluorescence lifetime, which allows the use of Nano-TRF detection to increase the robustness of an assay by suppressing background fluorescence, for example from library compounds in high-throughput screening (HTS). Second, Dbo is efficiently quenched by tryptophan and tyrosine, which allows single-label assays. And third, Dbo has a very small size and hydrophilicity compared to common aromatic hydrophobic fluorescent probes. It has been demonstrated that the combination of these properties affords a minimally invasive, yet very powerful approach to determine the activity of proteases, tyrosine kinases and phosphatases.

The second method introduces the use of water-soluble macrocycles and fluorescent dyes for enzyme assays, which presents an economic, convenient, and general assay principle. The assay is based on the competition of dye *versus* substrate and product in the reversible formation of a complex with the macrocycle. The enzyme thus converts a weak competitor (substrate) into a strong competitor (product) or *vice versa*, which leads to a different fraction of fluorescent dye bound to the macrocycle. Depending on whether the macrocycle/dye-complex is more or less fluorescent than the free dye, an increase or a decrease in fluorescence results, which signals the enzymatic activity. The method was applied to amino acid decarboxylases and arginase, and the possibility to derive enzyme kinetic parameters and inhibition constants has been demonstrated. Furthermore, the assays were conceptualized by supporting simulation.

– CHAPTER 1 –
INTRODUCTION

1. Introduction

1.1 Scope of the thesis

The scope of this thesis is the development of novel enzyme assays. In the most general sense, enzyme assays can be considered as transducers, which make chemical transformations available to human perception.[1,2] The importance of enzyme assays is underlined by the fact that a bewildering number of different techniques have been envisaged,[3,4] which have lead to numerous application areas, e.g. high-throughput screening (HTS) in the chemical and pharmaceutical industry.[5,6]

However, several problems still persist, which were recently addressed as follows:[7] "*There are compelling reasons to believe that the universal enzyme sensor, a user-friendly, noninvasive device that can detect all existing enzyme activities, belongs to the world of fiction and, despite functional proteomics, will never become reality.*"

This statement outlines important problems, which need to be faced while assaying enzymatic activity. i) Most of the available methods are limited to certain types of chemical transformation. ii) Most of the methods are invasive and disturb the natural progress of an enzymatic reaction, and iii) those methods, which are relatively universal and non-invasive, are not user-friendly, but rather tedious and time-consuming. The aim of the present thesis is therefore to fill some of the existing gaps: In particular it was planned to provide enzyme assays for new types of enzymatic transformations, which are less invasive but as simple as possible.

1.2 Spectrophotometric Enzyme Assays

The least invasive methods can be readily summarized as separation-based techniques, e.g. thin layer chromatography (TLC),[8] high-pressure liquid chromatography (HPLC),[9] capillary electrophoresis (CE)[10] or mass spectrometry (MS).[11] Furthermore, classical biochemical techniques, e.g. enzyme-linked immunosorbent assays (ELISA)[12,13] or radioimmunoassays,[14] may be added to this

group, because they require several steps of reagent addition and washing. The distinct advantage of these methods is that a natural enzyme substrate can be used in the assay. Usually, aliquots are taken from a reaction mixture after defined time intervals, which are then subjected to separation and detection. However, these methods are inherently time-consuming and often require additional derivatization steps to afford a sufficiently sensitive detection. They are therefore not suitable for HTS, although much effort is spent to decrease detection times, e.g. with LC/MS.

The most popular methods, which by-pass these tedious steps, are spectrophotometric techniques, in which the enzymatic reaction is coupled to a spectral change (absorbance or fluorescence).

1.2.1 Chromogenic and Fluorogenic Substrates

The most common targets for the design of spectrophotometric assays are proteases, lipases and esterases, which belong to the class of hydrolases (EC 3). In this case, the spectroscopic change can be directly coupled to the functional group interconversion, i.e. the hydrolysis transforms e.g. an amide into an amine, which display different absorption or fluorescence spectra (Scheme 1.1) as a consequence of a significant alteration of the chromophore properties as such.

Scheme 1.1. Representative examples of chromogenic and fluorogenic substrates for hydrolytic enzymes.

Proteases

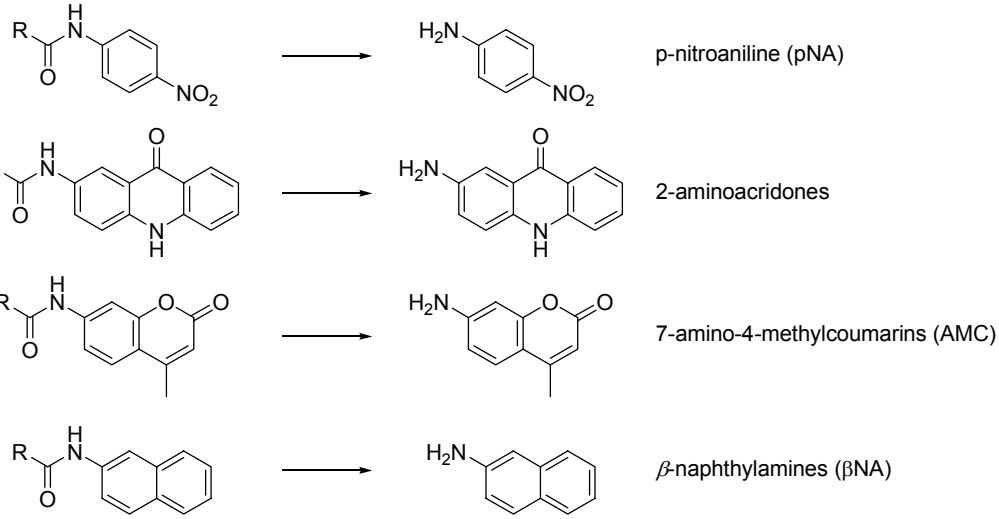

Phosphatase

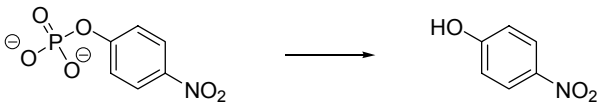

β-Glucosidase

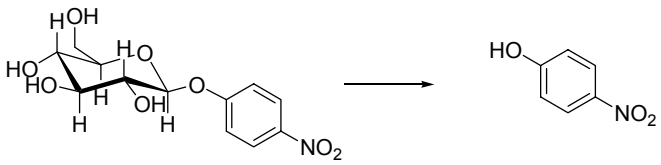

Esterase/Lipase

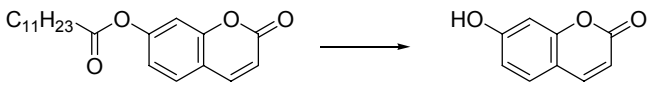

This method is quite simple and versatile, and in many cases other enzymatic conversions have been coupled to a hydrolytic step. This is for example the case in the catELISA[12,13] but applies also for coupled enzyme assays (Scheme 1.2), in which a rate-limiting amount of a non-hydrolytic enzyme transforms its substrate into a product, which can be hydrolyzed by a large excess of hydrolase. For example, peptidylprolyl isomerases (PPIases, EC 5.2.1.8), which catalyze the cis-trans isomerization around the proline amide bond, have been assayed in this way.[15]

Scheme 1.2. Example for a coupled enzyme assay. The protease, which is present in large excess in the assay mixture, selectively cleaves the substrate with a *trans* proline amide bond. The proline bond isomerization is rate-limiting under these conditions and the observed cleavage rate reflects the rate of cis-trans isomerization.

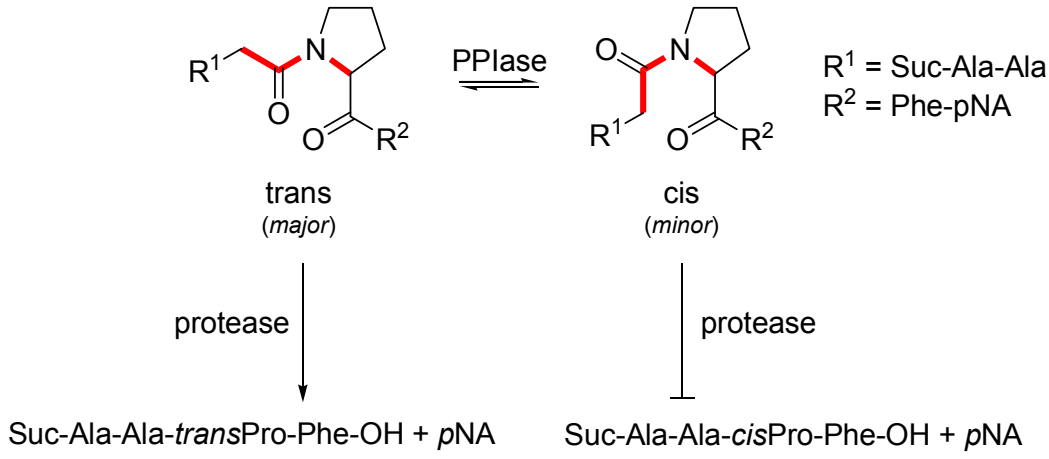

1.2.2 Intramolecularly Quenched Substrates

Despite the distinct advantages of chromogenic and fluorogenic substrates, several problems remained unsolved. In particular, the spatial proximity of an unnaturally large and hydrophobic extrinsic probe to the susceptible bond represents an enormous uncertainty in the design of chromogenic and fluorogenic substrates. In addition, desirable studies in enzymology, e.g. mutation of *C*-terminal and *N*-terminal residues, cannot be carried out with such assays.

Therefore, intramolecularly quenched substrates of the general type P–S–Q (probe–substrate–quencher) have been developed, which are more amenable to a flexible design. In these substrates, a fluorescent probe and a quencher are appended to both ends of a substrate (e.g., a peptide containing the

recognition sequence of a protease), a hydrolase cleaves the substrate and separates probe and quencher, which regenerates the fluorescence of the unquenched probe. Several distinct quenching mechanisms have been applied in the design of intramolecularly quenched substrates, which will be discussed in the following (*cf.* also Appendix 4.2, A. Hennig et. al., *Anal. Biochem.*, **2007**, *360*, 255-265).

1.2.2.1 Fluorescence Resonance Energy Transfer (FRET)

The most popular quenching mechanism is fluorescence resonance energy transfer (FRET), which proceeds *via* a radiationless interaction of the electric transition dipole moments of probe and quencher (which are commonly referred to as energy donor and acceptor in FRET).[16,17] The quenching efficiency (or transfer efficiency) E is given by eq. 1, in which the fluorescence intensities of the donor in the absence of acceptor (I_D) and presence of acceptor (I_{DA}) are related to the donor-acceptor distance (R).

$$E = 1 - \frac{I_{DA}}{I_D} = \frac{R_0^{\,6}}{R_0^{\,6} + R^6} \qquad (1)$$

With respect to applications in enzyme assay, the Förster distance R_0 (eq. 2) is nearly constant for a certain combination of donor and acceptor. A refractive index (n) of 1.33 and an orientation factor (κ^2) of 2/3 is a viable approximation for peptide substrates representing two freely diffusing molecules in water.[18,19] The two residual parameters, donor quantum yield (ϕ_D) and overlap integral ($J(\lambda)$), are calculated from the donor and acceptor spectra.

$$R_0 = 8.79 \times 10^{-5} \kappa^2 n^{-4} \phi_D J(\lambda) \qquad (2)$$

As can be seen from the equations (1) and (2), FRET reports on the distance between donor and acceptor and thus can be employed as a molecular "ruler".[17,19] Small perturbations can be readily measured by using suitable donor-acceptor pairs. This has been exploited for numerous fundamental studies, e.g., for determining the size of an enzyme active site,[20] for studying supramolecular assemblies,[21] and for determining the distance distribution of peptides.[19]

In enzyme assays, FRET should ideally work on an all-or-none basis, i.e. the donor fluorescence should be completely quenched in either the substrate or

the product. This is, however, not the case. Residual absorption of the acceptor at the excitation wavelength and efficient intermolecular FRET are unavoidable and sizable sources of error.[22,23] Note that with FRET, the latter is even problematic in concentration ranges for which a diffusion-limited dynamic contact-based quenching can be fully neglected.

Nevertheless, FRET represents nowadays the most simplistic approach to assay development. This is not only true for hydrolytic enzymes, in particular proteases, but also for fluoroimmunoassays, in which antibody and substrate are labeled with donor and acceptor (Scheme 1.3).[24-26]

Scheme 1.3. Principle of a fluoroimmunoassay. The substrate (●) and a product-specific antibody are labeled with FRET acceptor and donor, respectively. During an enzymatic reaction, the product (▼) is generated, which strongly binds to the antibody enabling efficient energy transfer.

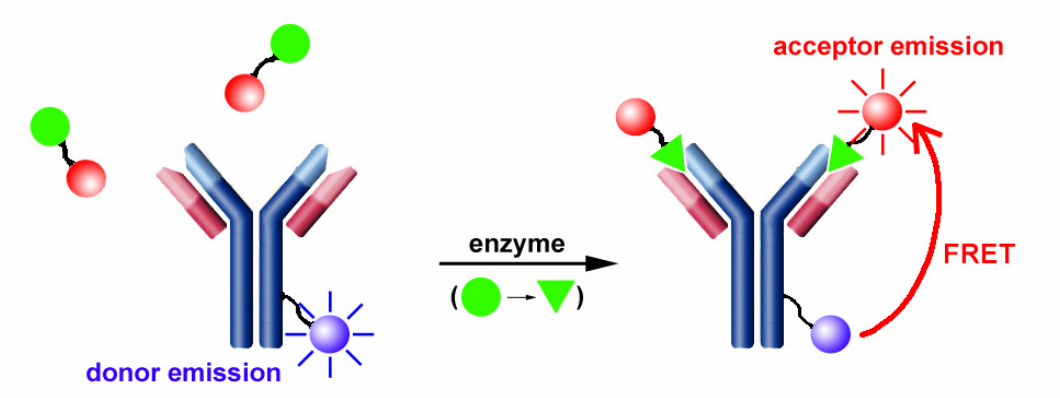

1.2.2.2 Contact-Induced Quenching Mechanisms

Shortly after the first report of a FRET-based protease assay had appeared,[27] another probe-quencher pair was introduced, in which no spectral overlap between probe and quencher was involved.[28] In this case, a contact-induced quenching mechanism was presumed, although this was never investigated in detail. Mechanistically, it is important to distinguish between static and dynamic quenching (Scheme 1.4).

Scheme 1.4. General scheme for the treatment of contact-induced fluorescence quenching.

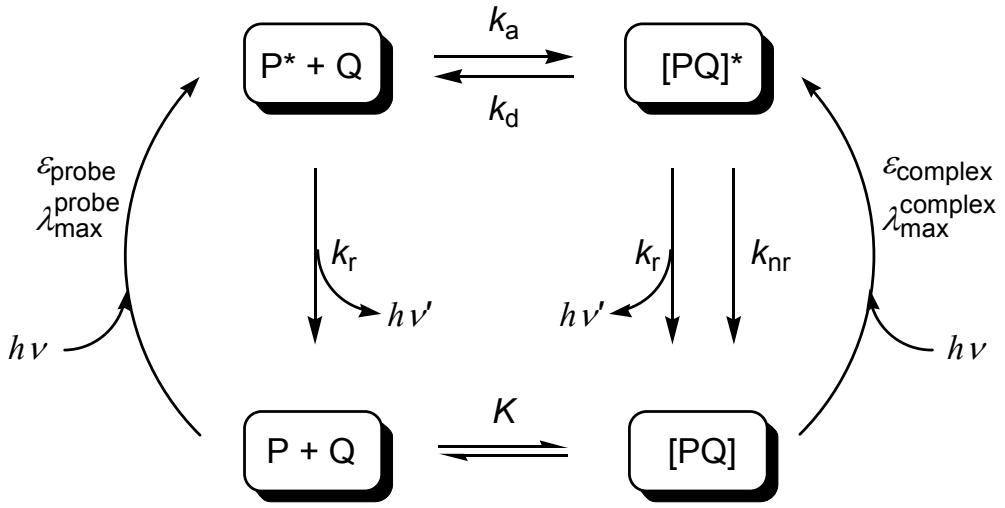

Static quenching occurs when the probe and the quencher form non-fluorescent ground-state complexes. In this case, the binding constant (K) is large, the complex has a different absorption spectrum (e.g. a shifted absorption maximum or a different extinction coefficient), and the nonradiative decay rate (k_{nr}) of the complex is large as well. Dynamic quenching requires other prerequisites. In this case, the fluorescence lifetime ($1/k_r$) of the probe needs to be sufficiently long to allow the association rate constant k_a to compete, i.e., to allow the formation of the excited-state complex (exciplex) within the fluorescence lifetime. Other cases are also known, for example the formation of fluorescent excited-state dimers (excimers) of pyrene.

Interestingly, shortly after it has been recommended[29] not to pursue the further development of these types of assays, contact-based quenching mechanisms have experienced a dramatic revival.[30,31]

1.2.3 Fluorescence Read-Outs

Besides the advantages of high sensitivity, short detection times, and robustness, fluorescence measurements offer the possibility for different read-out principles, which can be tailored to suit a desired application.[32] The simplest read-out is the steady-state fluorescence measurement, in which the intensity is followed at a particular wavelength during an enzymatic reaction. This is the most

popular method owing to its simplicity and the readily available instrumentation, although it is prone artifacts. Most commonly, stray lights, inner filter effects and adsorption to materials may tamper with the results even when the measurements are performed in quartz glass cuvettes. In microplates, which represent the preferred format for enzyme assays, additional complications arise due to background fluorescence of the plate material or adjacent wells and frequently the adsorption properties of the plastic materials interfere. Finally, in HTS, a strong and unpredictable background fluorescence from test compounds may interfere in steady-state mode.

To minimize complications owing to such artifacts, several improved methods have been envisaged. Direct read-out parameters such as lifetime and anisotropy, as well as more complex parameters (for example, energy transfer, which is calculated from two intensity measurements) have been applied, each with its advantages and limitations, which need to be considered in the design of enzyme assays.

1.2.3.1 Fluorescence Lifetime

The time-dependent decay of fluorescence intensity I after pulsed excitation can be described by the fluorescence lifetime τ_F according to $I(t) = I_0 \exp(-t/\tau_F)$. The fluorescence lifetime is related to the radiative and non-radiative rate constants (k_r and k_{nr}, *cf.* Scheme 1.4) by $\tau_F = 1/(k_r + k_{nr})$.

In contrast to the fluorescence intensity, which is a composite property of all fluorescing species, the fluorescence lifetime represents an intrinsic property of each emitting species, which is independent of its concentration and the instrumental setup. This renders assay development more robust, because the inner filter effect and reduced concentrations due to adsorption by sample container materials do not interfere. In addition, the measurement of the fluorescence decay profile may reveal the individual contribution of all emitting species, that is the decay law becomes multiexponential (eq. 3) in the case of i emitting species.

$$I(t) = \sum_i I_0^i \exp(-t/\tau_F^i) \qquad (3)$$

This feature has been exploited quite recently in lifetime-based assays,[33,34] in which two principally different approaches need to be considered: time-domain and frequency-domain measurements.[18] The time-domain measurements have led, in combination with confocal detection, to exciting new possibilities for miniaturization, which are nowadays summarized by the term ultra-HTS (uHTS).[34] The frequency-domain measurements are (although the instrumentation has not been available in our lab) more relevant, because extraordinary lifetimes, for example lifetimes that are longer than those of conventional fluorophores offer the possibility for an efficient background reduction.

The approach is based on preliminary work of Lakowicz *et. al.*, who demonstrated the extraction of the fluorescence lifetime of 9,10-diphenylanthracene (6 ns) from a mixture with scattered light (as imposed by colloidal silica), 2,2'-*p*-phenylene-bis-5-phenyloxazole (1.35 ns) and 9-cyanoanthracene (12 ns).[35] A general mathematical treatment and adjustment of the frequency-domain instrument to the lifetime of the desired probe component allowed the suppression of the background fluorescence.[35] This method has later been applied to ruthenium-based dyes, which display lifetimes in the range of 100-1000 ns, and commercialized as FLARe (Fluorescence lifetime assay repertoire) assay. The larger difference between probe lifetime and background lifetime allowed in this case an even more efficient suppression of the background components.[36]

1.2.3.2 Time-Gated Fluorescence

The time-gated fluorescence technique also takes advantage of the large difference between the lifetimes of emitting species. However, in contrast to the FLARe assays, the probe emission needs to have a much longer lifetime than the background for time-gated measurements.

The basic idea is to record the emission with a certain delay after the excitation pulse, which allows all short-lived emission to decay before detection. This principle has already been introduced in the 1960's in the form of a phosphoroscope, which records the long-lived triplet emission (phosphorescence) of an organic molecule and thereby reduces the undesirable interference from the

short-lived singlet emission (fluorescence).[37] Owing to the large difference between the lifetimes of fluorescence and phosphorescence, such a design required only relatively simple instrumentation with MHz switching times. With the availability of faster switching electric circuits, this method could later be applied to small differences in fluorescence lifetimes.[38] However, time-gated measurements first became popular with the development of lanthanide chelates which have a long-lived emission in a medium, which is suitable for enzyme assays (aerated water, conditions under which organic triplet states are quenched). These lanthanides allowed combining the advantages of a relatively cheap and simple detection with efficient background suppression.[25,39-41]

1.3 Supramolecular Sensor Systems

1.3.1 Classes of Macrocyclic Hosts in Sensor Applications

Supramolecular chemistry has its foundations in the discovery of the crown ethers by Charles Pedersen in 1967.[42,43] His reports were very inspiring and have immediately attracted the attention of numerous other research groups worldwide: Izatt and Christensen have proposed their use as models for ion transport through membranes,[44] refined polyethers with a polycyclic structure (cryptands) were devised by Lehn,[45] and Cram synthesized the first chiral crown ethers.[46] The development of the field progressed from then on rapidly and climaxed in awarding of the Nobel prize in 1987 to Pedersen, Lehn, and Cram.[47-49]

1.3.1.1 Cyclodextrins

Cyclodextrins are, in contrast to crown ethers, natural products, which are obtained from starch by an enzyme-catalyzed reaction. The first report dates back to 1891 and interestingly, the nature of their complexes with organic molecules was recognized to be of the inclusion type before the work of Pedersen.[50] However, most of the exciting progress in cyclodextrin chemistry has been made afterwards.

The most important, industrially available cyclodextrins are composed out of six to eight D-glucopyranose units, which are connected *via* an α-(1→4)-glycosidic bond (Chart 1.1). Depending on the number of monomeric units, they have been named α-, β-, and γ-cyclodextrin. Their shape resembles a hollow truncated cone with a wider upper rim carrying the C2 and C3 hydroxyl groups and a narrower lower rim carrying the C6 hydroxyl groups. The outer surface of the truncated cone is hydrophilic, which renders the cyclodextrins water soluble, while the inner surface is hydrophobic, which facilitates the inclusion of hydrophobic organic molecules.

Chart 1.1. Three representative examples from the family of cyclodextrins.

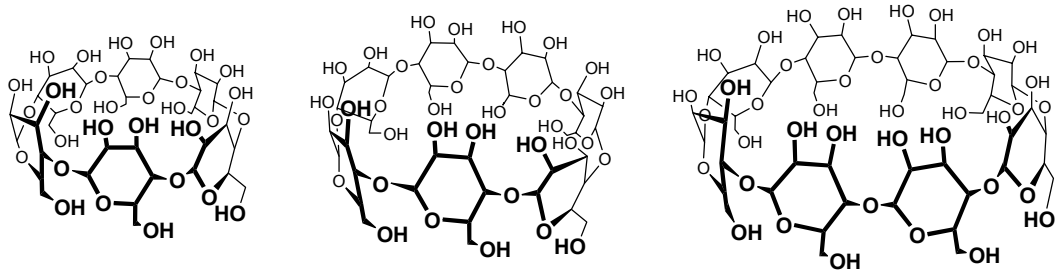

α-cyclodextrin β-cyclodextrin γ-cyclodextrin

Owing to their availability on a large scale and their apparent similarity to proteins, which comprises a hydrophilic surface and a hydrophobic cavity, suggested their use as suitable models for studies in molecular recognition.[51] The dependence of thermodynamic parameters (binding constant, enthalpy, entropy) and kinetic parameters on size, charge, and spatial arrangement of host and guest were studied by various techniques, e.g. nuclear magnetic resonance (NMR),[52] calorimetry,[53,54] absorption spectroscopy,[53,55-58] circular dichroism,[56-59] and steady-state[60,61] as well as time-resolved fluorescence spectroscopy.[55,57] These studies provided a deeper understanding of the fundamental requirements for highly efficient and selective binding and were inspiring for the construction of artificial enzymes based on the cyclodextrin scaffold.[62]

However, this challenge also required efficient methods for the attachment of functional groups to cyclodextrins. Much effort has therefore been spent towards the derivatization of cyclodextrins and methods for the selective mono-, di- and persubstitution at the C2, C3 and C6 hydroxy groups with well defined

substitution patterns are now available.[63] In addition, the synthesis of heterogeneous oligosaccharides composed of other monomeric units than only glucose has been demonstrated.[64]

Furthermore, the possibility to produce cyclodextrins in a multigrams- to tons-scale at fair prices, has enabled their application as drug carriers[65] and production aids in technical chemistry.[66]

1.3.1.2 Calixarenes

Calixarenes constitute a class of [1$_n$]metacyclophanes, which had been previously isolated as crystalline by-products in the curing of phenol-formaldehyde resins.[67] However, their exact constitution remained unsolved until Gutsche recognized their potential as hosts in the field of supramolecular chemistry,[68] and carried out more detailed investigations.[69,70] Calixarenes became immediately very popular owing to their convenient access and their ease of derivatization, in particular the *p-tert*-butylcalix[*n*]arenes (*n* indicating the number of aryl rings) with *n* = 4, 6, and 8 are accessible by a one-pot synthesis.[69] Nowadays, all ring sizes from *n* = 4-9 as well as some higher oligomers are known, and the derivatization of the upper rim and the lower rim (cf. Chart 1.2) is well established for every possible substitution pattern.[71]

Chart 1.2. Representative examples of calixarenes and resorcinarenes.

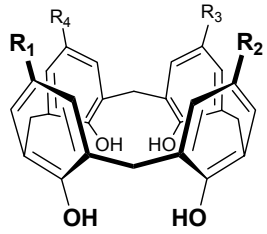

calix[4]arene

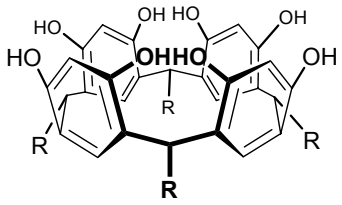

resorcinarene

Similarly, the condensation reaction of resorcinol with aldehydes affords resorcinarenes,[72,73] which are attractive owing to their possibility to rigidify the host cavity by bridging the upper rim hydroxyl groups, either by deprotonation and intramolecular hydrogen bonding[74] or by covalent modification.[75] The latter approach has enabled the construction of even larger host molecules, e.g.

deepened cavitands[76,77] and carcerands,[78-80] which were conceptualized as molecular containers.[81]

Calixarenes and related compounds have been used for similar studies in host-guest chemistry like cyclodextrins, because they are also featuring a hydrophobic microenvironment which is capable of forming strong intermolecular complexes: they have therefore been studied as enzyme models[82-85] and as receptors for biologically relevant analytes,[86-89] and they have been utilized as phase transfer catalysts[90,91] and as sensors for cations[92,93] and anions.[94] Despite the apparent similarity of calixarenes and cyclodextrins, interesting differences have been found, which have deepened the knowledge about the fundamentals of molecular recognition and which have led to complementary applications.[95,96] An interesting new application is their use as a scaffold for peptide structures[97] with the potential to modulate protein-protein interactions.[98-100]

1.3.1.3 Cucurbiturils

Cucurbiturils constitute one of the newest classes of macrocyclic hosts, although their history can be traced back to the year 1905.[101] The initial report did not provide a characterization of the compound and was therefore reinvestigated by Mock and co-workers in 1981.[102] They elucidated the structure of the uncharacterized compound and recognized that a pumpkin-shaped molecule comprising six glycoluril units had been formed, which was therefore given the name "cucurbituril".[102] Subsequently, the research groups of Buschmann[103] and Kim[104] entered the field and provided new insights into the complexation properties of cucurbituril.

Chart 1.3. The homologue series of cucurbit[*n*]urils with *n* = 5, 6, 7.

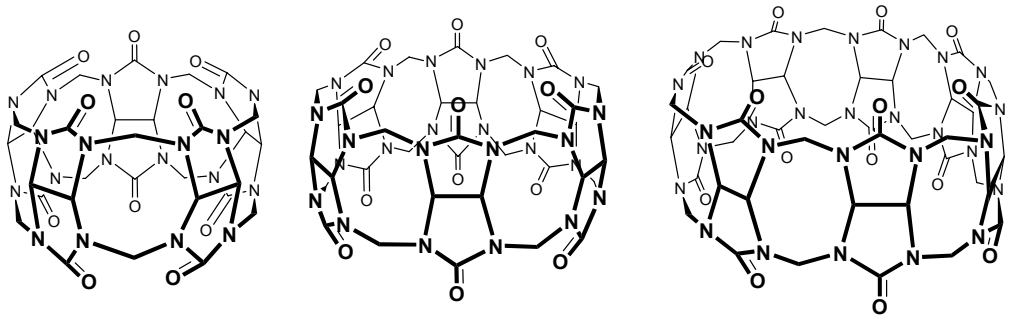

cucurbit[5]uril cucurbit[6]uril cucurbit[7]uril

The report of higher and lower homologues (Chart 1.3) of cucurbituril had finally been ground-breaking for the field.[105] Up to now, cucurbit[*n*]urils (*n* indicating the number of glycoluril units) with *n* = 5, 6, 7, 8, and 10[106] have been purified and characterized, but only few substituted cucurbit[*n*]urils have been synthesized,[107] which still presents a major challenge.

Regarding applications, cucurbiturils have proven to be as versatile and interesting as the aforementioned cyclodextrins and calixarenes, e.g. the construction of fluorescent sensors,[108] the selective molecular recognition of peptides,[109-111] and drug delivery systems[112,113] have been demonstrated. An outstanding facet of cucurbiturils, which is not found among cyclodextrins and calixarenes, is their propensity to bind cationic species with unprecedentedly high binding constants.[103,107,114,115] Furthermore, their complexation kinetics can be much slower than those of calixarenes and cyclodextrins,[116,117] which has led to their applications in self-sorting systems.[118]

Another outstanding feature is offered by the physical properties of their cavity. It has been demonstrated by determining the polarizability with a spectroscopic probe, that the interior of cucurbiturils represents a void, which shows properties similar to the gas phase.[119] This has enabled the application of cucurbiturils as dye-stabilizing additives for fluorescence measurements,[120,121] and explained previously observed effects on the enhancement of the fluorescence intensity of included dyes.[122,123] In addition, the fluorescence lifetime-enhancing properties of cucurbiturils have been predicted[124,125] on the basis of the Strickler-Berg equation,[126] which were afterwards demonstrated.[121]

1.3.2 Readout Principles for Supramolecular Sensors

In view of many macrocyclic receptors, which can be fine-tuned for the molecular recognition of biologically relevant analytes like neurotransmitters,[86,127,128] peptides,[110,129] and nucleotides,[130,131] it is not surprising that principles have been sought for to transform the recognition event into a spectroscopic signal. This directly affords a working device for sensory applications, which is important for the convenient determination of analyte

concentrations,[132] imaging of cell membranes,[133] or a little bit more far fetched, molecular computing.[134,135]

1.3.2.1 Covalent Tethering of Receptor and Fluorophore

The mostly employed approach is depicted in Scheme 1.5 and relies on the fluorophore-spacer-receptor approach. The receptor represents a macrocyclic unit, which is capable of binding the analyte of interest, the fluorophore is an organic fluorescent dye and the spacer serves as a mediator between the receptor and the fluorophore. The mechanisms, which have been used to induce a fluorescence change, comprise photoinduced electron transfer (PET), electronic energy transfer (EET), and modulation of charge-transfer excited states.[132]

Scheme 1.5. a) The fluorophore-spacer-receptor approach to the construction of supramolecular sensor systems. b) Application of the fluorophore-spacer-receptor approach to macrocyclic fluorescent dye complexes by a covalent tethering between macrocycle and dye. Note that the fluorescence can be likewise decreased upon binding of the analyte.

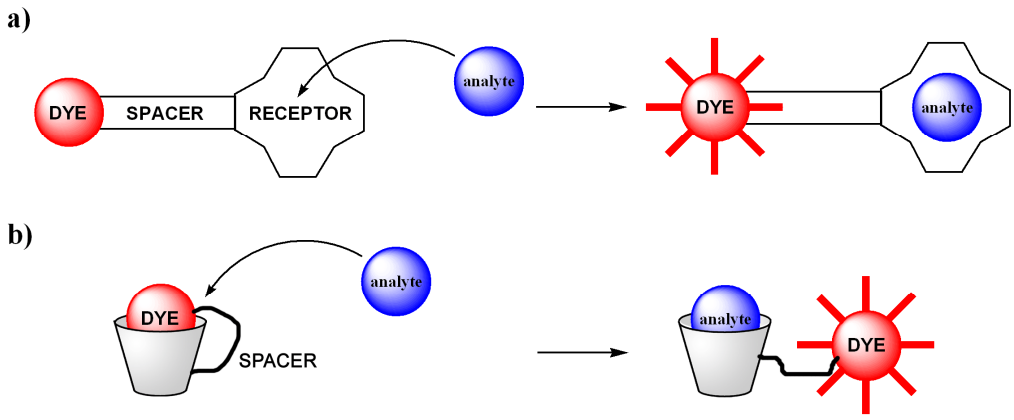

In a somewhat different approach, the receptor has been refined from simple crown ethers into cyclodextrins and calixarenes. Largely based on the pioneering works of Ueno and co-workers, the spacer has been replaced by a simple alkyl chain, which ties the fluorophore and receptor together,[136] and loses its role as a mediator of the fluorescence modulation. In this approach, the fluorescence intensity is solely determined by the different environments, i.e. exposed to the bulk solvent *versus* buried in the macrocyclic cavity. In a more

advanced approach, the alkyl chain has even been successfully replaced by an α-helical peptide backbone[137] and was applied to the detection of steroids.[138]

1.3.2.2 Displacement Assays

Although the method of dye displacement from a macrocyclic cavity has often been used to determine high binding constants,[87,139] which are not accessible by NMR, it took a relatively long time before it has been realized that this directly affords a sensor system.[86] The principle, which has been conceptualized by Anslyn as indicator displacement assays,[140,141] remedies the necessity to attach a covalent tethering between macrocycle and dye in Scheme 1.5b. However, this takes the toll that the dye might diffuse away from the analyte-receptor complex. This does not create any difficulties in homogeneous solution, but is undesirable in heterogeneous environments, for example in cellular imaging applications or solid state sensors. Nevertheless, the potential of this method has been overwhelming and afforded in combination with array recognition[142] an unprecedented amount of information in the analysis of amino acids,[143] proteins, or in complex media.[144]

1.4 Experimental Techniques

1.4.1 Synthesis

1.4.1.1 Synthesis of 2,3-Diazabicyclo[2.2.2]oct-2-ene (DBO)

All reagents for synthesis were purchased from Fluka or Aldrich, and solvent were from Applichem. The synthesis of DBO was performed according to the published route (Scheme 1.6). The synthesis of the parent fluorophore 2,3-diazabicyclo[2.2.2]oct-2-ene (DBO) was performed according to the literature,[145] *via* Diels-Alder reaction of freshly prepared 4-Methyl-4*H*-1,2,4-triazoline-3,5-dione (MTAD, 1) [146-148] with cyclohexadiene, hydrogenation, hydrolysis and oxidation.

Scheme 1.6. Synthesis of the parent fluorophore DBO (**5**).

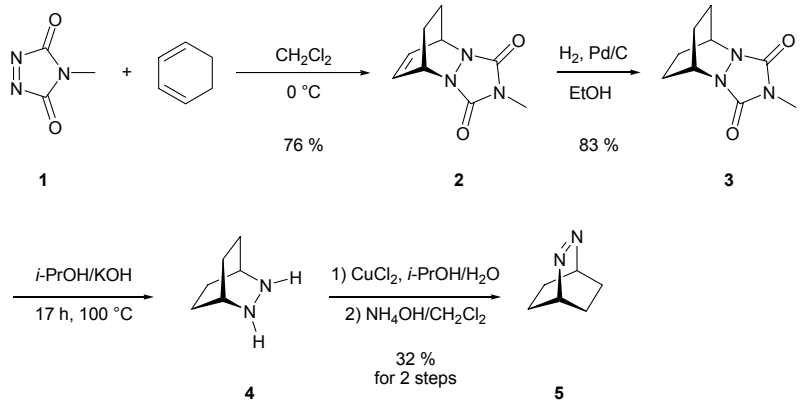

4-Methyl-4*H*-1,2,4-triazoline-3,5-dione (MTAD, 1).[146,147] MTAD is prepared from 4-methylurazole by oxidation with freshly prepared *tert*-butyl hypochlorite.[148] Therefore, 180 ml (0.39 mol) of 13 % sodium hypochlorite is cooled down to 0 °C and the reaction flask is covered with aluminum foil to prevent decomposition by intense light. A solution of 37 ml (0.39 mol) *tert*-butanol and 25.5 ml (0.43 mol) glacial acetic acid is added and the reaction mixture is stirred intensively for several minutes. Two phases form, which are separated. The lower, aqueous phase is discarded and the upper, yellowish, organic phase is washed with 50 ml 10 % sodium carbonate and 150 ml water.

The organic layer is dried over calcium chloride and yields 23.52 g (55 %) *tert*-butyl hypochlorite. ^{1}H-NMR ($CDCl_3$) δ TMS: 1.33 ppm (s).

4.72 g (43.4 mmol) of *tert*-butyl hypochlorite are added dropwise (over the course of 4 h) to a suspension of 5 g (43.4 mmol) 4-methylurazole in 100 ml dichloromethane at 0 °C. The solvent is removed from the dark-red solution and the obtained red crystals (4.27 g; 96 % crude yield) are dissolved in 60 ml ethyl acetate. The solution is filtered to remove a suspended white precipitate. The solution in ethyl acetate is stable overnight at 4 °C and is directly used for the next reaction. ^{1}H-NMR ($CDCl_3$, 400 MHz) δ TMS: 3.17 ppm (3H, s, NCH_3).

4-Methyl-2,4,6-triaza-tricyclo[5.2.2.0^{2,6}]undec-8-en-3,5-dion (2).[145] 4.27 g (41.7 mmol) freshly prepared **1** in 60 ml ethyl acetate is added dropwise during 4 h to an ice-cold solution of 3.34 g (41.7 mmol) cyclohexadiene in 120 ml ethyl acetate under inert atmosphere. The reaction is followed by disappearance of the red color. After complete addition, the reaction mixture is stirred for additional 30 minutes. The solvent is removed by rotary evaporation and excess cyclohexadiene is removed under high vacuum to obtain 6.03 g (76 %) pale yellow **2**. ^{1}H-NMR ($CDCl_3$) δ TMS: 1.53-1.58 (2H, m, bridge-CH), 2.10-2.20 (2H, m, bridge-CH), 3.00 (3H, s, CH_3), 4.82-4.87 (2H, m, CHN), 6.42 ppm (2H, dd, J = 4.04, 3.03 Hz, C=CH).

4-Methyl-2,4,6-triaza-tricyclo[5.2.2.0^{2,6}]undecan-3,5-dione (3). 6.03 g (31.5 mmol) **2** are dissolved in 300 ml abs. ethanol and 500 mg Pd/C are added. The reaction mixture is five times degassed and purged with hydrogen. Afterwards, the mixture is stirred until inspection by thin layer chromatography reveals complete disappearance of **2** (after ca. 90 min). The catalyst is removed by filtration over celite and the solvent is removed *in vacuo*. Drying under high vacuum yields 5.05 g (83 %) **3** as long needles. ^{1}H-NMR ($CDCl_3$) δ TMS: 1.75 und 1.95 ppm (4H, d, J = 8.08 Hz, bridge-CH), 3.03 (3H, s, NCH_3), 4.24 (2H, s, bridgehead-CH).

2,3-Diaza-bicyclo[2.2.2]octane (4). 17.22 g potassium hydroxide is dissolved in 200 ml *i*-propanol and 5.05 g (26.2 mmol) **3** are added. The mixture is heated under reflux for 17 h at 100 °C, during which a colorless solid precipitates. After

cooling down, the solid is filtered off and washed excessively with methanol and dichloromethane. The solvent of the combined extracts is removed by rotary evaporation yielding a highly viscous oil, which is dissolved in 200 ml water. The aqueous solution is four times extracted with 50 ml dichloromethane. The combined organic extracts are dried over magnesium sulfate and the solvent is removed by rotary evaporation, which yields 4.89 g crude product.

2,3-Diaza-bicyclo[2.2.2]oct-2-ene (DBO, 5). The obtained yellowish oil (4.89 g) is dissolved in 80 ml *i*-propanol and added dropwise to 200 ml 1 M copper(II) chloride in water. The reaction mixture is stirred for 2 h, and a dark-brown precipitate is formed. The solution is filtered, and the precipitate is washed with a diluted ammonium chloride-solution, ethanol and water, which reveals the red color of the copper adduct. The complex is decomposed by a mixture of 300 ml concentrated ammonia and 100 ml dichloromethane. The aqueous layer is extracted three times with dichloromethane and the combined extracts are dried over magnesium sulfate. Evaporation of the solvent yields a pale yellow solid, which affords after recrystallisation from hexane and sublimation (35 °C, 10^{-1} Torr) 0.91 g (32 % for last two steps) of **5** crystallizing as long, colorless needles. ^{1}H-NMR ($CDCl_3$) δ TMS: 1.30 und 1.59 ppm (4H, d, J = 8.08 Hz, bridge-CH), 5.11 (2H, s, bridgehead-CH). ^{13}C-NMR ($CDCl_3$) δ TMS: 21.2 ppm (bridge-C), 61.0 (bridgehead-C).

1.4.1.2 Synthesis of DBO-labeled asparagine and peptides

Reagents for synthesis were purchased from Fluka, Aldrich or Applichem, except Fmoc-Asp-OtBu, which was from Bachem. The synthesis of DBO-labeled asparagine was performed according to the published route (Scheme 1.7).[149] Starting with crotonaldehyde **6**, the hydroxymethyl-substituted cyclohexadiene **10** was prepared in four steps according to the method of Hünig and Kahanek.[150] Following the conventional[151] approach to DBO derivatives we reacted **10** with MTAD (**1**). After subsequent hydrogenation and hydrolysis the hydroxymethyl-substituted DBO **13** was obtained,[152] which was converted into the aminomethyl derivative **16** by tosylation,[153] azide substitution and reduction. The amine **16** was coupled with the help of *N*-ethoxycarbonyl-2-ethoxy-1,2-dihydroquinoline

(EEDQ)[154] to the side chain of Fmoc-Asp-OtBu, which was finally saponified by treatment with trifluoroacetic acid (TFA).[155] Overall yield referenced to the most expensive starting material MTAD was ca. 15 %.

The DBO-labeled asparagine was sent out for commercially available solid-phase peptide synthesis (Biosyntan, Berlin and Affina Immuntechnik, Berlin). The peptides were purified by preparative HPLC (LC-8A with UV-Vis detector SPD-6A) with a RP-18 column. For all peptides, no complications were ever reported during synthesis and no degradation of Dbo had been observed during purification.

Scheme 1.7. Synthesis of Fmoc-protected DBO-labeled asparagine (**18**).

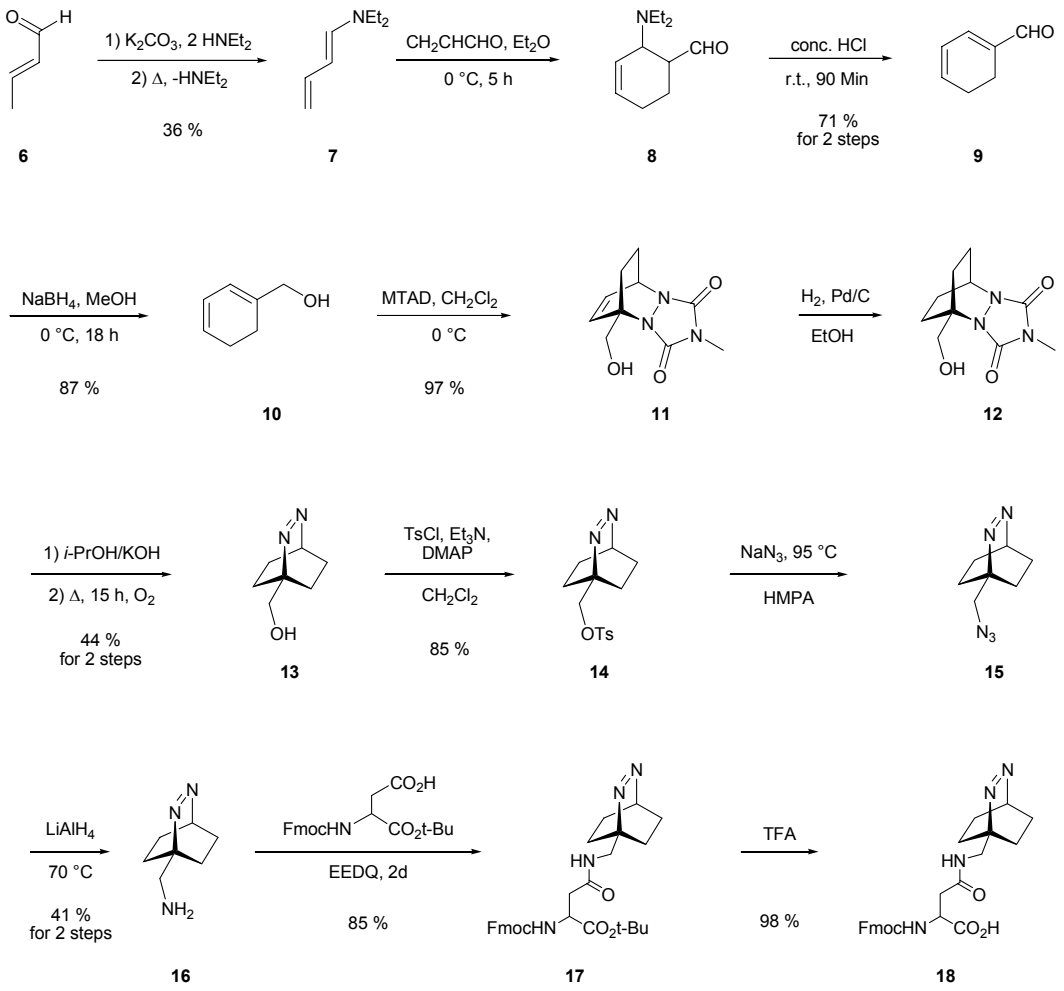

1-Diethylamino-butadiene (7). 185 ml (132 g, 1.80 mol) diethylamine and 24 g potassium carbonate are cooled down to –10 °C in an inert gas atmosphere. 50 ml (42 g, 0.60 mol) crotonaldehyde **1** are added dropwise to the reaction mixture,

while the temperature is carefully maintained below 0 °C. During addition the color changes from colorless to yellow. The reaction mixture is stirred for 4 h, while it is allowed to slowly warm up to room temperature. The reaction mixture is decanted from the potassium carbonate and 180 mg 9,10-phenanthrenequinone are added. Excess diethylamine is removed *in vacuo* at room temperature and 27.12 g (36 %) 1-dietyhlamino-butadiene is obtained as a pale yellow oil by vacuum distillation (boiling point: 60-65 °C; 18 mbar). ^{1}H-NMR ($CDCl_3$) δ TMS: 1.08 ppm (6H, t, ^{3}J = 7.07 Hz, NCH_2CH_3), 3.04 (4H, q, ^{3}J = 7.07 Hz, NCH_2CH_3), 4.44 (1H, dd, ^{2}J = 2.02 Hz, ^{3}J = 10.01 Hz, NCH=CH-CH=CH*H*), 4.69 (1H, dd, ^{2}J = 2.02 Hz, ^{3}J = 17.18 Hz, NCH=CH-CH=C*H*H), 5.02 (1H, dd, 3J = 10.61, 13.14 Hz, NCH=C*H*-CH=CH_2), 6.21 (1H, d, ^{3}J = 13.14 Hz, NC*H*=CH-CH=CH_2), 6.20-6.30 (1H, m, NCH=CH-C*H*=CH_2). ^{13}C-NMR ($CDCl_3$) δ TMS: 13.1 ppm (q, NCH_2CH_3), 45.1 (t, NCH_2CH_3), 98.3, 103.5, 137.6, 141.6 (C=C).

2-Diethylamino-cyclohex-3-ene carbaldehyde (8). A solution of 43.65 g (0.35 mol) **2** in 60 ml abs. diethylether is cooled down to −10 °C in an inert gas atmosphere. A solution of 23 ml (19.28 g, 0.35 mol) acroleine in 60 ml abs. diethylether is added dropwise, while the temperature is carefully maintained at −10 °C. The reaction mixture is allowed to warm up to room temperature overnight. The diethylether is removed by rotary evaporation and the crude product is directly used for the next reaction.

Cyclohexa-1,3-diene carbaldehyde (9). The crude **8** is mixed with 60 ml conc. HCl in 300 ml water and stirred for 5 h at room temperature. The reaction mixture is extracted 4 times with 100 ml diethylether. The combined extracts are washed with 100 ml water, 10 % Na_2CO_3-solution and twice with water. Subsequently the diethylether is removed by rotary evaporation to give 27.06 g (71 % for the last 2 steps) **9**. ^{1}H-NMR ($CDCl_3$) δ TMS: 2.25 ppm (2H, m, CH_2), 2.33 (2H, m, CH_2), 6.14 (1H, m, C=CH), 6.25 (1H, m, C=CH), 6.70 (1H, d, C=CH), 9.45 (1H, t, CHO).

Cyclohexa-1,3-dienyl-methanol (10). 27.06 g (0.250 mol) **9** is dissolved in 150 ml methanol and cooled down to 0 °C. 10 g (0.264 mol) $NaBH_4$ in 60 ml 10 % Na_2CO_3 are added dropwise within 10 minutes and the reaction mixture is stirred for 4 h at room temperature. The mixture is extracted three times with 200 ml

diethylether and the combined extracts are washed successively with 100 ml water and twice with 100 ml brine. After removal of the solvent by rotary evaporation and vacuum distillation (88-92 °C, 22 mbar) 24.05 g (87 %) **10** is obtained, which served as a stock for several synthesis of Fmoc-protected DBO-labeled asparagine **18**.

1-Hydroxymethyl-4-methyl-2,4,6-triaza-tricyclo[5.2.2.0^{2,6}]-undec-8-ene-3,5-dione (11). 6.54 g (59.3 mmol) freshly distilled **10** are dissolved in 75 ml dichloromethane. Under inert gas atmosphere 6.71 g (59.3 mmol) freshly prepared MTAD in 110 ml CH_2Cl_2 are added dropwise at 0 °C over the course of 3 h. During addition, the red colour of MTAD disappears immediately after dropping it into the solution. After complete addition, the reaction mixture is stirred for 1 h at room temperature, and the solvent is removed by rotary evaporation. Finally, excess **10** is removed under high vacuum, and 12.86 g (97 %) of colorless **11** are obtained. ^{1}H-NMR ($CDCl_3$) δ TMS: 1.38 ppm (1H, br, bridge-CH), 1.64 (1H, br, bridge-CH), 2.09 (1H, br, bridge-CH), 2.20 (1H, br, bridge-CH), 3.02 (3H, s, NCH_3), 4.00 (1H, br, CH_2OH), 4.20 (1H, br, CH_2OH), 4.50 (1H, br, OH), 4.93 (1H, br, bridgehead-CH), 6.49 (1H, br, C=CH), 6.59 (1H, br, C=CH). ^{13}C-NMR ($CDCl_3$) δ TMS: 23.6 ppm (t, bridge -C), 25.4 (q, NCH_3), 26.0 (t, bridge -C), 49.8 (d, bridgehead-C), 63.7 (s, bridgehead-C), 63.8 (d, CH_2OH), 130.2 (d, C=CH), 131.5 (d, C=CH), 155.4 (s, C=O), 156.3 (s, C=O).

1-Hydroxymethyl-4-methyl-2,4,6-triaza-tricyclo[5.2.2.0^{2,6}]-undecane-3,5-dione (12). 12.86 g (57.5 mmol) **11** is dissolved in 200 ml of abs. ethanol and 500 mg Pd/C (5 %) is added. The mixture is five times degassed and purged with hydrogen and the reaction mixture is stirred for 90 min at room temperature. Subsequently, Pd/C is removed by filtration over celite and the solvent is removed by rotary evaporation, which yields 12.90 g crude **12** as a colorless solid. ^{1}H-NMR ($CDCl_3$) δ TMS: 1.69 ppm (2H, br, bridge-CH_2), 1.91 (2H, br, bridge-CH_2), 2.03 (2H, br, bridge-CH_2), 2.13 (2H, br, bridge-CH_2), 3.10 (3H, s, NCH_3), 3.85 (2H, br, CH_2OH), 4.43 (1H, br, bridgehead-CH). ^{13}C-NMR ($CDCl_3$) δ TMS: 25.1 ppm (t, bridge-C), 25.5 (q, NCH_3), 27.6 (t, bridge-C), 47.6 (d, bridgehead-C), 62.2 (s, bridgehead-C), 65.3 (t, CH_2OH), 151.7 (s, C=O).

(2,3-Diaza-bicyclo[2.2.2]oct-2-en-1-yl)-methanol (13). 25 g potassium hydroxide is dissolved in 250 ml *i*-propanol and 12.90 g crude **12** is added under inert gas atmosphere. The reaction mixture is heated for 15 h under reflux, during which a white precipitate is formed. The reaction mixture is cooled down to room temperature, and the precipitate is removed by filtration. The filtrate is evaporated to dryness and the solid residue is excessively suspended in 250 ml dichloromethane and filtered over a short silica column with dichloromethane/methanol 10:1 as eluent. Purification by column chromatography (with a gradient from 99:1 to 90:10 dichloromethane/methanol) and subsequent recrystallization from hexane affords 3.65 g (44 % for the last two steps) **13**, which crystallizes as colorless long needles. ^{1}H-NMR ($CDCl_3$) δ TMS: 1.23-1.31, 1.32-1.40, 1.44-1.50, 1.62-1.69 ppm (je 2H, m, bridge-CH_2), 2.83 (1H, br, OH), 4.04 (2H, s, CH_2OH), 5.18 (1H, m, bridgehead-CH). ^{13}C-NMR ($CDCl_3$) δ TMS: 21.8 ppm (t, bridge-C), 23.1 (t, bridge-C), 62.1 (t, bridgehead-C), 67.6 (t, CH_2OH), 67.7 (s, bridgehead -C).

Toluene-4-sulfonyl-2,3-diaza-bicyclo[2.2.2]oct-2-en-1-ylmethylester (14). 2.73 g (19.5 mmol) **13** and 3.0 ml (2.18 g, 21.5 mmol) triethylamin are dissolved in 75 ml of dry dichloromethane under inert gas atmosphere. 3.75 g (19.7 mmol) toluenesulfonyl chloride in 25 ml dry dichloromethane is added to the well-stirred reaction mixture. 100 mg 4-dimethylaminopyridine is added as a catalyst and the reaction mixture is stirred for 18 h at room temperature. After this, 100 ml distilled water is added and the aqueous phase is extracted four times with 50 ml dichloromethane. The combined extracts are dried over magnesium sulfate and the solvent is removed by rotary evaporation. The crude product is purified by flash column chromatography (dichloromethane/methanol 98:2) over silica, which affords 4.86 g (85%) **14** as colorless solid. ^{1}H-NMR ($CDCl_3$) δ TMS: 1.08-1.16 ppm (2H, m, bridge-CH_2), 1.27-1.38 (2H, m, bridge-CH_2), 1.58-1.64 (4H, m, bridge-CH_2), 2.46 (3H, s, CH_3Ar), 4.56 (2H, s, CH_2OH), 5.15 (1H, m, bridgehead-CH), 7.37 (2H, d, J = 8.4 Hz, arom. CH), 7.86 (2H, d, J = 8.4 Hz, arom. CH). ^{13}C-NMR ($CDCl_3$) δ TMS: 21.2 ppm (t, bridge-C), 21.8 (t, CH_3), 23.3 (t, bridge-C), 61.8 (d, bridgehead-C), 65.7 (s, bridgehead-C), 74.3 (t, CH_2OH), 128.2 (d, arom. CH), 130.0 (d, arom. CH), 132.7 (s, arom. C), 145.1 (s, arom. C).

1-Azidomethyl-2,3-diaza-bicyclo[2.2.2]oct-2-ene (15). 4.86 g (16.5 mmol) **14** and 5.46 g sodium azide are dissolved in 140 ml freshly dried (over CaH_2 at 105 °C) and distilled (b.p. 113 °C at 17 mbar) HMPT under inert gas atmosphere. The reaction mixture is stirred for 18 h at 90 °C. After that the mixture was diluted with 200 ml water and extracted four times with 75 ml diethylether. The extracts were combined and the solvent was removed. The residue was taken up in diethylether and washed with water. The organic phase was dried over magnesium sulfate and the solvent was removed by rotary evaporation, which afforded 2.53 g crude azide **15**, which was directly used without further purification owing to its instability. ^{1}H-NMR ($CDCl_3$) δ TMS: 1.16-1.24 (2H, m, bridge-CH_2), 1.32-1.42 (2H, m, bridge-CH_2), 1.51-1.71 (2H, m, bridge-CH_2), 3.89 (2H, s, CH_2N_3), 5.18 (1H, m, bridgehead-CH).

***C*-(2,3-Diaza-bicyclo[2.2.2]oct-2-en-1-yl)methylamine (16)**. A solution of 2.27 g (13.7 mmol) **15** in 140 ml dry THF were added dropwise to a stirred suspension of 10.52 g (0.3 mol) lithium aluminium hydride in 70 ml THF under inert gas atmosphere. Subsequently, the reaction mixture is heated under reflux for 6 h, cooled to room temperature and slowly treated with 15 % NaOH until no more white, granular precipitate is formed. The precipitate is removed by filtration and washed excessively with THF. The combined washings are evaporated and the solid residue is dissolved in dichloromethane and dried over KOH pellets. Evaporation and flash chromatography (dichloromethane/methanol/triethylamine 100:10:1) gave 950 mg (41 % for the last two steps) amine **16** as a colorless wax. ^{1}H-NMR ($CDCl_3$) δ TMS: 1.20-1.31 ppm (2H, m, bridge-CH_2), 1.35-1.52 (4H, m, bridge-CH_2), 1.60-1.70 (2H, m, bridge-CH_2), 2.03 (2H, br, NH_2), 3.23 (2H, s, CH_2NH_2), 5.16 (1H, m, bridgehead-CH).

***N*-(2,3-Diaza-bicyclo[2.2.2]oct-2-en-1-ylmethyl)-2-(9H-fluoren-9-ylmethoxycarbonylamino)succinaminic acid-*tert*-butylester (17)**. 500 mg (3.59 mmol) **16**, 1.50 g (3.65 mmol) Fmoc-Asp-OtBu and 1.15 g (4.67 mmol) *N*-ethoxycarbonyl-2-ethoxy-1,2-dihydroquinoline (EEDQ) are dissolved in 100 ml abs. dichloromethane and stirred at room temperature for 2 days under nitrogen. The reaction mixture is diluted to 200 ml with dichloromethane and subsequently washed with 10 times 150 ml 5% citric acid, and once with 150 ml water, sat.

sodium hydrogencarbonate solution, water and brine. The combined organic phases are dried over magnesium sulfate. The crude product is purified by flash chromatography (dichloromethane/methanol 98:2), which affords 1.62 g (85 %) of **17** as a white solid. ^{1}H-NMR ($CDCl_3$) δ TMS: 1.08-1.17 (2H, m, bridge-CH_2), 1.24-1.36 (2H, m, bridge-CH_2), 1.47 (9H, s, t-Bu-CH_3), 1.52-1.66 (4H, m, bridge-CH_2), 2.79-2.82 (1H, m, β-CH_2 Asp), 2.91-2.93 (1H, m, Asp-β-CH_2), 3.82 (2H, d, J = 6.0 Hz, CH_2N), 4.17-4.26 (1H, m, Fmoc-CH), 4.28-4.32 (1H, m, Fmoc-CH_2), 4.36-4.42 (1H, m, Fmoc-CH_2), 4.46-4.54 (1H, m, Asp-α-CH), 5.16 (1H, br, bridgehead-CH), 6.06 (1H, br, Asp-NH), 6.56 (1H, br, DBO-NH), 7.30 (2H, m, arom. Fmoc), 7.40 (2H, m, arom. Fmoc), 7.58-7.62 (2H, m, arom. Fmoc), 7.76 (2H, m, arom. Fmoc).

***N*-(2,3-Diaza-bicyclo[2.2.2]oct-2-en-1-ylmethyl)-2-(9H-fluoren-9-ylmethoxycarbonylamino)succinamine acid (18, Fmoc-Dbo)**. 628 mg (1.18 mmol) Fmoc-DBO-OtBu are dissolved in 17.3 ml abs. dichloromethane under inert gas atmosphere at 0 °C. 10.4 ml trifluoroacetic acid (TFA) is added to the ice-cold solution and the reaction mixture is stirred for 3 h at room temperature. After removing a great fraction of the solvent, residual TFA is removed by coevaporation with toluene and acetonitrile as an azeotrop, which affords 550 mg (98 %) **18** as a colorless solid. ^{1}H-NMR ($CDCl_3$) δ TMS: 1.07-1.22 ppm (2H, m, bridge-CH_2), 1.30-1.39 (2H, m, bridge-CH_2), 1.53-1.61 (2H, m, bridge-CH_2), 1.64-1.71 (2H, m, bridge-CH_2), 2.79-2.82 (1H, m, Asp-β-CH_2), 2.98-3.00 (1H, m, Asp-β-CH_2), 3.84-3.88 (2H, m, CH_2N), 4.21 (1H, t, J = 7.1 Hz, Fmoc-CH), 4.34-4.43 (2H, m, Fmoc-CH_2), 4.51-4.56 (1H, m, Asp-α-CH), 5.24 (1H, s, br, bridge -CH), 6.13 (1H, m, Asp-NH), 7.15-7.18 (1H, m, DBO-NH), 7.31 (2H, arom. Fmoc-CH), 7.40 (2H, arom. Fmoc-CH), 7.56-7.60 (2H, m, arom. Fmoc-CH), 7.76 (2H, arom. Fmoc-CH).

1.4.1.3 Synthesis of other DBO derivatives

In addition to the parent fluorophore DBO and the DBO-labeled asparagine, for which the synthesis had been previously reported, two novel derivatives (**19** and **20**) were additionally synthesized (Scheme 1.8), which were however not yet investigated in detail. The bromomethyl derivative **19** was

obtained by substitution of the known[149] tosylate **14**. The DBO derivative carrying an aldehyde group in the bridgehead position **20** was obtained by Swern oxidation[156] from the alcohol **13**. Several other methods, e.g. pyridinium chlorochromate[157] or periodates[158] failed. Interestingly, the synthesis of the corresponding DBO acid proofed similarly challenging and also afforded surprisingly low yields,[159] which may be attributed to the radical-stabilizing character of these substituents.

Scheme 1.8. Synthesis of bromomethyl-DBO **19** and DBO aldehyde **20**.

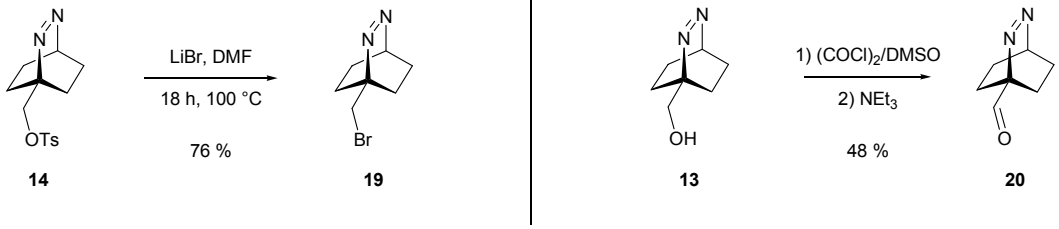

14 **19** **13** **20**

Bromomethyl-DBO (**19**): 494 mg (5.1 mmol) LiBr were dissolved in 9 ml abs. DMF under inert atmosphere. After addition of 250 mg (0.85 mmol) DBO tosylate (**14**), the reaction mixture was heated for 18 h at 100 °C. The reaction mixture was allowed to cool down, diluted with 10 ml water and extracted four times with 25 ml dichloromethane. After drying over $MgSO_4$, the solvent was removed by rotary evaporation. Flash column chromatography (dichloromethane/methanol 99:1) gave 131 mg (76 %) **19** as colorless crystals. ^{1}H NMR ($CDCl_3$, 400 MHz) δ (ppm): 1.18-1.27 (2H, m, CH_2), 1.32-1.42 (2H, m, CH_2), 1.55-1.76 (4H, m, CH_2), 3.95 (2H, s, CH_2Br), 5.14 (1H, br s, CH). ^{13}C NMR ($CDCl_3$, 100 MHz) δ (ppm): 21.9 (t, CH_2), 25.2 (t, CH_2), 39.9 (t, CH_2Br), 61.7 (d, CH), 66.1 (s, C_q).

DBO aldehyde (**20**): 55 mg (0.43 mmol) oxalylchloride were dissolved in 8 ml abs. dichloromethane and the reaction mixture was cooled down to −78 °C. Then, 67 mg (0.86 mmol) abs. DMSO in 2 ml abs. dichloromethane was added. Finally, 50 mg (0.36 mmol) **13** in 4 ml abs. dichloromethane were added dropwise over a period of 30 minutes. After 1 h of stirring at −78 °C 185 mg (1.80 mmol) triethylamine were added and the mixture was allowed to warm up to room temperature. The reaction mixture is hydrolyzed with 25 ml water. The biphasic

system is separated, and the aqueous layer is extracted three times with 25 ml dichloromethane. The combined organic layers are washed with 50 ml 0.5 M HCl and 50 ml water. After drying over $MgSO_4$, the solvent was removed. Purification by flash column chromatography (hexane/acetone 8:2) gave 24 mg (48 %) **15**. ^{1}H NMR ($CDCl_3$, 400 MHz) δ (ppm): 1.23-1.39 (4H, m, CH_2), 1.62-1.80 (4H, m, CH_2) 5.30 (1H, br s, CH), 10.69 (1H, s, CHO). ^{13}C NMR ($CDCl_3$, 100 MHz) δ (ppm): 20.7 (t, CH_2), 22.1 (t, CH_2) ,62.7 (d, CH), 73.7 (s, C_q), 203.7 (d, CHO).

1.4.2 Nano-TRF Assays

Stock solutions of the enzymes were prepared in the medium required to stabilize the enzyme and to avoid (in the case of proteases) self-digestion. In the case of solid enzyme preparations, an approximate amount of solid was weighed on a micro balance in aluminum boats. In the case of suspensions, the enzyme preparation was vortexed to homogeneity and the desired aliquot was immediately withdrawn by an Eppendorf pipette or a Hamilton syringe (for vials sealed with rubber stoppers). Trypsin and chymotrypsin were prepared in 1 mM HCl, carboxypeptidase A was prepared in 10 % LiCl. Acid phosphatase was prepared in reagent grade water and alkaline phosphatase in 0.1 M Tris-HCl, pH 8.5. Stability of the stock solutions was confirmed over 24 hours.

Leucine aminopeptidase was activated for 2 hours at 37 °C in 2 mM $MnCl_2$ and 0.05 M Tris (adjusted with HCl to pH 8.5) before use and was used for the respective day. Pepsin was always freshly prepared in the assay buffer. The concentrations of the enzyme stock solutions were determined by UV spectroscopy using the following extinction coefficients: ε_{278} = 64200 $M^{-1}cm^{-1}$ for carboxypeptidase A,[20] ε_{280} = 33600 for trypsin,[160] ε_{280} = 50000 for chymotrypsin,[161] ε_{280} = 50700 for pepsin,[162] and ε_{282} = 320000 for leucine aminopeptidase,[163] ε_{278} = 1.26 $mg^{-1}cm^{-1}ml$ for acid phosphatase and ε_{278} = 0.72 $mg^{-1}cm^{-1}ml$ for alkaline phosphatase.[164]

Stock solutions of the peptides were prepared at 1 mM in deionized water, which allowed their use for assays of several different enzymes by subsequent dilution in the respective buffer. The stock solutions were kept at +4 °C; no decomposition was observed over a period of up to six months. The

concentrations of the peptides were determined by assuming the same extinction coefficients as for the free amino acids Trp,[149] Tyr,[165] and pTyr.[166] The assays were conducted in the following buffers: Acid phosphatase in 0.15 M NaOAc (pH 5.0), alkaline phosphatase in 0.13 M glycine, 8.3 mM $MgCl_2$ (pH 8.8), chymotrypsin in 67 mM phosphate buffer (pH 7.0), trypsin in a 112 mM borate buffer (pH 8.0), pepsin in a 30 mM citrate buffer (pH 2.0), carboxypeptidase A in 1 M NaCl, 0.05 M Tris-HCl (pH 7.5), and leucine aminopeptidase in 0.05 M Tris-HCl (pH 7.8).

Steady-State and Time-Resolved Measurements in Cuvettes

A typical series of steady-state and time-resolved measurements were as follows: The enzyme and peptide stock solutions were prepared, following determination of the concentrations by UV. Then the required volumes of all stock solutions were calculated to afford the final concentrations in 500 µl total assay volume. The enzyme was diluted to have a 10fold higher concentration than required in the assay, so that 50 µl of enzyme solution must be added to 450 µl of substrate mixture.

The buffer required to yield the final volume was pipetted into semi-micro quartz glass cuvettes, and the background fluorescence intensity was determined. After addition of the peptide substrate, the fluorescence lifetime was determined by single-photon counting and the cuvette was placed into the steady-state fluorometer for the assay. After temperature equilibration the fluorescence intensity was recorded and the enzyme was added by rapidly taking out the cuvette, adding the enzyme and putting the cuvette back.

After reaching the final fluorescence intensity, the fluorometer was stopped and the fluorescence lifetime was again determined on the single-photon counting setup. After washing the cuvette with water, SODOSIL® RM 02 (detergent from Riedel de Haën, Seelze, Germany), water, and acetone, the cuvette was dried in water jet vacuum.

Nano-TRF Measurements in Microplates

Enzyme and peptide stock solutions were prepared and the concentrations were determined by UV spectroscopy. The required volumes of all stock solutions were calculated to afford the final concentrations in 50 µl total assay volume. The enzyme was diluted to have a 10fold higher concentration than required in the assay, so that 5 µl of enzyme solution must be added to 45 µl of substrate mixture. The substrate solutions were prepared in Eppendorf tubes, vortexed, and then transferred to the microplate to ensure efficient mixing.

Care was taken to also measure sufficient control wells, i.e. blanks containing only buffer to determine the background, wells with only enzyme to correct for potential fluorescent impurities, wells with only substrate to correct for potential time-dependent changes in the laser and to confirm the stability of the fluorescent probe. In the case of required additives (e.g. ATP for kinases or cucurbituril as inhibitors), they were also independently measured with buffer only, enzyme only and substrate only. All measurements were performed in triplicates.

After preparing the microplate with the substrate mixtures and control wells, the plate was measured once to exclude the possibility of mistakes during pipetting, e.g. the obtained fluorescence intensity was checked to be linearly dependent on the substrate concentration for measurements with different substrate concentrations. The enzyme was then added to the microplate by a programmable electronic Eppendorf pipette (5-100 µl). The "Dispensing"-program was used to minimize the required time, which allows aspiration of up to 100 µl and dispensing 20 times 5 µl into the microplate wells. Finally, the measurement of the microplate reader in the kinetic mode was initiated including a 5 s shake time to ensure mixing of substrate and enzyme.

1.4.3. Supramolecular Tandem Assays

The development of supramolecular tandem assays requires the choice of a macrocycle, the search for a suitable fluorescent dye and the determination of the binding constants of substrate and product, which involves several titrations before the actual assay performance can be tested. To obtain reliable binding

constants, it is essential to accurately know the concentrations of dyes and hosts. The dyes were used as received and the concentrations were either determined by weighing (Dapoxyl) or – if available – determined by published extinction coefficients (DBO derivatives). The purity of macrocycles was determined by NMR spectroscopy. The water content in *p*-sulfonatocalix[4]arene was accounted for by assuming 10% water content (as specified by the supplier). Two different fractions of cucurbit[7]uril were used throughout the thesis. The work on enzyme inhibition (Chapter 2.4) was carried out with a fraction containing 85 % cucurbit[7]uril as determined by NMR. The supramolecular tandem assays were carried out with a fraction containing cucurbit[7]uril in 98 % purity (NMR). The purity was corrected for and a water content of 13 water molecules per molecule of cucurbit[7]uril was assumed.

Titrations

Spectrophotometric titrations are most convenient, when the concentration of the dye is constant during the titration. It is therefore useful to titrate the macrocycle against the dye. In general, the titrations were carried out in 3.5 ml quartz glass cuvettes. The cuvette contained ca. 2 ml of the dye in an appropriate solvent or buffer. The titrant contained the same concentration of dye (which ensure a constant dye concentration during the titration even at higher host concentrations) and a host concentration, which is minimum 3 times higher than the concentration needed for complete (i.e. > 90%) complexation (see ref. [167] for a detailed discussion on choosing the right concentrations).

However, the initial points of the first titration were carried out with very low volumes of the titrant (e.g. 5 µl) to still obtain useful data although the binding constants were unexpectedly high. The host concentration $[H]_0$ for each titration point can be calculated by considering the actual volume in the cuvette V, the initial volume V_0, and the host concentration in the titrant $[H]_{\text{stock}}$ ($[H]_0 = [H]_{\text{stock}} V/V + V_0$). However, it was sometimes necessary to use larger volumes of the titrant, because of unexpectedly low binding constants. Then, the volume of the cuvette (already containing host with concentration $[H]_{\text{cuvette}}$) was reduced to V_{cuvette}. The concentration was then calculated according to:

$[H]_0 = ([H]_{\text{cuvette}} V_{\text{cuvette}} + [H]_{\text{stock}} V)/V_{\text{cuvette}} + V_0$. The competitive titrations were carried out in analogy to the host-guest titrations, i.e. to ensure a constant host and dye concentration during the titration, the titrant contained, besides the competitor, the host and dye (with concentrations equal the cuvette solution) and the competitor concentration in the titrant was adjusted to be minimum 3 times higher than the concentration needed for complete (i.e. > 90%) displacement of the dye from the host.

Enzyme Assays

Required for the assay are stock solutions of substrate, cucurbit[7]uril (CB7), dapoxyl, and enzyme. The stock solutions are prepared in 10 mM NH_4OAc buffer (pH 6.0); careful control of the pH was essential to obtain reliable and reproducible fluorescence intensities. The required volumes of all stock solutions were calculated to afford the final concentrations in 1 ml total assay volume. The 1 ml quartz glass cuvette containing the buffer was inserted into the fluorometer to allow temperature equilibration. Recording of the fluorescence intensity was started to obtain a value for the background fluorescence. Then, dapoxyl (final concentration 2.5 μM) was added and CB7 (final concentration 10 μM or 100 μM) was added. The increase in fluorescence intensity (to ca. 100 units for 10 μM CB7) was used as an independent control for accurate pH adjustment (instrument settings: λ_{exc} = 336 nm, λ_{em} = 380 nm, slit widths 5 nm, 345 nm cut-off filter in the emission beam). Finally, substrate and enzyme was added to the assay mixture, the order depending on the influence in fluorescence intensity; usually, the substance, which afforded the largest drop in fluorescence intensity, was added first. Then the cuvette was quickly taken out of the fluorometer, the second substance was added and the cuvette was inserted back into the fluorometer. After reaching the final fluorescence intensity, the fluorometer was stopped. Cleaning of the cuvette was as described for the Nano-TRF assays, except that washing with detergent was not necessary.

Alternatively, stock solutions of substrate, *p*-sulfonato-calix[4]arene (CX4), 1-aminomethyl 2,3-diazabicyclo[2.2.2]oct-2-ene (DBO-A), and enzyme can be used. The steps are the same as for the dapoxyl/CB7 assay with the

following modifications: 1) Slight variations of pH are not so detrimental for reproducible results, 2) CX4 was 200-400 µM and DBO-A was 100-400 µM, and 3) instrument settings were λ_{exc} = 365 nm, λ_{em} = 430 or 450 nm, slit widths: excitation 2.5-10 nm, emission: 10 nm.

1.4.4 Instrumentation

Time-resolved fluorescence spectroscopy was performed by time-correlated single photon counting (FLS920, Edinburgh Instruments) with a Picoquant picosecond pulsed diode laser as excitation source (λ_{exc} = 373 nm, fwhm ca. 50 ps). The lifetimes were recovered by tail-fitting or reconvolution with the instrument-specific software. The decay order was determined on the basis of reduced χ^2 around 1.0 and a random distribution of the weighted residuals around zero. Steady-state fluorescence spectroscopy was conducted with a Varian Eclipse spectrofluorometer. UV spectroscopy was performed on a Varian Cary 4000 or on a Varian Cary 50 spectrophotometer. Circular dichroism spectra were recorded on a Jasco J-810 spectropolarimeter. All spectrometers were equipped through feedback loops with circulating water baths and a temperatureprobe, which could be placed directly inside the cuvette to precisely maintain the desired temperature.

Nanosecond time-resolved assays were carried out in black 384-well microplates (Corning NBS) with an LF 402 NanoScan FI microplate reader (IOM, Berlin, Germany). An external nitrogen laser (MNL 200, Laser Technik Berlin, Germany) was coupled by to a dye laser module via glass fibers, which provided flexible adjustment of the excitation wavelength.

Photoreactions (also for photodecomposition quantum yield determinations) were carried out in a Luzchem LZC-4V photoreactor equipped with 14 Hitachi FL8BL-B UVA lamps ($\lambda_{max,em}$ = 350 nm). NMR-spectra were recorded on a JEOL JNM-ECX400 working at 400 MHz for ^{1}H and 100 MHz for ^{13}C measurements. pH measurements were performed with a WTW 330i pH meter equipped with a WTW SenTix Mic glass electrode. Conversion to pD values were performed by the method of Glasoe and Long.[168] Semi-empirical

computations were carried out by applying the AM1/UHF force field embedded within Hyperchem ver. 7.1 (Hypercube Inc., Gainesville, FL).

– CHAPTER 2 –
NANOSECOND TIME-RESOLVED FLUORESCENCE ASSAYS

2. Nanosecond Time-Resolved Fluorescence Assays

2.1 Introduction

The idea behind the "Nanosecond Time-Resolved Fluorescence" (Nano-TRF) is based on the outstanding chemical and photophysical properties of 2,3-diazabicyclo[2.2.2]oct-2-ene (DBO, **5**) derivatives. In particular, three properties are relevant in this regard: (i) DBO derivatives generally show an extremely long-lived fluorescence,[169,170] although a few exceptions have been reported,[159,171,172] (ii) the fluorescence of DBO is quenched by uncommon mechanisms, i.e. aborted electron and hydrogen atom transfer,[173,174] and (iii) DBO derivatives are small and hydrophilic probes in contrast to common large aromatic fluorescent dyes.

Combination of these properties afforded single-labeled protease and kinase assays, which are suitable for time-resolved fluorescence detection, an enhanced Nano-TRF assay by supramolecular complexation, as well as a supramolecular Nano-TRF sensor as demonstrated in the following. For the peptide substrates the DBO-labeled asparagine (Dbo, **21**) was introduced by solid phase synthesis using the Fmoc-derivative **18**. For the supramolecular Nano-TRF sensor, 1-aminomethyl 2,3-diazabicyclo[2.2.2]oct-2-ene (DBO-A, **16**) was used.

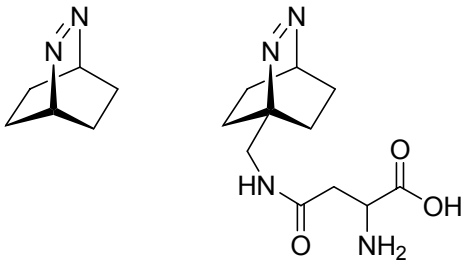

5
DBO

21
Dbo

2.2 Protease Assays

Corresponds to:

Appendix 4.1. A. Hennig, D. Roth, T. Enderle, W. M. Nau, Nanosecond Time-Resolved Fluorescence Protease Assays, *ChemBioChem* **2006**, *7*, 733-737.

Appendix 4.2. A. Hennig, M. Florea, D. Roth, T. Enderle, W. M. Nau, Design of Peptide Substrates for Nanosecond Time-Resolved Fluorescence Assays of Proteases: 2,3-Diazabicyclo[2.2.2]oct-2-ene as a Noninvasive Fluorophore, *Anal. Biochem.* **2007**, *360*, 255-265.

We first employed DBO for the construction of novel protease assays.[175,176] It was known from previous work[149] that DBO is efficiently quenched by the natural amino acids tryptophan and tyrosine and that the incorporation of DBO into peptides is feasible by the DBO-labeled asparagine derivative **18**. From the viewpoint of substrate synthesis this is very appealing, because the labeling is carried out directly during solid-phase peptide synthesis without any post-column modifications. In addition, the necessity to introduce an extrinsic quencher is remedied.

The proof of principle was carried out with carboxypeptidase A (CPA).[175] CPA is a member of the family of exopeptidases, i.e. a protease, which removes the *C*-terminal or *N*-terminal amino acid. Note that the investigation of such an enzyme is not possible with the more common double-labeling approach, in which an unnatural fluorescent dye would directly occupy the recognition site of the enzyme. CPA requires an aromatic *C*-terminal residue for maximal activity and we have consequently chosen tryptophan, because it is the most efficient quencher. It could be conclusively demonstrated by comparison to previously published data, that our probe has clear-cut different influence on the enzymatic activity than common aromatic probes, which might be very helpful in future mutation studies. These findings were further corroborated by applying the new assay to trypsin, chymotrypsin, pepsin, and leucine aminopeptidase (the latter one is another exopeptidase).[176]

Most importantly, the exceedingly long unquenched fluorescence lifetime of DBO derivatives allowed the use of time-gated fluorescence detection as introduced in Chapter 1.2.3.2. This technique has become popular with lanthanide chelates which have decay times in the range of milliseconds, and is known as time-resolved fluorescence (TRF) detection in the context of enzyme assays. In contrast, DBO has lifetimes which are <1 µs and we have consequently coined the term nanosecond time-resolved fluorescence (Nano-TRF) for this technique.[175] The advantages of a long unquenched fluorescence lifetime can be seen from Figure 2.1.

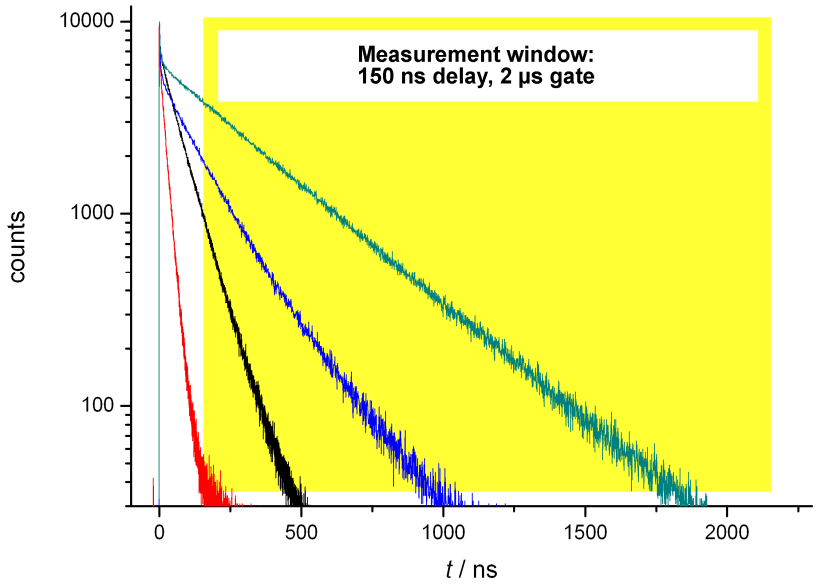

Figure 2.1. Nanosecond time-resolved fluorescence detection demonstrated with the fluorescence lifetimes for different peptides (X = Dbo): H-WTLTGKX-NH_2 (27 ns, red), H-WQIFVKX-NH_2 (90 ns, black), H-YQIFVKX-NH_2 (172 ns, blue), and H-X-NH_2 (355 ns, green), the last one being the common cleavage product by trypsin. Note the yellow time window which reflects the standard integration window employed for Nano-TRF detection.

The small peak at $t \approx 0$ ns refers to background fluorescence, which can be conveniently suppressed by detecting the fluorescence only in the yellow time-window. This efficiently reduces any interfering background fluorescence and

thus increases the sensitivity of the assay. This was demonstrated by creating an up to 500-times stronger artificial background fluorescence (by addition of 7-amino-4-methylcoumarin), in which the activity of the enzyme could still be conveniently detected.[175] In addition, it is also possible to increase the differentiation between substrate and product. Consider for this the red (substrate) and the green (product) lifetime trace in Figure 2.1. When applying the time-gate as depicted in Figure 2.1 it is apparent that also the substrate fluorescence is suppressed by Nano-TRF detection. By carefully adjusting the position of the time-gate, for example to 500 ns it is also possible to suppress the fluorescence of the black trace and so on. By this method it was possible to enhance the differentiation of substrate and product from 1.8times in the steady-state mode to ca. 14times in Nano-TRF mode.[176] This can also be seen from Figure 2.2, which compares the steady-state and Nano-TRF kinetic traces.

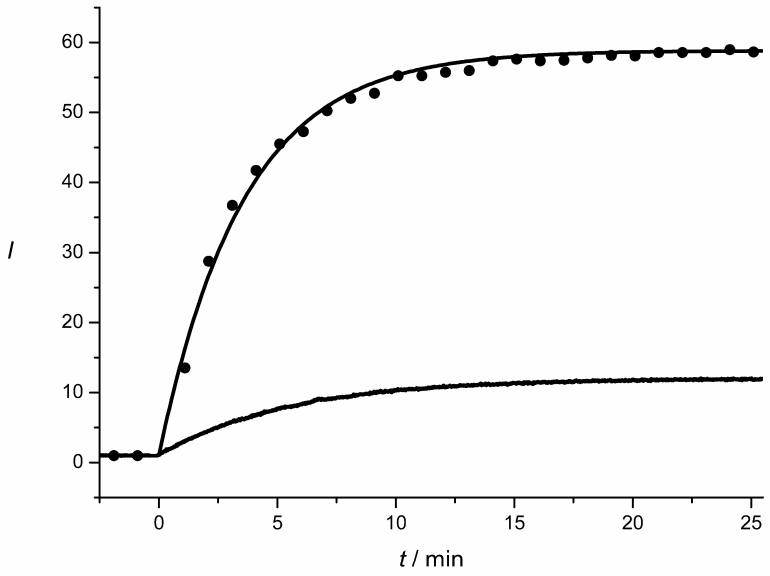

Figure 2.2. Comparison of the fluorescence increase (initial intensity was normalized to 1) of H-WTLTGKX-NH_2 (20 μM) upon digestion with 300 nM trypsin at pH 8. The lower trace was recorded in steady state mode and the upper one in Nano-TRF mode ($_{delay}$ = 150 ns, $_{gate}$ = 2 μs).

2.3 Tyrosine Phosphorylation Assays (Kinases and Phosphatases)

Corresponds to

Appendix 4.3. H. Sahoo, A. Hennig, M. Florea, D. Roth, T. Enderle, W. M. Nau, Single-Label Kinase and Phosphatase Assays for Tyrosine Phosphorylation Using Nanosecond Time-Resolved Fluorescence Detection, *J. Am. Chem. Soc.* **2007**, *51*, 15927-15934.

After establishing the spectroscopic method and the desirable biochemical compatibility of Dbo, we tackled the design of a new kinase and phosphatase assay. Kinases and phosphatases catalyze the phosphorylation and dephosphorylation of tyrosine residues in proteins, which is one of the most important regulatory mechanisms of biological signal transduction. The aberrant function of these enzymes plays therefore a vital role in numerous diseases, like pathogenic infections[177] or cancer,[178,179] and assays, which are suitable for HTS, have long been sought for.[180-184]

Scheme 2.1. Principle of a single-labeled kinase and phosphatase assay based on aborted hydrogen atom transfer from the phenolic O–H group of tyrosine.

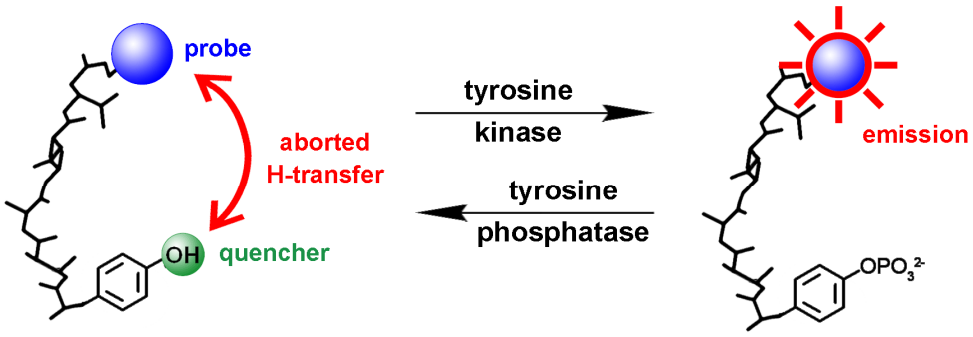

The susceptibility of Dbo towards quenching by phenolic O–H groups offers the possibility to apply the aforementioned (see Chapter 2.2) single-labeling approach also to the design of a kinase and phosphatase assay. Phosphorylation by a kinase transforms the good hydrogen atom donor (phenolic O–H group), which

provides efficient quenching, into the phosphate group, which is not capable of quenching the Dbo fluorescence. Thus, an increase in fluorescence intensity results upon phosphorylation (Scheme 2.1). Conversely, this principle is applicable to assay the activity of tyrosine phosphatases, which catalyze the reverse reaction.

Regarding simplicity, this novel assay principle represents a new benchmark, which is only comparable to a very recently introduced assay by Lawrence and co-workers,[184] who exploited the differential propensity of tyrosine and phosphotyrosine to form non-fluorescent ground-state complexes with pyrene. However, the latter strategy takes its toll that a large aromatic and hydrophobic probe needs to be introduced in close proximity to the enzyme recognition site, which often tampers with reliable determinations of enzyme kinetics in mutation studies or may even lead to a loss of enzyme activity against such a substrate.[185,186]

We selected two kinases (src kinase[187,188] and EGFR kinase[188-190]) and two phosphatases (alkaline and acid phosphatase) to demonstrate the working principle in Scheme 2.1 and investigated in total nine different peptides in combination with these enzymes. The extraction of the kinetic parameters (catalytic turnover number k_{cat} and Michaelis-Menten constant K_M) for three substrates of src kinase was demonstrated and the inhibition of acid phosphatase and alkaline phosphatase by sodium molybdate was determined.

Besides the biocompatibility, the possibility to use Nano-TRF detection is the most appealing asset of the Dbo-based assay, which is made feasible by the exceedingly long fluorescence lifetime of the fluorescent probe Dbo. Nano-TRF detection can be conveniently applied to suppress background fluorescence and to increase the differentiation of substrate and product.[175,176] This has been elaborated for the protease assay, and could be successfully transferred to the phosphorylation assay (Figure 2.3). In addition to Nano-TRF detection, a further enhancement in the substrate-product differentiation could be demonstrated by adding a base (for example in a stopped assay) to increase the pH to 12 or by working in D_2O instead of H_2O. The former decreases the fluorescence lifetime of the unphosphorylated peptide by switching from a hydrogen atom abstraction to

an exciplex-induced quenching mechanism,[173] while the latter increases the fluorescence lifetime of the phosphorylated peptide by a less efficient solvent-induced quenching (see inset of Figure 2.3).[191] In summary, the application of Nano-TRF, addition of base, and the use of D_2O increased the differentiation of substrate and product from 2.8 in a steady-state assay to 18.4 for the same substrate.

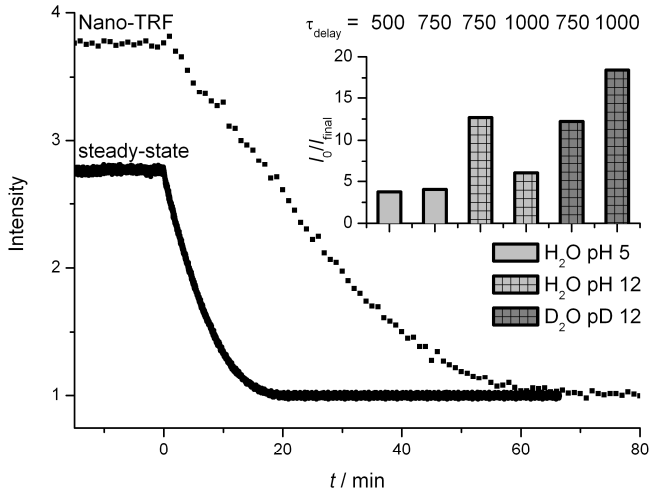

Figure 2.3. Optimization of a phosphatase assay by Nano-TRF detection. For the experiments H-Dbo-EEEEpY-OH has been dephosphorylated by acid phosphatase at pH 5. The steady-state trace refers to 30 µM peptide and 100 µg/ml acid phosphatase. The continuous Nano-TRF trace was recorded with 10 µM peptide and 20 µg/ml phosphatase (t_{delay} = 500 ns, t_{gate} = 2 µs). The final intensity of the traces was normalized to demonstrate the better differentiation in the Nano-TRF mode. The inset demonstrates the further possibility to enhance the substrate/product-differentiation by adding a base (which increases the pH to 12) or by using D_2O (see text) in a Nano-TRF measurement (all measurements in the inset were recorded with 10 µM of peptide).

2.4 Interaction of Cucurbit[7]uril with Protease Substrates: Drug Delivery Systems and Improved Background Suppression in Nano-TRF Assays

Corresponds to

Appendix 4.4. A. Hennig, G. Ghale, W. M. Nau, Effects of Cucurbit[7]uril on Enzyme Activity, *Chem. Comm.* **2007**, 1614-1616.

Appendix 4.5. A. Hennig, D. Roth, T. Enderle, W. M. Nau, Interaction of Cucurbit[7]uril with Protease Substrates: Application to Nanosecond Time-Resolved Fluorescence Assays, *in preparation*.

The motivation for this project were the beneficial effects of cucurbit[7]uril (CB7) on the fluorescence properties of DBO, which had been previously reported.[119,124,125,192] The extremely low polarizability of the inner CB7 cavity[119] affords a reduced radiative decay rate and thus a prolonged (unquenched) fluorescence lifetime,[125,126] which is desirable for TRF assays.[124] In addition, CB7 acts as an efficient "protection shield" against contact-based quenching,[192] which should increase the stability and reliability of an assay; for example, library compounds, which quench the fluorescent probe, will be immediately identified as false hits in the presence of CB7.

First, it was necessary to find a new quencher for Dbo, which is not based on a contact-based quenching mechanism. Most prominently, FRET fulfills this requirement and we have chosen for 3-nitrotyrosine as a FRET quencher. The spectral properties for this system were determined in a wide pH range, which suggested its excellent performance for 10-mer peptides at pH > 6. Additionally, the system has been characterized in view of the effects of donor-acceptor diffusion during the long fluorescence lifetime, which must not be neglected for the microsecond time range.[193-196]

Trypsin and chymotrypsin were chosen as model enzymes and a model peptide has been designed, which suited the recognition motifs of both enzymes. Preliminary experiments in absence of CB7 were promising and afforded a very high increase in fluorescence upon proteolytic digestion. However, it was further

necessary to ascertain the binding properties with CB7 to enable a rational design of further CB7-enhanced fluorescence assays.

UV spectroscopy and fluorescence spectroscopy were employed to determine the binding sites of CB7 to the peptide and the binding constants for each site. In addition, enzyme inhibition experiments revealed information about the affinity to the recognition site. In summary, a comprehensive binding model (Scheme 2.2) was derived. At low CB7 concentration, the substrate is selectively complexed at the *C*-terminal Dbo residue with a binding constant K_1. However, the upper rim is still void, such that the complexation of small cationic residues can still take place. Intramolecular host-guest complexation with the arginine side chain thus follows in the second step with a binding constant K_2, which also provides an efficient masking of the arginine side chain against enzymatic cleavage by trypsin (*vide infra*). Finally, at high CB7 concentrations the 3-nitrotyrosine residue is also complexed with a binding constant K_3.

This binding model is mechanistically a very interesting finding, since it has never been described before. It may form the basis for cucurbiturils as potential stabilizers of peptide-based drugs with cationic side chains and thus provides a complementary application to cyclodextrins, which have been used as stabilizing agents for drugs with hydrophobic residues.[65,197-201] Consequently, the possibility to stabilize peptides by complexation with cucurbituril has been demonstrated with six further model substrates for chymotrypsin, trypsin, and leucine aminopeptidase.[202] This study revealed that cucurbituril has indeed a significant potential as a drug stabilizing additive, which provides under certain circumstances an even more efficient stabilization than cyclodextrins.

The results regarding the desired application, i.e. an enhancement in Nano-TRF assays, were mixed. The inhibition of trypsin, which has been used to elucidate the binding model proposed in Scheme 2.2, precludes continuous measurements of this enzyme. On the other hand, a stopped assay is still feasible, and CB7 might be useful in this regard as the stopping reagent. Chymotrypsin, which was not inhibited by CB7, could still be measured. In this case, a lifetime enhancement was in fact observed. Owing to the reduced steady-state fluorescence intensity of the Dbo-CB7 complex, it turned out that the application

of CB7 in Nano-TRF assays is most useful for measuring with long delay times (> 200 ns). This is useful for enhancing the substrate-product differentiation of peptides, which show otherwise a poor increase in fluorescence upon proteolytic cleavage. However, the improved robustness of the assay against contact-based quenchers still persists.

Scheme 2.2. Proposed interactions between CB7 and the protease substrate H-(NO_2)Tyr-Gly-Ser-Gly-Phe-Arg-Gly-Dbo-NH_2. The complexation of the substrate by CB7 proceeds in three steps. After complexation of the *C*-terminal Dbo residue, an intramolecular complex formation follows, which complexes the arginine side chain and provides an efficient inhibition against cleavage by trypsin. At high concentrations of CB7 the *N*-terminal 3-nitrotyrosine residue is also complexed.

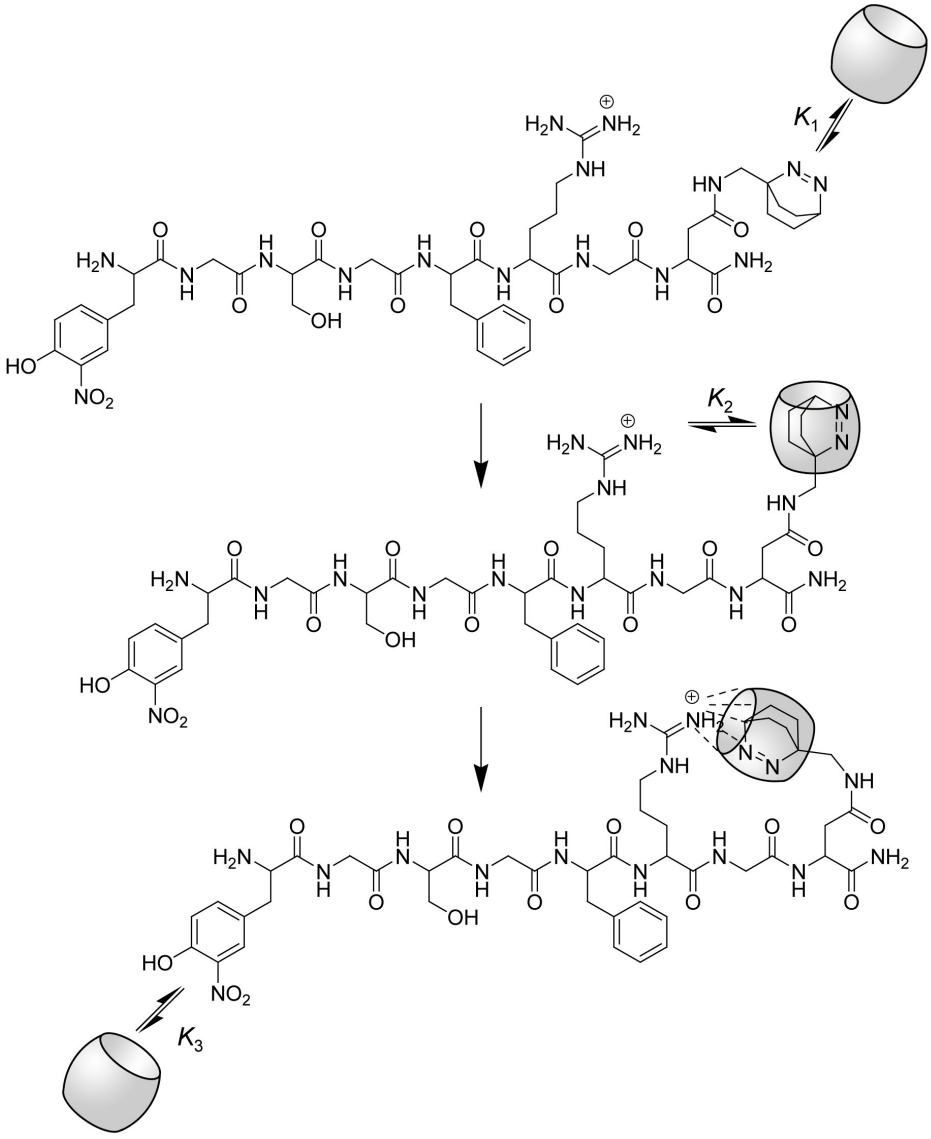

2.5 A Supramolecular Nanosecond Time-Resolved Fluorescence Sensor System for the Detection of Biogenic Amines

On-going Project: A. Hennig, H. Bakirci, W. M. Nau.

The binding of the parent DBO towards *p*-sulfonato-calix[4]arene (CX4) has been recently introduced as an appealing supramolecular sensor system for multivalent cations[93] and neurotransmitters.[89] Similarly, DBO-A (**16**) is even more strongly bound by CX4 owing to the additional Coulomb interaction between the positively charged ammonium group (at pH < 9.5) and the negatively charged sulfonato groups of CX4. This allows lowering the detection limit of the sensor system, because the complex of the sensor system is already formed at much lower concentrations.[203] Consequently, the latter DBO-A/CX4-system has been applied for the subsequent studies.

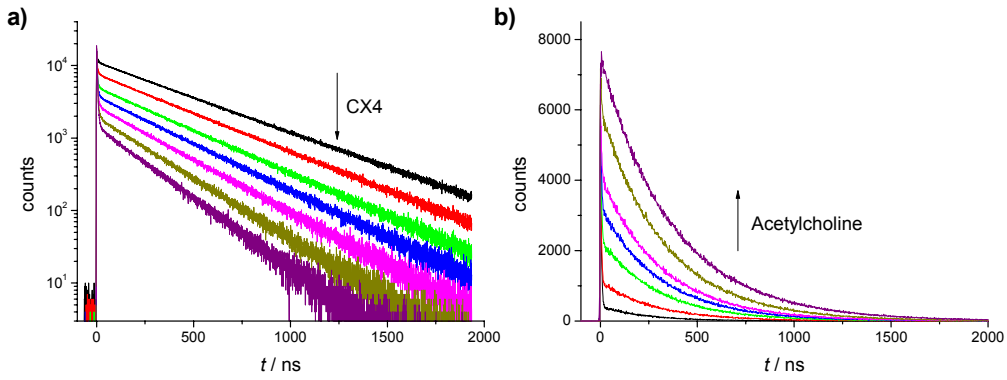

Figure 2.4. a) Fluorescence lifetime traces for a DBO-A/CX4 titration. b) Fluorescence lifetime traces for a competitive titration of acetylcholine with the DBO-A/CX4 reporter system. The traces were obtained by TCSPC. Note the logarithmic scale in a).

The binding of DBO-A by CX4 is accompanied by a strong fluorescence quenching and addition of an analyte leads to a regeneration of the fluorescence owing to the displacement principle (see Chapter 1.3.2.2). More interesting, addition of CX4 to a DBO-A solution changes the fluorescence decay trace from a single-exponential decay to a biexponential decay with a long-lived and a much

shorter-lived component. The two lifetime components are assigned to the free DBO-A and the DBO-A/CX4-complex, respectively (see Figure 2.4a). Addition of a competitor (for example acetylcholine) leads to a step-by-step regeneration of the long-lived lifetime component (see Figure 2.4b), which verifies this conjecture. Therefore, this sensor system should be suitable for Nano-TRF monitoring and background suppression (compare Figure 2.1) as has been previously demonstrated in the context of protease assays.[175]

The cation receptor properties of CX4 suggest its use for sensing cationic analytes. In this report, biogenic amines (i.e. amines derived from decarboxylation of naturally occurring amino acids) have been chosen due to their importance in cell maturation,[204] cancer,[205] signal transduction,[206] and in food analysis.[207] As could be demonstrated the sensor system is very selective for the amines and the respective amino acids do not interfere. This enables the detection of these amines in complex media by Nano-TRF, in which otherwise a high background fluorescence might interfere.

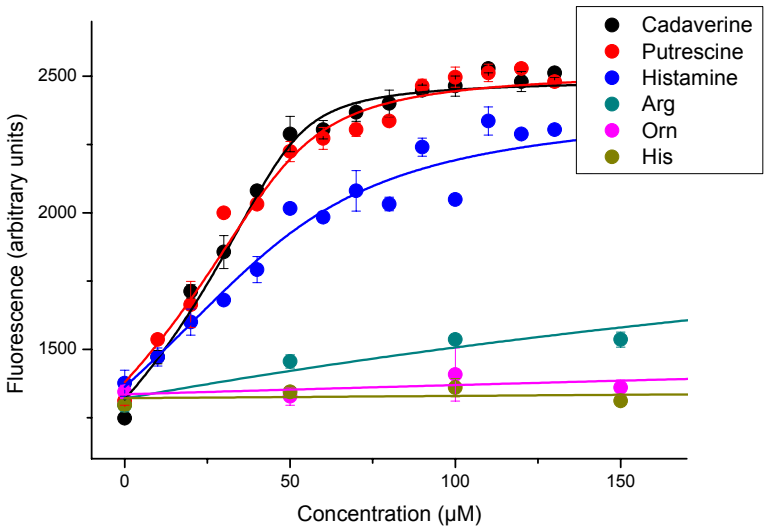

Figure 2.5. Representative competitive titrations of cadaverine, putrescine, and histamine. Addittional titrations of Arg, Orn and His demonstrate that amino acids do not interfere with the sensing of the amines. The solid lines are derived from a fitting according to a competitive binding model.

– CHAPTER 3 –
SUPRAMOLECULAR TANDEM ASSAYS

3. Supramolecular Tandem Assays

Corresponds to

Appendix 4.6. A. Hennig, H. Bakirci, W. M. Nau, Label-Free Continuous Enzyme Assays with Macrocycle-Fluorescent Dye Complexes, *Nature Methods*, **2007**, *4*, 629-632.

and **Appendix 4.7.** A. Hennig, W. M. Nau, Determination of Arginase Inhibition by a Substrate-Coupled Supramolecular Tandem Assay, *in preparation*.

and **Appendix 4.8.** A. Hennig, T. Schwarzlose, W. M. Nau, Bridgehead Carboxy-Substituted 2,3-Diazabicyclo[2.2.2]oct-2-enes: Synthesis, Fluorescent Properties and Host-Guest Complexation Behavior, *Arkivoc*, **2007**, *8*, 341-357.

3.1 Introduction

The previous chapter had been devoted to the development of a new spectroscopic method for assaying enzymatic activity. This chapter now deals with a new analytical technique, which for the first time uses macrocyclic hosts for assaying the activity of enzymes or more generally to follow chemical reactions. This novel method is fast, cheap, and features an unprecedented simplicity for assaying reactions, for which so far only time-consuming colorimetric assays or antibody-based methods have been used.

The method is based on the principle of displacement assays,[140,141] which has been briefly introduced in Chapter 1.3.2.2. It is now worth recalling that displacement assays are, in principle, an application of competitive binding titrations, which are ubiquitous in supramolecular chemistry literature.[86,87,89,93,108,140,141] To illustrate, an arbitrary titration is shown in Figure 3.1. In the exemplified case, the fluorescent dye is quenched upon inclusion into the macrocyclic cavity (Figure 3.1a, part 1); an analyte, which is added to the mixture, replaces the fluorescent dye from the cavity, whereupon the fluorescence

of the free dye is regenerated (Figure 3.1a, part 2). The step-by-step addition of increasing amounts of analyte affords binding isotherms as shown in Figure 3.1b, from which binding constants can be determined.

Most often, such binding titrations have been used to demonstrate certain selectivity for an analyte, although it still remains a major challenge to devise receptors with high selectivity for specific analytes. As an alternative Anslyn and co-workers have introduced the concept of differential receptor arrays.[142,143,208] Therein, a combination of different receptors and dyes is exposed to the analyte. By using a neural network statistical analysis, it is sufficient that the receptors of the array respond with a different magnitude to the desired analytes, such that a specific analyte creates an indicative signal pattern with several receptors.

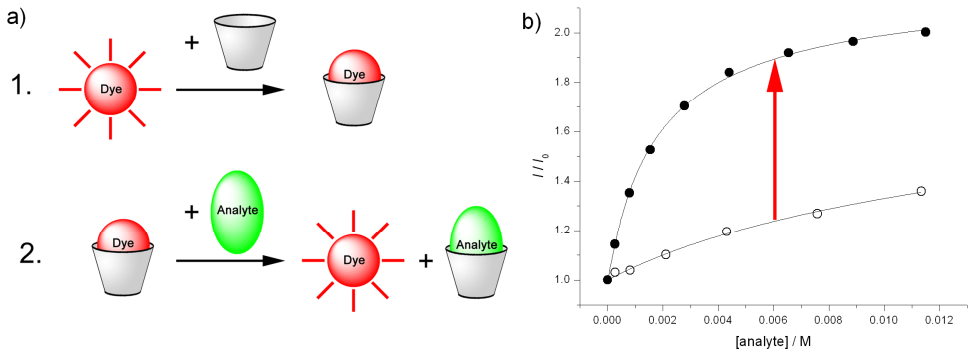

Figure 3.1. Fluorescence regeneration method for determining binding constants of analytes to macrocyclic hosts. a) For sensing purposes, the macrocycle-dye complex is formed. In presence of an analyte the dye is replaced from the macrocyclic cavity and the fluorescence is regenerated. b) Example of a competitive binding titration with two different analytes. One can expect an increase in fluorescence upon enzymatic transformation, assuming that the analyte, which has a higher propensity for binding with the macrocyclic receptor (solid circles), is the product and that the analyte with a lower propensity for binding (open circles) is the substrate.

Our idea was instead to exploit the differential binding of the substrate and the product of an enzymatic reaction to the macrocyclic receptor. In this way it was possible to apply the principle of displacement assays to the area of enzyme assays for the first time. To illustrate, assume that the lower binding isotherm Figure 3.1b represents the substrate and the upper binding isotherm the product of

an enzymatic reaction. In this case, addition of an enzyme transforms a weak competitor into a strong competitor, such that the fluorescence intensity changes during the reaction as indicated by the red arrow. In principle (*vide infra*), the reverse reaction, i.e. when a strong competitor is transformed to a weak competitor (reverse the red arrow in Figure 3.1b), can also be monitored by this method.

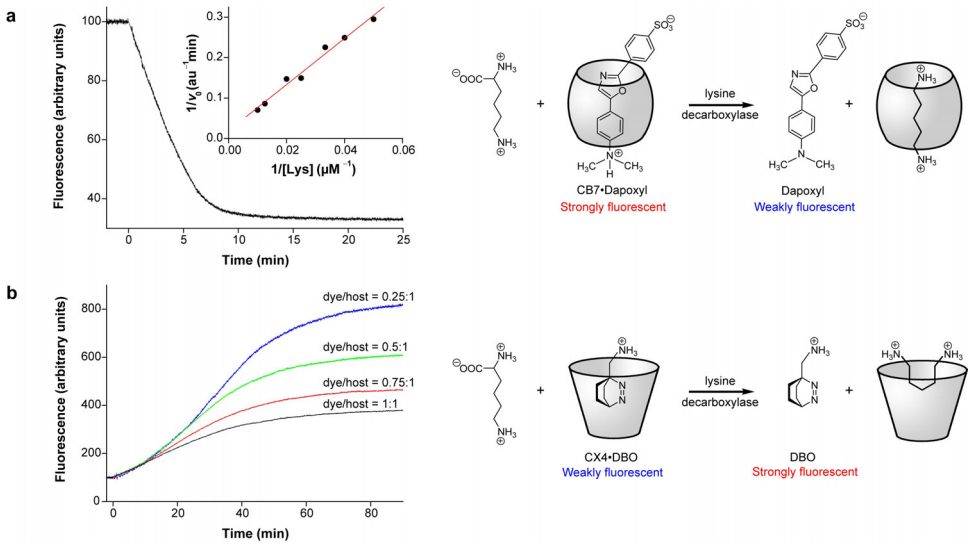

Figure 3.2. Continuous fluorescence enzyme assays for lysine decarboxylase (in 10 mM NH_4OAc buffer at pH 6.0) **a)** with the CB7/Dapoxyl macrocycle/dye pair (40 µg/ml enzyme, 100 µM lysine, 2.5 µM Dapoxyl, 10 µM CB7, λ_{exc} = 336 nm, λ_{em} = 380 nm) and **b)** with the CX4/DBO macrocycle/dye pair (500 µM lysine, 400 µM CX4, 0.4 mg/ml enzyme, and 100-400 µM DBO, λ_{exc} = 365 nm, λ_{em} = 450 nm). The inset in a) shows the Lineweaver-Burk plot obtained for varying substrate concentrations. The assay principles are shown on the right.

As a proof of principle we chose to investigate the enzyme class of amino acid decarboxylases, which remove the carboxyl group from amino acids. CB7 was chosen as a macrocyclic host for this system stimulated by the well-known preference of cucurbiturils to bind diamines.[107,110,209] Dapoxyl was used as the fluorescent dye, which was previously reported to afford an up to 200fold enhanced fluorescence upon CB7 complexation.[210] Determination of the binding constants of six selected amino acids (Lys, Arg, His, Orn, Tyr, Trp) and their respective decarboxylated products revealed in fact an excellent discrimination (expressed as the ratio of binding constants) in the range of 80 to 16500. This

assay afforded therefore a decrease in fluorescence upon enzymatic activity (Figure 3.2a). Owing to the excellent differentiation of substrate and product by CB7, it was even possible to approximately determine the enzyme kinetics by a Lineweaver-Burk plot.

However, an increase in fluorescence is generally more desirable such that DBO-A and *p*-sulfonato-calix[4]arene (CX4), which had been previously introduced as a displacement-based sensor for neurotransmitters and metal cations,[89,93] has been tested. DBO-A and CX4 seemed attractive for two reasons: First, CX4 carries four negatively charged sulfonato groups and can thus be considered as a cation receptor, which should afford a stronger binding with the doubly positively charged diamines than with the singly positively charged (net charge at relevant pH) amino acids, and second, DBO-A is quenched upon complexation by CX4. These combined properties provided the desired increase in fluorescence as expected (Figure 3.2b). However, the differential binding was not as pronounced as for the CB7/dapoxyl system (the ratio of binding constants ranges from 160 to 1240), which resulted in sigmoidal progress curves. Therefore, different macrocycle/dye ratios were probed, which afforded more common progress curves at higher dye concentrations, although the optimal increase in fluorescence intensity needed to be sacrificed.

3.2 Concept of Supramolecular Tandem Assays

These successful initial studies and the appearance of ubiquitous displacement sensors,[86,87,89,93,108,140,141] motivated us to develop this macrocyclic approach to enzyme assays into a more generalized concept. It can be seen from Figure 3.2 that depending on the photophysical properties of the fluorescent dye and the macrocycle, a decrease or an increase in fluorescence results such that accordingly the terms “OFF-assay” and “ON-assay” were coined. In addition, the reverse reaction can in principle also be monitored. In the former case (Figure 3.2), the product binds to the macrocycle; in the latter case (reversed reaction), the substrate binds to the macrocycle. In summary, four different types of assays result (Figure 3.3): a product-coupled ON-assay, a substrate-coupled ON-assay, a product-coupled OFF-assay, and a substrate-coupled ON-assay. The whole

concept has been termed supramolecular tandem assays to emphasize the interrelation of the supramolecular and biomolecular component of the assay system by several binding equilibria.

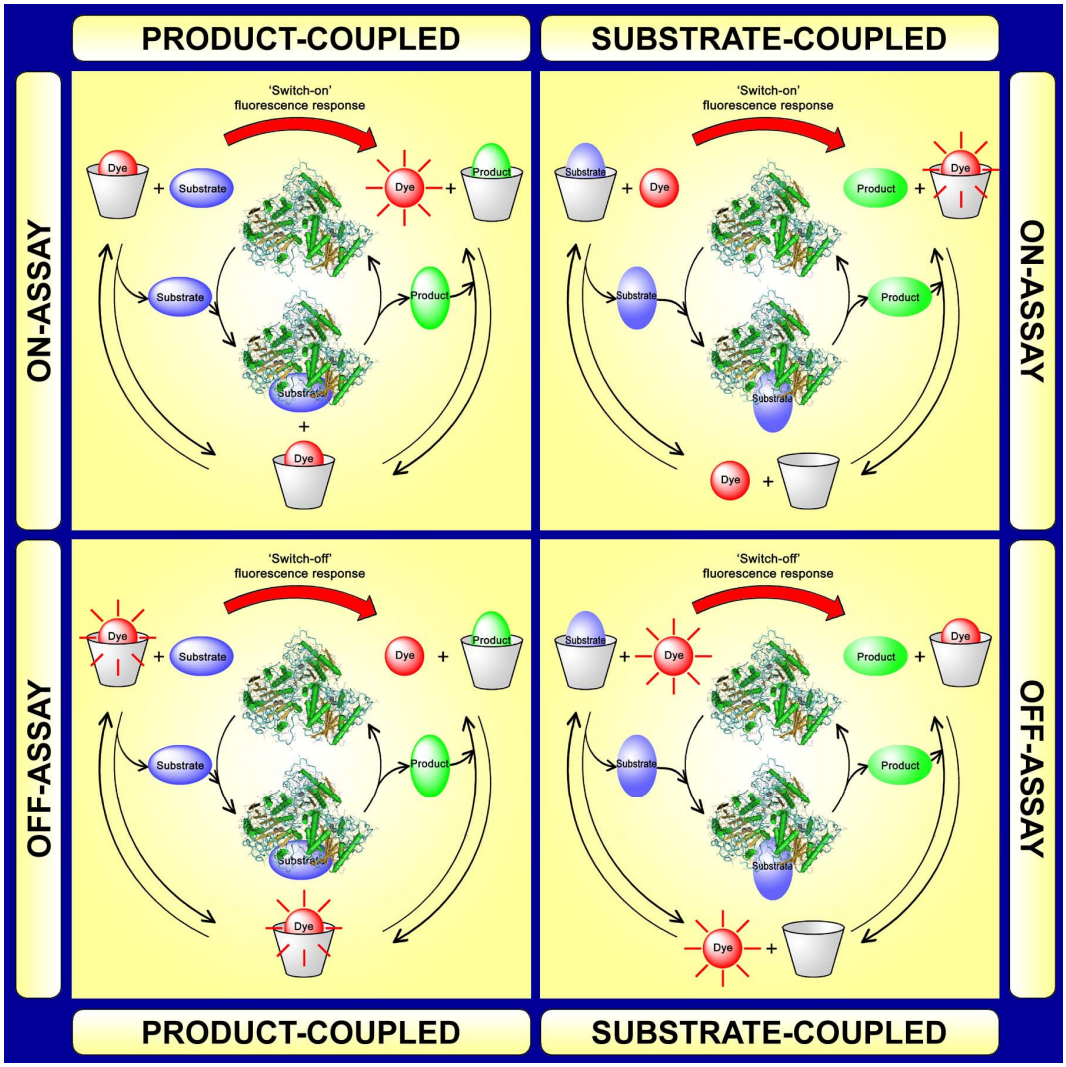

Figure 3.3. Concept for different types of supramolecular tandem assays. A product-coupled assay results, when the product is more strongly bound by the macrocycle than the substrate; conversely, a substrate-coupled assay results, when the macrocycle binds stronger with the substrate than with the product (left *versus* right column). Depending on the photophysical properties of the fluorescent dye-macrocycle combination, the fluorescence can be turned ON or OFF during the enzymatic transformation.

With the concept scheme (Figure 3.3) at hand it is worth considering some well-known fundamental principles of supramolecular chemistry in more detail.[211] First of all, there is a known charge selectivity of macrocyclic receptors, i.e. a

receptor carrying negatively charged groups will preferentially bind cations[93] and a receptor carrying positively charged groups will preferentially bind anions.[87,139] It can be concluded from numerous studies that any change in charge status of a guest results in a different propensity to bind with a complementary receptor, although care needs to be taken regarding the spatial alignment of the oppositely charged groups (*cf.* Chapter 3.4.1).[159] This has been demonstrated, for example, for metal cation binding by CX4,[93] tri- and diphosphate nucleotide binding to calixarenes,[87] cyclodextrins,[139] and cyclophanes[212] or peptide recognition by cucurbiturils.[110] This means that a cation receptor will bind dications more strongly than monocations or an uncharged molecule. Conversely, an anion receptor will bind dianions more strongly than monoanions or uncharged molecules. This principle can also be extended to ion-dipole interactions, which lead to the very strong binding of diamines and certain amino acid derivatives towards cucurbiturils.[107,110,202,209]

Another inherent principle in supramolecular chemistry is the size selectivity of macrocyclic receptors, which had already been reported as early as Pedersen's work on crown ethers.[42,43] Such a size selectivity has subsequently often been reported for other macrocyclic hosts, for example for complexation of azoalkanes by cucurbiturils,[117] bicyclic alkanes by cyclodextrins,[53] or quaternary ammonium cations by calixarenes[89] and cavitands.[213] It is important to note, that these two properties, namely size and charge, are key properties, which are changed by nearly any enzymatic reaction.[2]

From these two established concepts in supramolecular chemistry, i.e. the charge and size selectivity, it is possible to derive guidelines for the development of supramolecular tandem assays (Table 3.1). If a change in charge is involved during the enzymatic transformation, one should apply a macrocyclic receptor, which is complementary to the analyte (first four rows of Table 3.1), e.g. if a cationic charge is removed from the analyte (the product could either be still positively charged or could become uncharged) a cation receptor should be chosen. Of course, Table 3.1 can only provide a rough guide for choosing a macrocyclic receptor, and many more aspects of supramolecular chemistry need to be considered to afford efficient differentiation between substrate and product.

Table 3.1. Guidelines for the development of supramolecular tandem assays.[a]

substrate		product	suitable receptor	resulting assay[b]
⊕⊕	→	⊕	cation receptor[c]	substrate-coupled
⊕	→	⊕⊕	cation receptor[c]	product-coupled
⊖⊖	→	⊖	anion receptor[c]	substrate-coupled
⊖	→	⊖⊖	anion receptor[c]	product-coupled
⊕	→	⊕	large cation receptor small cation receptor	substrate-coupled product-coupled
⊖	→	⊖	large anion receptor small anion receptor	substrate-coupled product-coupled
◯	→	○	large anion receptor small anion receptor	product-coupled substrate-coupled
○	→	◯	large anion receptor small anion receptor	substrate-coupled product-coupled
R *S*	→ →	*S* *R*	chiral receptor	substrate/product-coupled assay

[a] Circles with a plus or minus sign indicate positively and negatively charged analytes. Two circles indicate a higher charge status of the analyte than in the corresponding substrate or product column. Large and small circles indicate the size of the analyte. [b] Relates to the nomenclature introduced in Figure 3.3. It solely depends on the photophysical properties of the macrocycle-dye combination whether an ON or an OFF-assay results. [c] In these cases the singly charged analytes could also be uncharged.

3.3 Assay Simulation and Optimization of Assay Parameters

3.3.1 Derivation of a Binding Scheme

Commonly, there is a proportional relation between the product concentration and the fluorescence intensity in fluorogenic enzyme assays, which simplifies data analysis. However, as it transpires from Figure 3.2b this is not the case in supramolecular tandem assays. In fact, the underlying binding equilibria afford quite often counterintuitive results, such that a more elaborate treatment by data simulation was initiated. As a starting point, Scheme 3.1 is introduced, which shows all relevant equilibria.

Scheme 3.1. Binding scheme for the equilibria involved during enzymatic transformation in a supramolecular tandem assay.

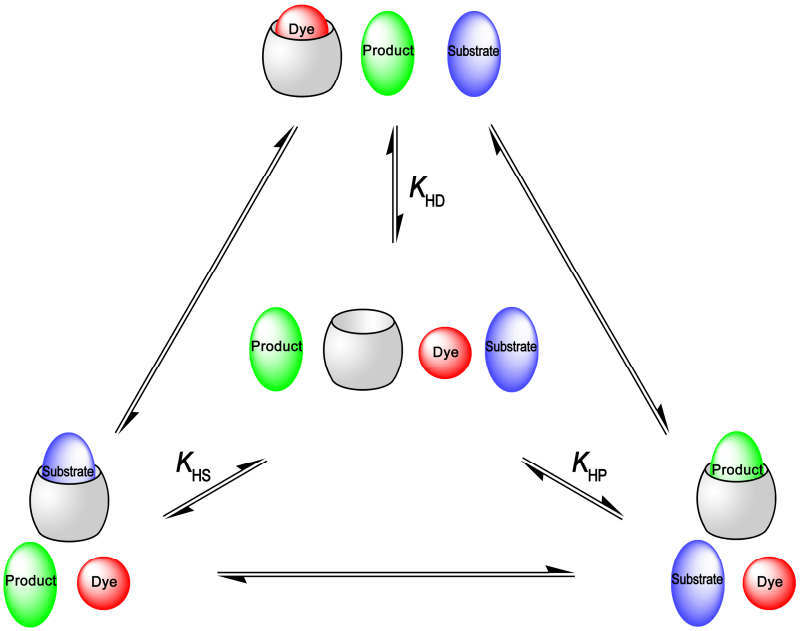

The system (so far neglecting biomolecular interactions) can be described by considering the concentrations of the free macrocyclic host $[H]$, fluorescent dye $[D]$, substrate $[S]$, and product $[P]$. Three binding equilibria, i.e. binding of the dye to the host (K_{HD}, top in Scheme 3.1) forming the host-dye complex $[HD]$, of the substrate to the host (K_{HS}, bottom left in Scheme 3.1) forming the host-substrate complex $[HS]$, and of the product to the host (K_{HP}, bottom right in Scheme 3.1) forming the host-product complex $[HP]$, suffice to comprehensively describe the system. Thus, three equations can be formulated (eqn (4)-(6)).

$$[HD] = K_{HD}[H][D] \tag{4}$$

$$[HS] = K_{HS}[H][S] \tag{5}$$

$$[HP] = K_{HP}[H][P] \tag{6}$$

The residual equilibria do not need to be considered, because they can be described by a thermodynamic cycle. Furthermore, the law of mass conservation requires that the concentration of the individual species sum up to the total concentrations of host $[H]_0$, dye $[D]_0$, substrate $[S]_0$, and product $[P]_0$, which leads to eqn (7)-(10).

$$[H]_o = [H] + [HD] + [HS] + [HP] \quad (7)$$

$$[D]_o = [D] + [HD] \quad (8)$$

$$[S]_o = [S] + [HS] \quad (9)$$

$$[P]_o = [P] + [HP] \quad (10)$$

Combining eqn 4-10 yields a system of seven interrelated non-linear equations, in which seven parameters are unknown (note that this requires the prior knowledge of binding constants from independent titrations). The system can thus be solved, which was achieved by the quasi-Newton-Raphson method as implemented in the MathWorks Matlab® 7.3 package. This provided the concentrations of all species involved under a given set of total host, dye, substrate, and product concentrations.

Finally, the enzymatic activity needs to be introduced to describe the conversion of substrate into product in a time-dependent manner. Generally, this can be achieved by numerically integrating the Michaelis-Menten equation (eq. 11) for each time step of the simulation, in which $[E]$ is the enzyme concentration, k_{cat} the catalytic turnover number, and K_M the Michaelis-Menten constant. $[S]'$ and $[P]'$ are the substrate and product concentration during an enzymatic reaction, so far assuming them to be independent of the equilibria involved in the supramolecular tandem cycle (*vide infra*).

$$\frac{d[P]'}{dt} = \frac{k_{cat}[E][S]'}{K_M + [S]'} \quad (11)$$

Alternatively, at low substrate concentrations ($[S]' << K_M$), eq. 11 simplifies to eq. 12, which can be solved analytically to yield eq. 13, in which k_{cat}/K_M reduces to the pseudo first-order rate constant k.

$$\frac{d[P]'}{dt} = k_{cat}/K_M [E][S]' \quad (12)$$

$$[P]' = [S]' - [S]' \exp(-k[E]t) \quad (13)$$

To arrive at the final simulated plots of fluorescence intensity I *versus* time, the molar fractions of the free dye x_D and the host-dye complex x_{HD} are contributing to the fluorescence intensity with its intrinsic fluorescence I_D and I_{HD} (eq. 14).

$$I = x_{HD} I_{HD} + x_D I_D = \frac{[HD]}{[D]_o} I_{HD} + \frac{[D]}{[D]_o} I_D \qquad (14)$$

3.3.2 Simulations with the CB7/dapoxyl System

3.3.2.1 Simulating the Experimental Decarboxylase Results

Initially, a comparison of experimental data from Figure 3.2a with simulated data was undertaken. It is instructive to compare the simulated fluorescence intensity data with the actual product concentration (Figure 3.4), which is available on the side from the same simulation. In contrast to common fluorogenic assays, in which the whole product progress curve is manifested in the intensity plot, this supramolecular tandem assay affords under the conditions specified in Figure 3.4 only the initial part of the progress curve. However, this suffices for the determination of the initial rate,[214] which is needed, for example, in the determination of the enzyme kinetic parameters[175] or for inhibition assays.[202]

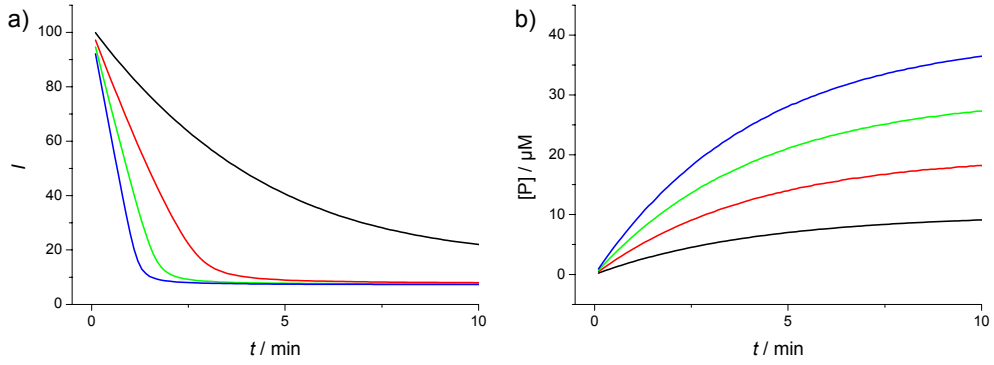

Figure 3.4. Comparison of the a) fluorescence intensity progress curves with the b) product concentration progress curves for a product-coupled OFF-assay. The data has been generated with the following parameters: $[H]_0$ = 10 µM, $[D]_0$ = 2.5 µM, K_D = 2.0 × 10^4 M^{-1}, K_S = 1000 M^{-1}, K_P = 1.4 × 10^7 M^{-1}, I_{HD} = 600, I_D = 7, $[S]_0$ = 10 (black), 20 (red), 30 (green), and 40 µM (blue), all of which have been obtained from the experimental results (CB7/dapoxyl system, substrate: lysine, and product: cadaverine). The enzyme kinetic parameters were arbitrarily chosen as K_M = 10 mM, k_{cat} = 8000 $M^{-1}min^{-1}$, and [*E*] = 300 nM.

CB7 is an excellent macrocyclic host for decarboxylase assays, because of the extremely high binding constants of diamines[107,209] (up to 1.4×10^7 M^{-1}) and the resulting excellent discrimination from the amino acid products. Although binding constants are generally much lower for macrocyclic complexes (in the range of 10^3 to 10^5 M^{-1}),[57,87,89,127,139] this presents no further limitation to apply supramolecular tandem assays since a differential binding rather than a very high absolute binding is required. In addition, these assays offer the opportunity to fine-tune the assay performance by several strategies as will be demonstrated in the following Chapters 3.3.2.2 to 3.3.3.2.

3.3.2.2 Simulation of a CB7/Dapoxyl Substrate-Coupled ON-Assay for Amine Oxidases

The decarboxylase-assay was a product-coupled assay, in which the substrate has a lower binding constant than the product. In particular, the amino acids had such a low affinity towards CB7 that the substrates could be considered as uncomplexed under the applied conditions. This rendered the assay design and the analysis straight-forward. However, the situation becomes much more complex in the case of a substrate-coupled assay, in which the substrate is complexed. For the simulation of a substrate-coupled assay, a reaction was considered, in which the substrate displays a much higher binding constant than the product. Amine oxidases, which transform an amine into the corresponding aldehyde,[215,216] represent a viable example for this simulation. The binding constants of the substrates (e.g. cadaverine, putrescine) are known, and it seems likely that the products have binding constants of <5000 M^{-1}, such that this value was chosen as an upper limit for the simulation.

The simulations revealed that substrate binding has two effects on the feasibility of such a substrate-coupled assay, which could be readily dissected by slight modifications in the simulations. First, consider the dashed curves in Figure 3.5, in which it has been assumed that substrate complexation has no effect on the enzymatic reaction, i.e. $[S]' = [S]_0$ (*cf.* eqn 9 and 11). The product concentration curves (Figure 3.5b) are unbiased as expected, but the fluorescence intensity curves (Figure 3.5a) show an initial lag phase. This is due to the excess substrate

($[S]_0 > [H]_0$), which is still capable of fully displacing the dye from the macrocyclic cavity, although the enzymatic reaction has already considerably progressed. Consequently, the fluorescence intensity does not change before the residual substrate concentration is smaller than the host concentration.

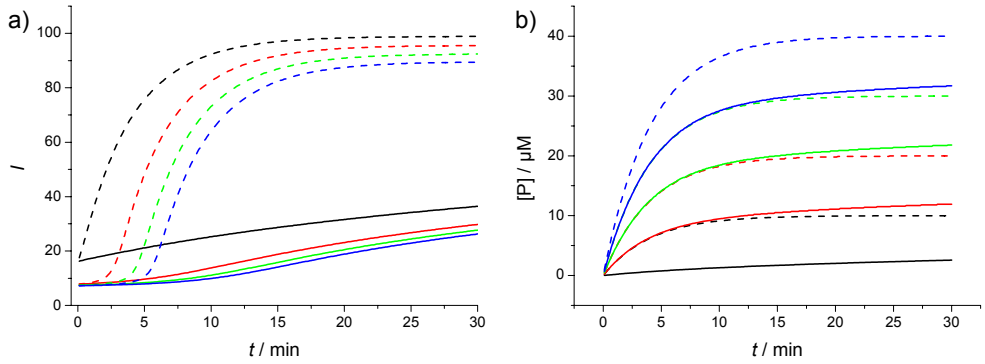

Figure 3.5. a) Fluorescence intensity progress curves and b) product concentration progress curves for an substrate-coupled ON-assay. The curves have been generated with the following parameters: $[H]_0$ = 10 µM, $[D]_0$ = 2.5 µM, K_D = 2.0 × 10^4 M^{-1}, K_S = 1.4 × 10^7 M^{-1}, K_P = 5000 M^{-1}, I_{HD} = 600, I_D = 7, $[S]_0$ = 10 (black), 20 (red), 30 (green), and 40 µM (blue). The values have partially been taken from experimental results (CB7/dapoxyl system, substrate: cadaverine). The enzyme kinetic parameters were arbitrarily chosen as K_M = 10 mM, k_{cat} = 8000 $M^{-1}min^{-1}$, and [*E*] = 300 nM. The solid lines indicate, that [*S*]' = [*S*]; the dashed lines indicate that [*S*]' = $[S]_0$ (see text).

An additional complication arises from the highly efficient enzyme inhibition by substrate complexation, which is known from previous work with cucurbiturils[202,204] (cf. also Chapter 2.4) and cyclodextrins.[65,197-201] Consider the unbiased product progress curves (dashed lines in Figure 3.5b) and the considerably deteriorated curves in presence of the macrocyclic host (solid lines in Figure 3.5b), which reveal that the enzymatic reaction progresses with its unbiased rate as long as sufficient free substrate is available. As soon as nearly all free substrate is consumed, the conversion rate dramatically decreases as a consequence of the extremely low residual substrate, which is still free in solution (equilibrium concentration). An implementation of the inhibitory effect into the intensity progress curves (by assuming that $[S]' = [S]$, *cf.* eqn 9 and 11) reveals that, as a consequence of the highly efficient substrate binding, any useful

information about the initial rates of the enzymatic reaction will be lost (solid lines in Figure 3.5a).

3.3.3. Simulations with the CX4/DBO-A System

3.3.3.1 The Advantage of Low Binding Constants in a Substrate-Coupled Assay

As a possible solution for this puzzling phenomenon, simulations with relatively low binding constants of the substrate (<1 × 10^4 M^{-1}, which is also a more typical binding constant for macrocyclic hosts)[53,89,96,127,212] were initiated. In this case, the host/dye system plays more the role of a passive spectator of the enzymatic reaction rather than directly interacting with the enzyme kinetics. This is demonstrated by Figure 3.6b, in which the product progress curves are shown, assuming an interaction of the substrate with the macrocycle ($[S]' = [S]$, dotted lines) and without an interaction ($[S]' = [S]_0$, solid lines). Both progress curves are very similar and the enzymatic reaction can thus be followed by the supramolecular tandem assay in a much more reliable manner than in the case of highly efficient substrate binding (compare Figures 3.5 and 3.6).

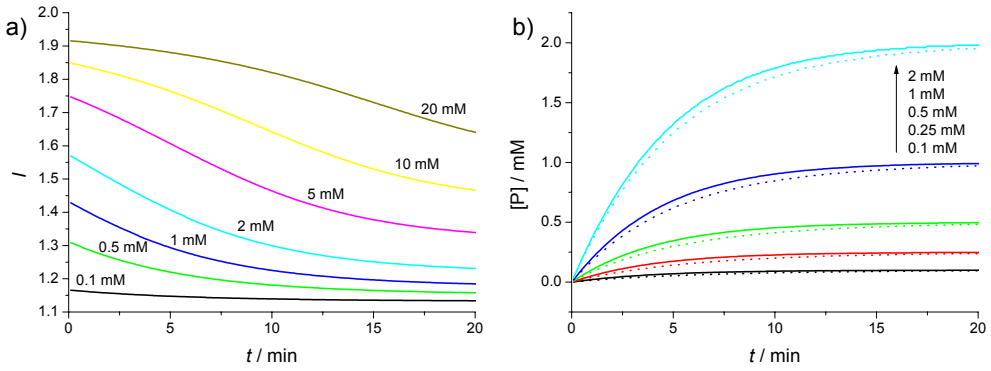

Figure 3.6. a) Comparison of fluorescence intensity progress curves for varying substrate concentration. b) Comparison of the product progress curves for varying substrate concentration. In the case of the solid lines, the total substrate is available to the enzyme, i.e. $[S]' = [S]_0$; the dotted line represents the progress curve, considering that only the free substrate is available to the enzyme, i.e. $[S]' = [S]$. The other parameters are $[H]_0$ = 200 µM, $[D]_0$ = 100 µM, K_D = 6.1 × 10^4 M^{-1}, K_S = 6.4 × 10^3 M^{-1}, K_P = 550 M^{-1}, I_{HD} = 1, and I_D = 2. The values have partially been taken from experimental results (CX4/DBO-A system, substrate: arginine, product: ornithine, pH 9.5). The enzyme kinetic parameters were arbitrarily chosen as K_M = 10 mM, k_{cat} = 8000 $M^{-1}min^{-1}$, and [*E*] = 300 nM.

This can also be seen in the fluorescence intensity progress curves in Figure 3.6a, which illustrate that enzymatic reactions can be followed over a much larger substrate concentration range. Most importantly, the actual activity of the enzyme can be judged from the intensity progress curves, i.e. the change in fluorescence intensity progresses roughly as long as the enzymatic reaction proceeds. However, the possibility to determine enzyme kinetic parameters is a major challenge for this case, because many uncertain parameters would need to be considered to obtain an initial rate from the intensity progress curves. The reason lies in the low binding constants, which are required for a substrate-coupled assay. As a consequence, neither the initial nor the final fluorescence intensity of the enzymatic reaction is linearly dependent on the respective concentrations, such that approximations, which could be conveniently used for the product-coupled assays, no longer hold true. This becomes more obvious from the plot of normalized fluorescence intensity (Figure 3.7), which reveals crossing curves and a dependence of the ratio of fluorescence intensities before the reaction I_0 and the intensities after the reaction I_{final} on the substrate concentration.

However, this presents not a limiting factor for applications, in which a constant substrate concentration is used, for example: inhibitor screening, or screening of enzymes with different activities (*cf.* Chapter 3.4.2.1).

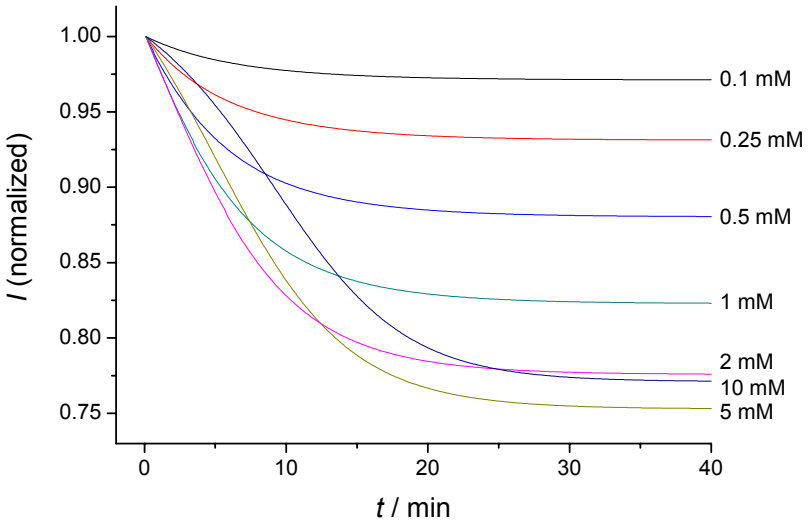

Figure 3.7. Normalized fluorescence intensity progress curves for varying substrate concentration. The parameters are as specified in Figure 3.6.

3.3.3.2 Methods for Improving the Substrate-Product Differentiation

A challenge encountered when working with low substrate binding constants is that the fluorescence intensities before the reaction I_0 and the intensities after the reaction I_{final} do not differ to a large extent, i.e. a relatively low substrate to product differentiation results. By considering the simple titration curve in Figure 3.1b this can be traced back to an incomplete displacement of the dye from the macrocycle at low substrate concentrations.

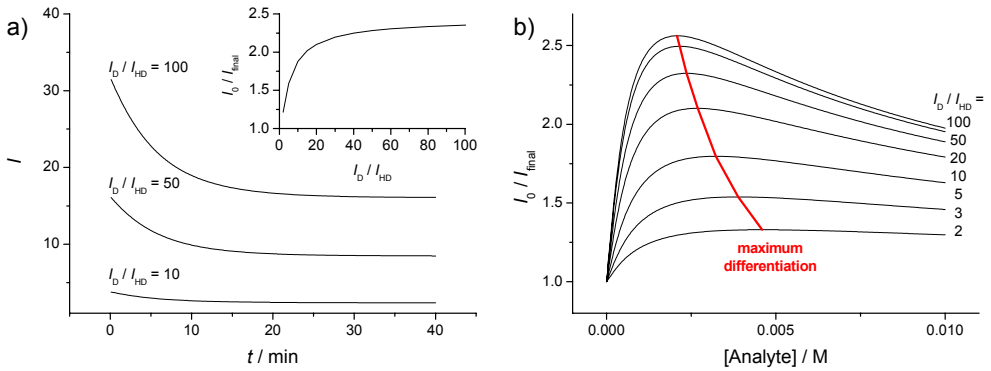

Figure 3.8. a) Comparison of the fluorescence intensity progress curves for different ratios of the fluorescence intensity of free dye and host-dye complex (I_D/I_{HD}). Substrate concentration was set to 500 µM. The inset shows the dependence of the substrate-product differentiation (I_0/I_{final}) at different ratios of the fluorescence intensity of free dye and host-dye complex (I_D/I_{HD}). b) This graph shows the dependence of the expected substrate-product differentiation (I_0/I_{final}) on the initial substrate concentration for several I_D/I_{HD}. All parameters herein are the same as specified in Figure 3.6 if not stated otherwise.

However, the flexibility of supramolecular tandem assays provides several potential remedies. First, another fluorescent dye could be selected, which displays a more efficient fluorescence quenching upon complexation, i.e. the ratio I_D/I_{HD} is increased. A simulation (Figure 3.8a) verified this assumption. Interestingly, this effect tends to decrease at higher ratios I_D/I_{HD} and reaches a nearly constant value (see inset of Figure 3.8a) at which a higher I_D/I_{HD} does not further improve the differentiation of substrate and product (I_0/I_{final}).

Second, the substrate concentration could be varied such that I_0/I_{final} becomes maximal (Figure 3.8b). Note that each fluorescent dye (as represented by

a specific I_D/I_{HD}) affords a different optimal substrate concentration, which decreases with an increasing I_D/I_{HD}. This reveals that an improved I_D/I_{HD} leads to a more sensitive assay, in which lower amounts of substrate could be used.

Finally, there is the possibility to improve the substrate-product differentiation (I_0/I_{final}) by carefully adjusting the concentrations of host and dye for a given system (at constant I_D/I_{HD}). As an example, Figure 3.9 is shows the dependence of the substrate-product differentiation on the host concentration, which demonstrates that a maximum but constant I_0/I_{final} is obtained at low dye concentrations. This remedies the necessity to use very low concentrations of dye and again demonstrates the flexibility of supramolecular tandem assays.

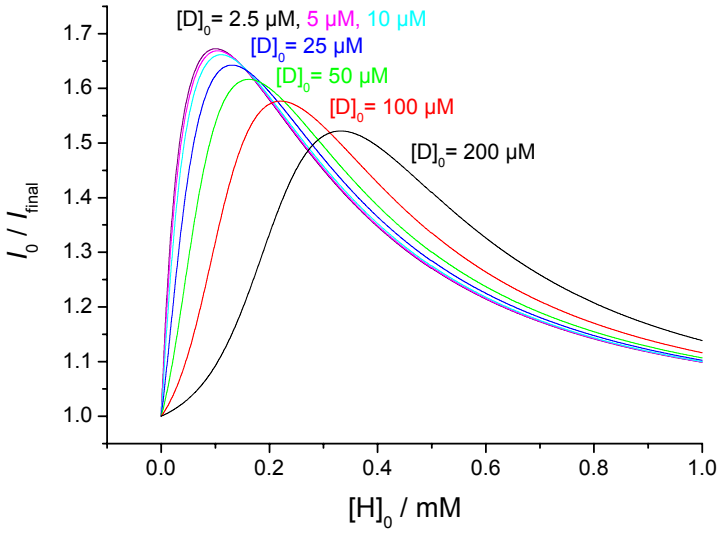

Figure 3.9. Optimization of the dye and host concentration to achieve maximum differentiation of substrate and product. The other parameters are $[S]_0 = 250$ µM, $K_D = 6.1 \times 10^4$ M^{-1}, $K_S = 6.4 \times 10^3$ M^{-1}, $K_P = 550$ M^{-1}, $I_{HD} = 1$, and $I_D = 100$.

In conclusion, the interrelating binding equilibria of supramolecular tandem assays lead to a considerable degree of complexity. However, this also affords an enormous potential to fine-tune assay conditions to meet certain desired criteria, for example sensitivity, substrate-product differentiation or an increased dynamic range. It finally seems to be plausible to derive the following guidelines

for the design of a supramolecular tandem assay (Scheme 3.2) from the present limited considerations and simulations.

Scheme 3.2. Binding scheme for the equilibria involved during enzymatic transformation in a supramolecular tandem assay.

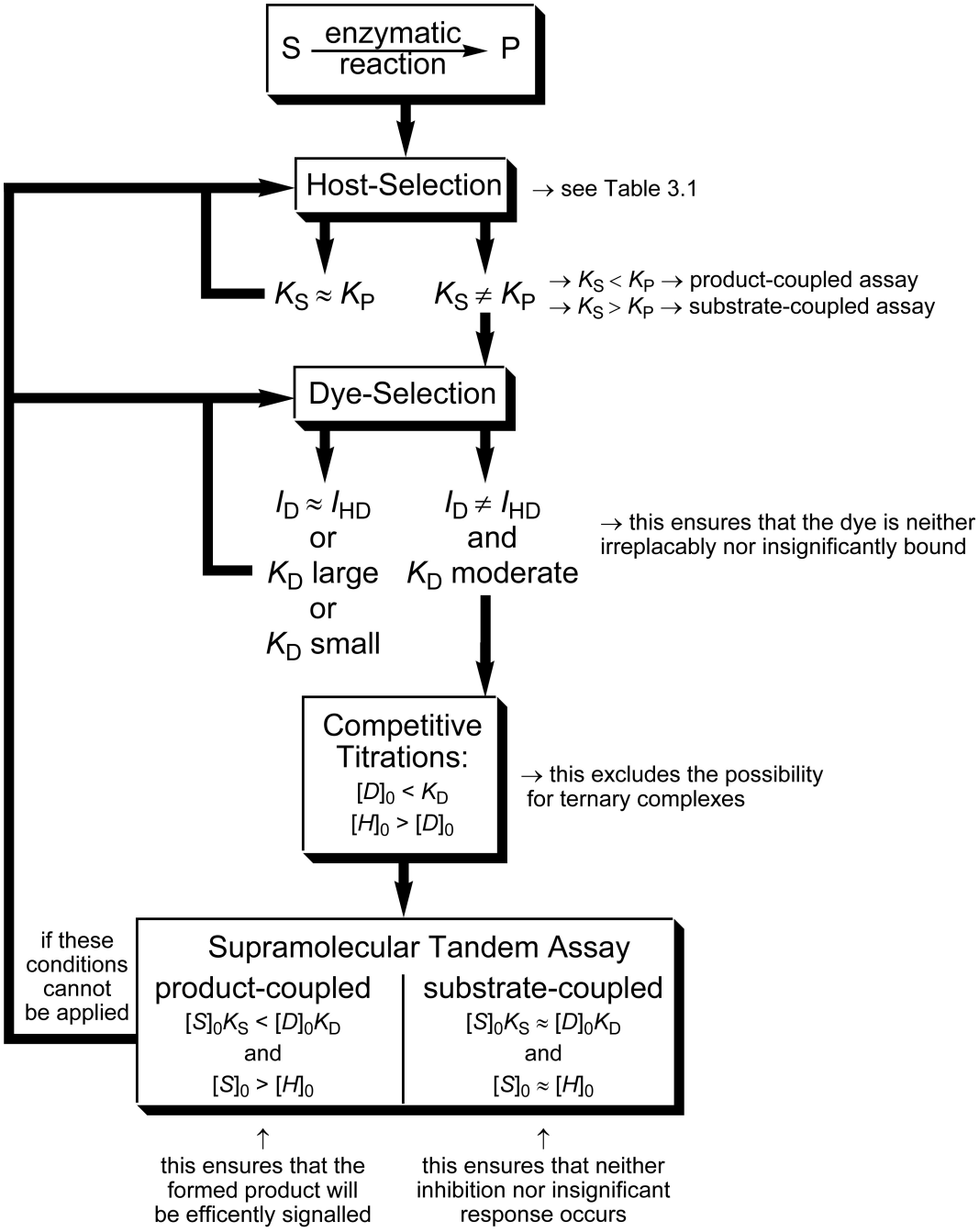

3.4 Future Developments of Supramolecular Tandem Assays

3.4.1 Development of a Supramolecular Tandem Assay for Anions[159]

Chapter 3.1 introduces the use of CB7 and the anionic *p*-sulfonato-calix[4]arene (CX4) as potential hosts for supramolecular tandem assays, which involve cationic products or substrates. According to Table 3.1 it would be additionally desirable to have an anion receptor, which would pave the way for assaying anionic analytes. As a particular appealing analyte, nucleotides have been envisaged, which are important cofactors for numerous enzymes. An example are the phosphotransferases (enzyme class 2.7.x.x), which contain more than 200 enzymes including important regulatory enzymes such as kinases.[179,183,189,217] Interestingly, supramolecular receptors for nucleotides, which should be principally suitable for the development of a tandem assay, have been previously reported.[87,139,212] Aminosubstituted cyclodextrins showed a high preference for ATP over AMP, but ADP or other di- and triphosphates were not investigated.[139] Interestingly, the aminocyclodextrins were also able to distinguish between d-5′-GTP and 5′-GTP as well as between 3′-ATP and 5′-ATP.[139] Aminosubstituted calix[*n*]arenes (with *n* ranging from 4 to 8) showed a high preference of ATP over ADP,[87] and a recently reported cyclophane was an excellent host for ATP, ADP and GTP.[212]

It was therefore appealing to initially search for a suitable fluorescent dye. It was known from previous studies[57,89,96] that DBO derivatives bind strongly with calixarenes and cyclodextrins, in particular when they carry complementarily charged functional groups.[85] The simplest anionic DBO derivatives, which could be envisaged, are the carboxylic acids **22** and **23**.

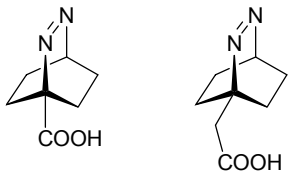

22 **23**

The synthesis of the bridgehead carboxy-substituted derivative **22** was accomplished by the conventional synthesis route based on MTAD (*cf.* Chapter

1.4.1).[151] A complete photophysical characterization of **22** revealed that it has a very low fluorescence quantum yield and rapidly decomposes under intense illumination, due to the radical stabilizing effect of the bridgehead carboxyl substituent.[218,219] Because this renders the derivative **22** unsuitable for the desired application, the methylcarboxyl derivative **23** was synthesized from **13** by tosylation, cyanide substitution, and hydrolysis. As expected, the latter derivative had an amenable quantum yield of 0.21 because the methylene group in the bridgehead-position is less prone to stabilize radicals.[218,219] **23** should thus be more suitable for application in enzyme assays.

The exploratory studies with tetrakis(*N*,*N*'-dimethylammoniomethyl)tetrahydroxycalix[4]arene revealed unexpectedly low binding constants of **23** (< 2000 M^{-1}), presumably owing to the 1,3-alternate conformation of the calixarene,[220] which prevents efficient Coulombic attractions between the ammonium groups of the calixarene and the carboxylic acid group of **23**. In addition to the tetrahydroxy derivative, tetrakis(*N*,*N*',*N*''-dimethylammoniomethyl)tetrapropoxy-calix[4]arene was tested.[221] In the latter case, the cone conformation of the calixarene is fixed by the four propoxy groups at the lower rim.[71] However, this afforded an even lower binding constant with **23** (< 100 M^{-1}), which is presumably due to a much smaller cavity. It can be assumed that the sterically demanding propoxy groups compress the cavity such that a bicyclic derivative like DBO no longer fits into the cavity.

The studies of the binding with β-cyclodextrin also revealed unexpectedly low binding constants (< 120 M^{-1} at pH 7.0). This is in stark contrast to previously reported binding constants of the related alicyclic alkanes (e.g. for the bicycle[2.2.2]octane analogue of **22** a binding constant of 9.7×10^4 M^{-1} has been reported).[53] This has been rationalized by the higher hydrophilicity of azoalkanes, which lowers the hydrophobic contribution to the driving force of complexation. This assumption is corroborated by a more than 8fold increase in the binding constants for the protonated form and has been similarly observed for the protonated and unprotonated form of the DBO ammonium derivative **16**.[57]

This study outlines some potential pitfalls, which need to be avoided in the design of future tandem assays. Further experiments with other potentially suitable macrocycles are underway.

3.4.2 Applications of Supramolecular Tandem Assays

3.4.2.1 Screening for Enzyme Inhibitors

It has been suggested in Chapters 3.3.2 and 3.3.3 that a substrate-coupled assay might work best with low binding constants of substrate and product. In fact, it was possible to demonstrate this with the conversion of arginine to ornithine, which is catalyzed by arginase (Figure 3.10).[222-225] Arginase belongs to the enzyme class of hydrolases and is thought to play a major role in erectile function[222] and sexual arousal,[224] in immune response,[224] and in asthma.[225] So far, arginase has been assayed by laborious colorimetric techniques involving heating to 100 °C,[226] or by a chromogenic derivative, which needs to be synthesized.[227]

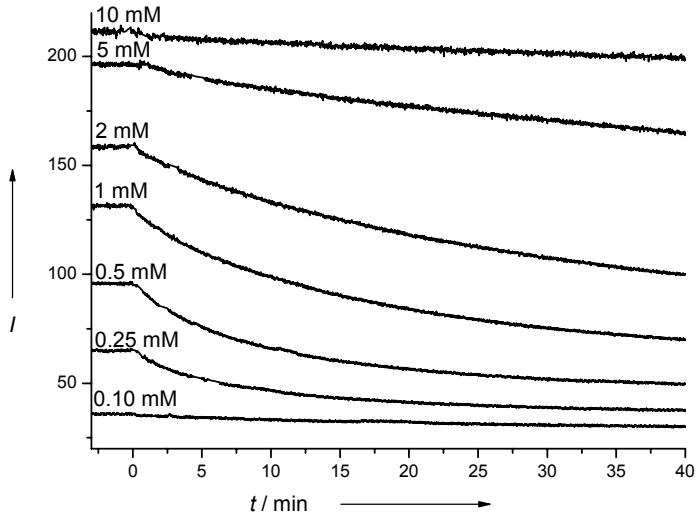

Figure 3.10. Evolution of fluorescence intensity of the DBO-A/CX4 (100 μM and 200 μM) system during enzymatic hydrolysis of arginine by arginase (16 μg/ml) at different substrate concentrations.

As previously discussed in Chapter 3.3.3.1, it was not possible to find a handy method to derive enzyme kinetic parameters from the fluorescence progress

curves owing to the complex dependence of the fluorescence intensity under different initial substrate concentrations. However, it was possible to compare the inhibition of two known inhibitors of arginase. This is feasible because a specific fluorescence intensity reflects a specific progress of the enzymatic reaction. Depending on the time at which this intensity is reached an approximated initial rate for the enzymatic reaction can be derived. Finally, a Hill analysis of the plot is adequate to compare the potential of different inhibitors.[214] Unfortunately, there is so far no method to further determine the properties of the inhibitor by supramolecular tandem assay, i.e. it remains elusive whether the inhibitor is a competitive or an uncompetitive inhibitor. However, the simplicity of the supramolecular approach would make this method highly attractive for a primary HTS to diminish the number of library compounds for a secondary screening with more elaborate methods.

3.4.2.2 Highly Selective Sensing and Quantification

The natural specificity of enzymes has frequently been used in combination with optical[2,228-231] or electrochemical transducers[232-235] for the highly selective sensing of lysine,[228] uranium,[229] AMP,[234] and glucose.[231,235] Recent advances in the field include the application of supramolecular multifunctional pores[2,230] and indicator displacement assays as optical transducers.[231]

This allows the possibility to exploit supramolecular tandem assays as optical transducers for the highly selective sensing of analytes. For example, the established decarboxylase assay system (Chapter 3.1) is as well suitable for a qualitative and quantitative determination of the amino acids Lys, Arg, His, Orn, Trp, and Tyr in the micromolar range. This is made feasible by the extreme specificity of the decarboxylases, which are able to distinguish between these closely related amino acids without any known cross-reactions.[228,236-239] To test a sample for the presence of an amino acids, addition of the dye, the host, and the decarboxylase would suffice. Any time-dependent change of fluorescence intensity in the assay mixture would thus indicate the presence of the respective amino acid.

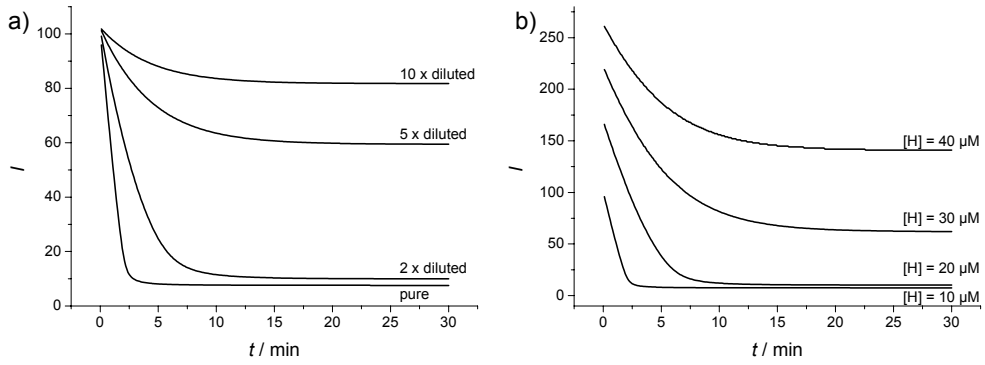

Figure 3.11. Simulation of the detection and quantification of a 25 µM lysine sample by supramolecular tandem assays. a) Since the dye is completely displaced with the undiluted sample, a dilution series (2, 5, and 10 times) can adjust the concentration accordingly (the parameters are the same as in Figure 3.4) to allow the subsequent quantification by a calibration curve. b) Alternatively, the host concentration can be adjusted, such that naked eye inspection already suggests an analyte concentration between 20 and 30 µM (all other parameters as in Figure 3.4).

In addition, a quantitative determination of the amino acid is also feasible like demonstrated in Figure 3.11. In the one case (Figure 3.11a) a dilution series affords the dilution factor at which the dye is not yet completely displaced. In this specific example a (*a priori* unknown) concentration of 25 µM lysine was chosen. A complete displacement results with the undiluted sample, a 5fold dilution reveals that the dye is no longer fully displaced, and a 2fold dilution is just capable of displacing the dye. In this case the common conditions of the CB7/dapoxyl sensor system were chosen, i.e. 2.5 µM dapoxyl and 10 µM CB7. The results from the dilution series thus suggest that the actual sample concentration is around 20 µM by naked eye inspection.

As an alternative to diluting the sample, a series of measurements with different host concentrations could be performed (Figure 3.11b). To demonstrate, the same sample (25 µM lysine) was chosen. Again, increasing the host concentration affords a concentration at which the host concentration exceeds the analyte concentration, such that residual dye remains complexed and the fluorescence intensity does not decrease to the intensity of the free dye (Figure 3.11b). As in the dilution series, a naked eye inspection suggests a concentration

of ca. 20 μM, and, most likely, more elaborate data treatment by calibration curves will reveal the accurate concentrations.

3.4.2.3 Chiral Recognition

The determination of the enantiomeric excess is of utmost importance for high-throughput screening of asymmetric catalysts and protein engineering for biotechnological applications.[240,241] Chromogenic or fluorogenic methods are as for enzyme assays most desirable, because of the possibility of a rapid read-out. As demonstrated for the highly selective sensing, it is likewise possible to utilize the stereoselectivity of enzymes for chiral recognition. The established decarboxylase assay thus makes the determination of the enantiomeric excess of the D-enantiomer of Lys, Arg, His, and Orn feasible, because the decarboxylases specifically convert L-amino acids into the respective amines.[237-239]

A general requirement for the viability of *e.e.* determinations by supramolecular tandem assays is a sufficiently different binding constant of substrate and the product. The reason is that the enzyme converts specifically one enantiomer to the product, while the other enantiomer remains unconverted. It is thus essential that very small amounts of product are detectable and quantifiable in the presence of the remaining substrate (enantiomer).

For demonstrating the viability with the present CB7/dapoxyl system, consider a titration of lysine and cadaverine. The fluorescence in absence of any analyte is ca. 100 units, in presence of 1 mM lysine (regardless of the enatiomer) ca. 70 and in presence of 10 μM cadaverine ca. 5. This suggests that an *e.e.* of ca. 99 % could be easily and reliably determined by the present system.

References

1. In this context it should be noted, that the use of the term "enzyme assay" does not imply any limitation to enzymes; in principle any chemical reaction, e.g. also those catalyzed by antibodies (abzymes), supramolecular enzyme mimics, or metal catalysts could be followed.
2. Das, G.; Matile, S., *Chem. Eur. J.* **2006,** *12*, 2936-2944.
3. Reymond, J. L., *Enzyme Assays*. Wiley-VCH: Weinheim, 2005.
4. Eisenthal, R.; Danson, M. J., *Enzyme Assays: A Practical Approach*. Oxford University Press: Oxford, 2002.
5. Hüser, J., *High-Throughput Screening in Drug Discovery*. Wiley-VCH: Weinheim, 2006.
6. Carter, J. M., *A Guide to HTS Assay Development*. D&MD: Westborough, 2004.
7. Sordé, N.; Das, G.; Matile, S., *Proc. Natl. Acad. Sci. USA* **2003,** *100*, 11964-11969.
8. Reymond, J. L.; Koch, T.; Schröer, J.; Tierny, E., *Proc. Natl. Acad. Sci. USA* **1996,** *93*, 4251-4256.
9. Syed, S. E. H., In *Enzyme Assays - A Practical Approach*, Eisenthal, R.; Danson, M. J., Eds. Oxford University Press: Oxford, 2002; pp 103-140.
10. Chang, H.-T.; Huang, Y.-F.; Chiou, S.-H.; Chiu, T.-C.; Hsieh, M.-M., *Curr. Proteomics* **2004,** *1*, 325-347.
11. Liesener, A.; Karst, U., *Anal. Bioanal. Chem.* **2005,** *382*, 1451-1464.
12. Tawfik, D. S.; Green, B. S.; Chap, R.; Sela, M.; Eshhar, Z., *Proc. Natl. Acad. Sci. USA* **1993,** *90*, 373-377.
13. Benedetti, F.; Berti, F.; Flego, M.; Resmini, M.; Bastiani, E., *Anal. Biochem.* **1998,** *256*, 67-73.
14. Hughes, K. T., In *Enzyme Assays - A Practical Approach*, Eisenthal, R.; Danson, M. J., Eds. Oxford University Press: Oxford, 2002; pp 79-102.
15. Fischer, G.; Bang, H.; Mech, C., *Biomed. Biochim. Acta* **1984,** *43*, 1101-1111.
16. Förster, T., *Ann. Phys.* **1948,** *437*, 55-75.
17. Stryer, L.; Haugland, R. P., *Proc. Natl. Acad. Sci. U. S. A.* **1967,** *58*, 719-726.
18. Lakowicz, J. R., *Principles of fluorescence spectroscopy*. 2. ed.; Kluwer Academic/Plenum: New York, London, 1999; p 698 p.
19. Sahoo, H.; Roccatano, D.; Zacharias, M.; Nau, W. M., *J. Am. Chem. Soc.* **2006,** *128*, 8118-8119.

20. Latt, S. A.; Auld, D. S.; Vallee, B. L., *Biochemistry* **1972,** *11*, 3015-3022.

21. Castellano, R. K.; Craig, S. L.; Colin, N.; Rebek Jr., J., *J. Am. Chem. Soc.* **2000,** *122*, 7876-7882.

22. Grüninger-Leitch, F.; Schlatter, D.; Küng, E.; Nelböck, P.; Döbeli, H., *J. Biol. Chem.* **2002,** *277*, 4687-4693.

23. Alves, A. C. V.; Rogana, E.; Barbosa, C. d. F.; Ferreira-Alves, D. L., *J. Biochem. Biophys. Meth.* **2007**, in press.

24. Lim, C. S.; Miller, J. N.; Bridges, J. W., *Anal. Biochem.* **1980,** *108*, 176-184.

25. Hemmilä, I.; Dakubu, S.; Mukkala, V.-M.; Siitari, H.; Lövgren, T., *Anal. Biochem.* **1984,** *137*, 335-343.

26. Karvinen, J.; Laitala, V.; Mäkinen, M.-L.; Mulari, O.; Tamminen, J.; Hermonen, J.; Hurskainen, P.; Hemmilä, I., *Anal. Chem.* **2004,** *76*, 1429-1436.

27. Latt, S. A.; Auld, D. S.; Vallee, B. L., *Anal. Biochem.* **1972,** *50*, 56-62.

28. Carmel, A.; Kessler, E.; Yaron, A., *Eur. J. Biochem.* **1977,** *73*, 617-625.

29. Knight, C. G., *Methods Enzymol.* **1995,** *248*, 18-34.

30. Packard, B. Z.; Toptygin, D. D.; Komoriya, A.; Brand, L., *Proc. Natl. Acad. Sci. U. S. A.* **1996,** *93*, 11640-11645.

31. Johansson, M. K.; Cook, R. M., *Chem. Eur. J.* **2003,** *9*, 3466-3471.

32. Pope, A. J.; Haupts, U. M.; Moore, K. J., *Drug Discovery Today* **1999,** *4*, 350-362.

33. Moger, J.; Gribbon, P.; Sewing, A.; Winlove, C. P., *J. Biomol. Screen.* **2006,** *11*, 765-772.

34. Turconi, S.; Bingham, R. P.; Haupts, U.; Pope, A. J., *Drug Discovery Today* **2001,** *6*, S27-S39.

35. Lakowicz, J. R.; Jayaweera, R.; Joshi, N.; Gryczynski, I., *Anal. Biochem.* **1987,** *160*, 471-479.

36. French, T. E.; Owicki, J. C.; Modlin, D. N.; Deshpande, S. S.; Mineyev, I.; Crawford, K.; Burton, W., *Proc. SPIE* **1998,** *3259*, 209-218.

37. O'Haver, T. C.; Winefordner, J. D., *Anal. Chem.* **1966,** *38*, 602-607.

38. Haugen, G. R.; Lytle, F. E., *Anal. Chem.* **1981,** *53*, 1554-1559.

39. Saha, A. K.; Kross, K.; Kloszewski, E. D.; Upson, D. A.; Toner, J. L.; Snow, R. A.; Black, C. D. V.; Desai, V. C., *J. Am. Chem. Soc.* **1993,** *115*, 11032-11033.

40. Selvin, P. R.; Rana, T. M.; Hearst, J. E., *J. Am. Chem. Soc.* **1994,** *116*, 6029-6030.

41. Hemmilä, I.; Webb, S., *Drug Discovery Today* **1997,** *2*, 373-381.

42. Pedersen, C. J., *J. Am. Chem. Soc.* **1967,** *89*, 2495-2496.

43. Pedersen, C. J., *J. Am. Chem. Soc.* **1967,** *89*, 7017-7036.
44. Izatt, R. M.; Rytting, J. H.; Nelson, D. P.; Haymore, B. L.; Christensen, J. J., *Science* **1969,** *164*, 443-444.
45. Dietrich, B.; Lehn, J.-M.; Sauvage, J.-P., *Tetrahedron Lett.* **1969,** *10*, 2885-2888.
46. Kyba, E. P.; Siegel, M. G.; Sousa, L. R.; Sogah, G. D. Y.; Cram, D. J., *J. Am. Chem. Soc.* **1973,** *95*, 2691-2692.
47. Pedersen, C. J., *Angew. Chem. Int. Ed.* **1988,** *27*, 1021-1027.
48. Lehn, J.-M., *Angew. Chem. Int. Ed.* **1988,** *27*, 89-112.
49. Cram, D. J., *Angew. Chem. Int. Ed.* **1988,** *27*, 1009-1020.
50. Szejtli, J., *Chem. Rev.* **1998,** *98*, 1743-1754.
51. Connors, K. A., *Chem. Rev.* **1997,** *97*, 1325-1358.
52. Schneider, H.-J.; Hacket, F.; Rüdiger, V.; Ikeda, H., *Chem. Rev.* **1998,** *98*, 1755-1786.
53. Eftink, M. R.; Andy, M. L.; Bystrom, K.; Perlmutter, H. D.; Kristol, D. S., *J. Am. Chem. Soc.* **1989,** *111*, 6765-6772.
54. Harries, D.; Rau, D. C.; Parsegian, V. A., *J. Am. Chem. Soc.* **2005,** *127*, 2184-2190.
55. Nau, W. M.; Zhang, X., *J. Am. Chem. Soc.* **1999,** *121*, 8022-8032.
56. Zhang, X.; Nau, W. M., *Angew. Chem. Int. Ed.* **2000,** *39*, 544-547.
57. Zhang, X.; Gramlich, G.; Wang, X.; Nau, W. M., *J. Am. Chem. Soc.* **2002,** *124*, 254-263.
58. Bakirci, H.; Zhang, X.; Nau, W. M., *J. Org. Chem.* **2005,** *70*, 39-46.
59. Harata, K.; Uedaira, H., *Bull. Chem. Soc. Jpn.* **1975,** *48*, 375-378.
60. Wagner, B. D.; Fitzpatrick, S. J., *J. Inclusion Phenom. Macrocyclic Chem.* **2000,** *38*, 467-478.
61. Wagner, B. D.; MacDonald, P. J., *J. Photochem. Photobiol. A* **1998,** *114*, 151-157.
62. Breslow, R.; Dong, S. D., *Chem. Rev.* **1998,** *98*, 1997-2011.
63. Khan, A. R.; Forgo, P.; Stine, K. J.; D'Souza, V. T., *Chem. Rev.* **1998,** *98*, 1977-1996.
64. Gattuso, G.; Nepogodiev, S. A.; Stoddart, J. F., *Chem. Rev.* **1998,** *98*, 1919-1958.
65. Uekama, K.; Hirayama, F.; Irie, T., *Chem. Rev.* **1998,** *98*, 2045-2076.
66. Hedges, A. R., *Chem. Rev.* **1998,** *98*, 2035-2044.
67. Zinke, A.; Ziegler, E., *Ber. Dtsch. Chem. Ges.* **1944,** *77*, 264-272.
68. Gutsche, C. D.; Muthukrishnan, R., *J. Org. Chem.* **1978,** *43*, 4905-4906.

69. Gutsche, C. D.; Dhawan, B.; No, K. H.; Muthukrishnan, R., *J. Am. Chem. Soc.* **1981,** *103*, 3782-3792.

70. Gutsche, C. D., *Acc. Chem. Res.* **1983,** *16*, 161-170.

71. Böhmer, V., *Angew. Chem. Int. Ed.* **1995,** *34*, 713-745.

72. Högberg, A. G. S., *J. Org. Chem.* **1980,** *45*, 4498-4500.

73. Högberg, A. G. S., *J. Am. Chem. Soc.* **1980,** *102*, 6046-6050.

74. Schneider, H.-J.; Güttes, D.; Schneider, U., *Angew. Chem. Int. Ed.* **1986,** *25*, 647-649.

75. Moran, J. R.; Kerbach, S.; Cram, D. J., *J. Am. Chem. Soc.* **1982,** *104*, 5826-5828.

76. Rudkevich, D. M.; Rebek Jr., J., *Eur. J. Org. Chem.* **1999**, 1991-2005.

77. Biros, S. M.; Rebek Jr., J., *Chem. Soc. Rev.* **2007,** *36*, 93-104.

78. Pina, F.; Parola, A. J.; Ferreira, E.; Maestri, M.; Armaroli, N.; Ballardini, R.; Balzani, V., *J. Phys. Chem.* **1995,** *99*, 12701-12703.

79. Warmuth, R., *Eur. J. Org. Chem.* **2001,** *2001*, 423-437.

80. Warmuth, R.; Kerdelhué , J.-L.; Carrera, S. S.; Langenwalter, K. J.; Brown, N., *Angew. Chem. Int. Ed.* **2002,** *41*, 96-99.

81. Cram, D. J., *Nature* **1992,** *356*, 29-36.

82. Atwood, J. L.; Orr, G. W.; Robinson, K. D.; Hamada, F., *Supramol. Chem.* **1993,** *2*, 309-317.

83. Molenveld, P.; Engbersen, J. F. J.; Kooijman, H.; Spek, A. L.; Reinhoudt, D. N., *J. Am. Chem. Soc.* **1998,** *120*, 6726-6737.

84. Bakirci, H.; Koner, A. L.; Schwarzlose, T.; Nau, W. M., *Chem. Eur. J.* **2006,** *12*, 4799-4807.

85. Bakirci, H.; Koner, A. L.; Dickman, M. H.; Kortz, U.; Nau, W. M., *Angew. Chem. Int. Ed.* **2006,** *45*, 7400-7404.

86. Koh, K. N.; Araki, K.; Ikeda, A.; Otsuka, H.; Shinkai, S., *J. Am. Chem. Soc.* **1996,** *118*, 755-758.

87. Shi, Y.; Schneider, H.-J., *J. Chem. Soc. Perkin Trans. 2* **1999**, 1797-1803.

88. Liu, S.-Y.; He, Y.-B.; Qing, G.-Y.; Xu, K.-X.; Qin, H.-J., *Tetrahedron: Asymmetry* **2005,** *16*, 1527-1534.

89. Bakirci, H.; Nau, W. M., *Adv. Funct. Mat.* **2006,** *16*, 237-242.

90. Shimizu, S.; Shirakawa, S.; Sasaki, Y.; Hirai, C., *Angew. Chem. Int. Ed.* **2000,** *39*, 1256-1259.

91. Baur, M.; Frank, M.; Schatz, J.; Schildbach, F., *Tetrahedron* **2001,** *57*, 6985-6991.

92. Kim, S. K.; Lee, S. H.; Lee, J. Y.; Lee, J. Y.; Bartsch, R. A.; Kim, J. S., *J. Am. Chem. Soc.* **2004,** *126*, 16499-16506.

93. Bakirci, H.; Koner, A. L.; Nau, W. M., *Chem. Commun.* **2005**, 5411-5413.

94. Miyaji, H.; Kim, H.-K.; Sim, E.-K.; Lee, C.-K.; Cho, W.-S.; Sessler, J. L.; Lee, C.-H., *J. Am. Chem. Soc.* **2005,** *127*, 12510-12512.

95. Liu, Y.; Han, B.-H.; Chen, Y.-T., *J. Phys. Chem. B* **2002,** *106*, 4678-4687.

96. Bakirci, H.; Koner, A. L.; Nau, W. M., *J. Org. Chem.* **2005,** *70*, 9960-9966.

97. Casnati, A.; Sansone, F.; Ungaro, R., *Acc. Chem. Res.* **2003,** *36*, 246-254.

98. Hamuro, Y.; Calama, M. C.; Park, H. S.; Hamilton, A. D., *Angew. Chem. Int. Ed.* **1997,** *36*, 2680-2683.

99. Memmi, L.; Lazar, A.; Brioude, A.; Ball, V.; Coleman, A. W., *Chem. Commun.* **2001**, 2474-2475.

100. Park, H. S.; Lin, Q.; Hamilton, A. D., *Proc. Natl. Acad. Sci. USA* **2002,** *99*, 5105-5109.

101. Behrend, R.; Meyer, E.; Rusche, F., *Liebigs Ann. Chem.* **1905,** *339*, 1-37.

102. Freeman, W. A.; Mock, W. L.; Shih, N.-Y., *J. Am. Chem. Soc.* **1981,** *103*, 7367-7368.

103. Buschmann, H.-J.; Cleve, E.; Schollmeyer, E., *Inorg. Chim. Acta* **1992,** *193*, 93-97.

104. Wang, D.; Heo, J.; Park, J. H.; Kim, K., *Angew. Chem. Int. Ed.* **1998,** *37*, 78-80.

105. Kim, J.; Jung, I.-S.; Kim, S.-Y.; Lee, E.; Kang, J.-K.; Sakamoto, S.; Yamaguchi, K.; Kim, K., *J. Am. Chem. Soc.* **2000,** *122*, 540-541.

106. Liu, S.; Zavalij, P. Y.; Isaacs, L., *J. Am. Chem. Soc.* **2005,** *127*, 16798-16799.

107. Lagona, J.; Mukhopadhyay, P.; Chakrabarti, S.; Isaacs, L., *Angew. Chem. Int. Ed.* **2005,** *44*, 4844 – 4870.

108. Sindelar, V.; Cejas, M. A.; Raymo, F. M.; Chen, W.; Parker, S. E.; Kaifer, A. E., *Chem. Eur. J.* **2005,** *11*, 7054-7059.

109. Buschmann, H.-J.; Schollmeyer, E.; Mutihac, L., *Thermochim. Acta* **2003,** *399*, 203-208.

110. Bush, M. E.; Bouley, N. D.; Urbach, A. R., *J. Am. Chem. Soc.* **2005,** *127*, 14511-14517.

111. Heitmann, L. M.; Taylor, A. B.; Hart, P. J.; Urbach, A. R., *J. Am. Chem. Soc.* **2006,** *128*, 12574-12581.

112. Wheate, N. J.; Day, A. I.; Blanch, R. J.; Arnold, A. P.; Cullinane, C.; Collins, J. G., *Chem. Commun.* **2004**, 1424-1425.

113. Wheate, N. J.; Buck, D. P.; Day, A. I.; Collins, J. G., *Dalton Trans.* **2006**, 451-458.

114. Lee, J. W.; Samal, S.; Selvapalam, N.; Kim, H.-J.; Kim, K., *Acc. Chem. Res.* **2003,** *36*, 621-630.

115. Jeon, W. S.; Moon, K.; Park, S. H.; Chun, H.; Ko, Y. H.; Lee, J. Y.; Lee, E. S.; Samal, S.; Selvapalam, N.; Rekharsky, M. V.; Sindelar, V.; Sobransingh, D.; Inoue, Y.; Kaifer, A. E.; Kim, K., *J. Am. Chem. Soc.* **2005,** *127*, 12984-12989.

116. Márquez, C.; Nau, W. M., *Angew. Chem. Int. Ed.* **2001,** *40*, 3155-3160.

117. Márquez, C.; Hudgins, R. R.; Nau, W. M., *J. Am. Chem. Soc.* **2004,** *126*, 5806-5816.

118. Liu, S.; Ruspic, C.; Mukhopadhyay, P.; Chakrabarti, S.; Zavalij, P. Y.; Isaacs, L., *J. Am. Chem. Soc.* **2005,** *127*, 15959-15967.

119. Márquez, C.; Nau, W. M., *Angew. Chem. Int. Ed.* **2001,** *40*, 4387-4390.

120. Mohanty, J.; Nau, W. M., *Angew. Chem. Int. Ed.* **2005,** *44*, 3750-3754.

121. Nau, W. M.; Mohanty, J., *Int. J. Photoenergy* **2005,** *7*, 133-141.

122. Wagner, B. D.; Fitzpatrick, S. J.; Gill, M. A.; MacRae, A. I.; Stojanovic, N., *Can. J. Chem.* **2001,** *79*, 1101-1104.

123. Wagner, B. D.; MacRae, A. I., *J. Phys. Chem. B* **1999,** *103*, 10114-10119.

124. Marquez, C.; Huang, F.; Nau, W. M., *IEEE Trans. Nanobiosci.* **2004,** *3*, 39-45.

125. Mohanty, J.; Nau, W. M., *Photochem. Photobiol. Sci.* **2004,** *3*, 1026-1031.

126. Strickler, S. J.; Berg, R. A., *J. Chem. Phys.* **1962,** *37*, 814-822.

127. Hof, F.; Trembleau, L.; Ullrich, E. C.; Rebek Jr., J., *Angew. Chem. Int. Ed.* **2003,** *42*, 3150-3153.

128. Lam, R. T. S.; Belenguer, A.; Roberts, S. L.; Naumann, C.; Jarrosson, T.; Otto, S.; Sanders, J. K. M., *Science* **2005,** *308*, 667-669.

129. Tashiro, S.; Tominaga, M.; Kawano, M.; Therrien, B.; Ozeki, T.; Fujita, M., *J. Am. Chem. Soc.* **2005,** *127*, 4546-4547.

130. Teulade-Fichou, M.-P.; Carrasco, C.; Guittat, L.; Bailly, C.; Alberti, P.; Mergny, J.-L.; David, A.; Lehn, J.-M.; Wilson, W. D., *J. Am. Chem. Soc.* **2003,** *125*, 4732-4740.

131. Baudoin, O.; Gonnet, F.; Teulade-Fichou, M.-P.; Vigneron, J.-P.; Tabet, J.-C.; Lehn, J.-M., *Chem. Eur. J.* **1999,** *5*, 2762-2771.

132. de Silva, A. P.; Gunaratne, H. Q. N.; Gunnlaugsson, T.; Huxley, A. J. M.; McCoy, C. P.; Rademacher, J. T.; Rice, T. E., *Chem. Rev.* **1997,** *97*, 1515-1566.

133. Leevy, W. M.; Gammon, S. T.; Jiang, H.; Johnson, J. R.; Maxwell, D. J.; Jackson, E. N.; Marquez, M.; Piwnica-Worms, D.; Smith, B. D., *J. Am. Chem. Soc.* **2006,** *128*, 16476-16477.

134. de Silva, A. P.; McClenaghan, N. D., *Chem. Eur. J.* **2004,** *10*, 574-586.

135. de Silva, A. P., *Nat. Mater.* **2005,** *4*, 15-16.

136. Ueno, A.; Kuwabara, T.; Nakamura, A.; Toda, F., *Nature* **1992,** *356*, 136-137.

137. Hossain, M. A.; Hamasaki, K.; Takahashi, K.; Mihara, H.; Ueno, A., *J. Am. Chem. Soc.* **2001,** *123*, 7435-7436.

138. Hossain, M. A.; Mihara, H.; Ueno, A., *Bioorg. Med. Chem. Lett.* **2003,** *13*, 4305-4308.

139. Eliseev, A. V.; Schneider, H.-J., *J. Am. Chem. Soc.* **1994,** *116*, 6081-6088.

140. Wiskur, S. L.; Ait-Haddou, H.; Lavigne, J. J.; Anslyn, E. V., *Acc. Chem. Res.* **2001,** *34*, 963-972.

141. Nguyen, B. T.; Anslyn, E. V., *Coord. Chem. Rev.* **2006,** *250*, 3118-3127.

142. Wright, A. T.; Anslyn, E. V., *Chem. Soc. Rev.* **2006,** *35*, 14-28.

143. Folmer-Andersen, J. F.; Kitamura, M.; Anslyn, E. V., *J. Am. Chem. Soc.* **2006,** *128*, 5652-5653.

144. Piatek, A. M.; Bomble, Y. J.; Wiskur, S. L.; Anslyn, E. V., *J. Am. Chem. Soc.* **2004,** *126*, 6072-6077.

145. Engel, P. S.; Hayes, R. A.; Keifer, L.; Szilagyi, S.; Timberlake, J. W., *J. Am. Chem. Soc.* **1978,** *100*, 1876-1882.

146. Nelsen, S. F.; Petillo, P. A.; Chang, H.; Frigo, T. B.; Dougherty, D. A.; Kaftory, M., *J. Org. Chem.* **1991,** *56*, 613-618.

147. Cookson, R. C.; Gupte, S. S.; Stevens, I. D. R.; Watts, C. T., *Org. Syn.* **1971,** *51*, 121.

148. Mintz, M. J.; Walling, C., *Org. Syn. Coll.* **1973,** *V*, 184.

149. Hudgins, R. R.; Huang, F.; Gramlich, G.; Nau, W. M., *J. Am. Chem. Soc.* **2002,** *124*, 556-564.

150. Hünig, S.; Kahanek, H., *Chem. Ber.* **1957,** *90*, 238-246.

151. Adam, W.; De Lucchi, O., *Angew. Chem. Int. Ed.* **1980,** *19*, 762-779.

152. Engel, P. S.; Horsey, D. W.; Scholz, J. N.; Karatsu, T.; Kitamura, A., *J. Phys. Chem.* **1992,** *96*, 7524-7535.

153. Yoshida, Y.; Sakakura, Y.; Aso, N.; Okada, S.; Tanabe, Y., *Tetrahedron* **1999,** *55*, 2183-2192.

154. Belleau, B.; Malek, G., *J. Am. Chem. Soc.* **1968,** *90*, 1651-1652.

155. Atherton, E.; Wellings, D. A., In *Houben-Weyl Methods of Organic Chemistry. Synthesis of Peptides and Peptidomimetics*, Goodman, M.; Felix, A.; Moroder, L.; Toniolo, C., Eds. Georg Thieme Verlag: Stuttgart, 2001; Vol. E22a, pp 740-754.

156. Mancuso, A. J.; Swern, D., *Synthesis* **1981**, 165.

157. Piancatelli, G.; Scettri, A.; D'Auria, M., *Synthesis* **1982**, 245.

158. Wirth, T., *Angew. Chem. Int. Ed.* **2001,** *40*, 2812-2814.

159. Hennig, A.; Schwarzlose, T.; Nau, W. M., *Arkivoc* **2007**, 341-357.

160. Labouesse, J.; Gervais, M., *Eur. J. Biochem.* **1967,** *2*, 215-223.

161. Martin, C. J.; Marini, M. A., *J. Biol. Chem.* **1967,** *242*, 5736-5743.

162. Knowles, J. R.; Sharp, H.; Greenwell, P., *Biochem. J.* **1969,** *113*, 343-351.

163. Misselwitz, R.; Zirwer, D.; Frohne, M.; Hanson, H., *FEBS Lett.* **1975,** *55*, 233-236.

164. Anderson, R. A.; Bosron, W. F.; Scott, K. F.; Vallee, B. L., *Proc. Nat. Acad. Sci. USA* **1975,** *72*, 2989-2993.

165. Du, H.; Fuh, R.-C. A.; Li, J.; Corkan, L. A.; Lindsey, J. S., *Photochem. Photobiol.* **1998,** *68*, 141-142.

166. Cousins-Wasti, R. C.; Ingraham, R. H.; Morelock, M. M.; Grygon, C. A., *Biochemistry* **1996,** *35*, 16746-16752.

167. Hirose, K., *J. Inclusion Phenom. Macrocyclic Chem.* **2001,** *39*, 193-209.

168. Glasoe, P. K.; Long, F. A., *J. Phys. Chem.* **1960,** *64*, 188-190.

169. Nau, W. M.; Wang, X., *ChemPhysChem* **2002,** *3*, 393-398.

170. Nau, W. M.; Huang, F.; Wang, X.; Bakirci, H.; Gramlich, G.; Márquez, C., *Chimia* **2003,** *57*, 161-167.

171. Engel, P. S.; Horsey, D. W.; Keys, D. E.; Nalepa, C. J.; Soltero, L. R., *J. Am. Chem. Soc.* **1983,** *105*, 7108-7114.

172. Adam, W.; Nikolaus, A.; Sauer, J., *J. Org. Chem.* **1999,** *64*, 3695-3698.

173. Pischel, U.; Nau, W. M., *J. Am. Chem. Soc.* **2001,** *123*, 9727-9737.

174. Nau, W. M.; Pischel, U., In *Organic Photochemistry and Photophysics*, Ramamurthy, V.; Schanze, K. S., Eds. CRC Press: 2006; Vol. 14, pp 75-129.

175. Hennig, A.; Roth, D.; Enderle, T.; Nau, W. M., *ChemBioChem* **2006,** *7*, 733-737.

176. Hennig, A.; Florea, M.; Roth, D.; Enderle, T.; Nau, W. M., *Anal. Biochem.* **2007,** *360*, 255-265.

177. Manger, M.; Scheck, M.; Prinz, H.; von Kries, J. P.; Langer, T.; Saxena, K.; Schwalbe, H.; Fürstner, A.; Rademann, J.; Waldmann, H., *ChemBioChem* **2005,** *6*, 1749-1753.

178. van der Geer, P. V.; Hunter, T.; Lindberg, R. A., *Annu. Rev. Cell Biol.* **1994,** *10*, 251-337.

179. Johnson, L. N.; Lewis, R. J., *Chem. Rev.* **2001,** *101*, 2209-2242.

180. Park, Y.-W.; Cummings, R. T.; Wu, L.; Zheng, S.; Cameron, P. M.; Woods, A.; Zaller, D. M.; Marcy, A. I.; Hermes, J. D., *Anal. Biochem.* **1999,** *269*, 94-104.

181. Parker, G. J.; Law, T. L.; Lenoch, F. J.; Bolger, R. E., *J. Biomol. Screen.* **2000,** *5*, 77-88.

182. Simeonov, A.; Bi, X.; Nikiforov, T. T., *Anal. Biochem.* **2002,** *304*, 193-199.

183. Shults, M. D.; Imperiali, B., *J. Am. Chem. Soc.* **2003,** *125*, 14248-14249.

184. Wang, Q.; Cahill, S. M.; Blumenstein, M.; Lawrence, D. S., *J. Am. Chem. Soc.* **2006,** *128*, 1808-1809.

185. Soleilhac, J. M.; Cornille, F.; Martin, L.; Lenoir, C.; Fournié-Zaluski, M. C.; Roques, B. P., *Anal. Biochem.* **1996,** *241*, 120-127.

186. Anne, C.; Cornille, F.; Lenoir, C.; Roques, B. P., *Anal. Biochem.* **2001,** *291*, 253-261.

187. Haskell, M. D.; Slack, J. K.; Parsons, J. T.; Parsons, S. J., *Chem. Rev.* **2001,** *101*, 2425-2440.

188. Thomas, S. M.; Brugge, J. S., *Annu. Rev. Cell Dev. Biol.* **1997,** *13*, 513-609.

189. Oda, K.; Matsuoka, Y.; Funahashi, A.; Kitano, H., *Mol. Syst. Biol.* **2005,** *1*, E1-E17.

190. Wells, A., *Int. J. Biochem. Cell Biol.* **1999,** *31*, 637-643.

191. Nau, W. M.; Greiner, G.; Rau, H.; Wall, J.; Olivucci, M.; Scaiano, J. C., *J. Phys. Chem. A* **1999,** *103*, 1579-1584.

192. Márquez, C.; Pischel, U.; Nau, W. M., *Org. Lett.* **2003,** *5*, 3911-3914.

193. Thomas, D. D.; Carlsen, W. F.; Stryer, L., *Proc. Nat. Acad. Sci. USA* **1978,** *75*, 5746-5750.

194. Steinberg, I. Z.; Katchalski, E., *J. Chem. Phys.* **1968,** *48*, 2404-2410.

195. Elkana, Y.; Feitelson, J.; Katchalski, E., *J. Chem. Phys.* **1968,** *48*, 2399-2404.

196. Birks, J. B.; Georghiou, S., *J. Phys. B (Proc. Phys. Soc.)* **1968,** *1*, 958-965.

197. Irwin, W. J.; Dwivedi, A. K.; Holbrook, P. A.; Dey, M. J., *Pharm. Res.* **1994,** *11*, 1698-1703.

198. Matsubara, K.; Ando, Y.; Irie, T.; Uekama, K., *Pharm. Res.* **1997,** *14*, 1401-1405.

199. McGarraghy, M.; Darcy, R., *J. Inclusion Phenom. Macrocyclic Chem.* **2000,** *37*, 259-264.

200. Monteiro, J. B.; Chiaradia, L. D.; Brandão, T. A. S.; Dal Magro, J.; Yunes, R. A., *Int. J. Pharm.* **2003,** *267*, 93-100.

201. Koralewska, A.; Augustyniak, W.; Temeriusz, A.; Kanska, M., *J. Inclusion Phenom. Macrocyclic Chem.* **2004,** *49*, 193-197.

202. Hennig, A.; Ghale, G.; Nau, W. M., *Chem. Commun.* **2007**, 1614-1616.

203. Bakirci, H. Bicyclic Azoalkanes as probes and sensors in supramoecular chemistry. International Univeristy Bremen, Bremen, 2006.

204. Isobe, H.; Sato, S.; Lee, J. W.; Kim, H.-J.; Kim, K.; Nakamura, E., *Chem. Commun.* **2005**, 1549-1551.

205. Gerner, E. W.; Meyskens, F. L., *Nat. Rev. Cancer* **2004,** *4*, 781-792.

206. Handley, S. A.; Dube, P. H.; Miller, V. L., *Proc. Natl. Acad. Sci. USA* **2006,** *103*.

207. Innocente, N.; Biasutti, M.; Padovese, M.; Moret, S., *Food Chem.* **2007,** *101*, 1285-1289.

208. Wright, A. T.; Griffin, M. J.; Zhong, Z.; McCleskey, S. C.; Anslyn, E. V.; McDevitt, J. T., *Angew. Chem. Int. Ed.* **2005,** *44*, 6375-6378.

209. Mock, W. L.; Shih, N.-Y., *J. Org. Chem.* **1986,** *51*, 4440-4446.

210. Koner, A. L.; Nau, W. M., *Supramol. Chem.* **2007,** *19*, 55-66.

211. Lehn, J.-M., *Supramolecular Chemistry - Concepts and Perspectives*. 1 ed.; VCH Verlagsgesellschaft mbH: Weinheim, 1995.

212. Neelakandan, P. P.; Harihan, M.; Ramaiah, D., *J. Am. Chem. Soc.* **2006,** *128*, 11334-11335.

213. Ballester, P.; Sarmentero, M. A., *Org. Lett.* **2006,** *8*, 3477-3480.

214. Copeland, R. A., *Anal. Biochem.* **2003,** *320*, 1-12.

215. Nara, S.; Gomes, B.; Yasunobu, K. T., *J. Biol. Chem.* **1966,** *241*, 2774-2780.

216. Tabor, H.; Tabor, C., *Adv. Enzymol.* **1972,** *36*, 203.

217. von Ahsen, O.; Bomer, U., *ChemBioChem* **2005,** *6*, 481-490.

218. Dube, M. F.; Timberlake, J. W., *Tetrahedron* **1980,** *36*, 1753-1756.

219. Luedtke, A.; Meng, K.; Timberlake, J. W., *Tetrahedron Lett.* **1987,** *28*, 4255-4258.

220. Nagasaki, T.; Sisido, K.; Arimura, T.; Shinkai, S., *Tetrahedron* **1992,** *48*, 797-804.

221. Florea, M.; Hennig, A.; Nau, W. M., unpublished results.

222. Kim, N. N.; Cox, J. D.; Baggio, R. F.; Emig, F. A.; Mistry, S. K.; Harper, S. L.; Speicher, D. W.; Morris Jr., S. M.; Ash, D. E.; Traish, A.; Christianson, D. W., *Biochemistry* **2001,** *40*, 2678-2688.

223. Christianson, D. W., *Acc. Chem. Res.* **2005,** *38*, 191-201.

224. Bronte, V.; Zanovello, P., *Nat. Rev. Immunol.* **2005,** *5*, 641-654.

225. Ricciardolo, F. L. M.; Zaagsma, J.; Meurs, H., *Expert Opin. Invest. Drugs* **2005,** *14*, 1221-1231.

226. Kuchel, P. W.; Nichol, L. W.; Jeffrey, P. D., *J. Biol. Chem.* **1975,** *250*, 8222-8227.

227. Baggio, R.; Cox, J. D.; Harper, S. L.; Speicher, D. W.; Christianson, D. W., *Anal. Biochem.* **1999,** *276*, 251-253.

228. Hong, L.; Huarui, H.; Wolfbeis, O. S., *Biosens. Bioelectron.* **1992,** *7*, 725-732.

229. Liu, J.; Brown, A. K.; Meng, X.; Cropek, D. M.; Istok, J. D.; Watson, D. B.; Lu, Y., *Proc. Nat. Acad. Sci. USA* **2007,** *104*, 2056-2061.

230. Litvinchuk, S.; Sordé, N.; Matile, S., *J. Am. Chem. Soc.* **2005,** *127*, 9316-9317.

231. Zhang, T.; Anslyn, E. V., *Org. Lett.* **2007,** *9*, 1627-1629.

232. Phadke, R. S., *Biosystems* **1992,** *27*, 203-206.

233. Rechnitz, G. A., *Science* **1975,** *190*, 234-238.

234. Papastathopoulos, D. S.; Rechnitz, G. A., *Anal. Chem.* **1976,** *48*, 862-864.

235. Kalayci, S.; Somer, G.; Ekmekci, G., *Talanta* **2005,** *65*, 87-91.

236. Pegg, A. E., *J. Biol. Chem.* **2006,** *281*, 14529-14532.

237. Tanase, S.; Guirard, B. M.; Snell, E. E., *J. Biol. Chem.* **1985,** *260*, 6738-6746.

238. Soda, K.; Moriguchi, M., *Biochem. Biophys. Res. Comm.* **1969,** *34*, 34-39.

239. Blethen, S. L.; Boeker, E. A.; Snell, E. E., *J. Biol. Chem.* **1968,** *243*, 1671-1677.

240. Reetz, M. T., *Angew. Chem. Int. Ed.* **2001,** *40*, 284-310.

241. Finn, M. G., *Chirality* **2002,** *14*, 534-540.

– CHAPTER 4 –
APPENDIX

Appendix 1: Fitting Functions for Origin

Titrations for 1:1 Host-Guest Binding

Suitable for NMR in the fast exchange limit, absorbance, and fluorescence intensity

The underlying binding model is as follows:

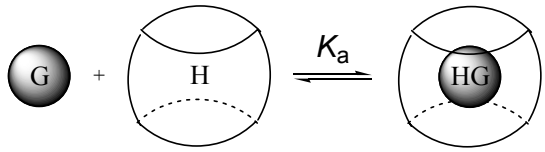

The association constant of a 1:1 binding is given by the law of mass action.

$$K_a = \frac{[HG]}{[H][G]} \quad \Leftrightarrow \quad [HG] = K_a \times [H][G] \tag{1}$$

Conservation of mass requires that

$$[H] = [H]_0 - [HG] \tag{2}$$

$$[G] = [G]_0 - [HG] \tag{3}$$

From eqs. 1-3 one obtains

$$[HG] = K_a([H]_0 - [HG])([G]_0 - [HG])$$

$$\Leftrightarrow \quad [HG] = K_a\left([H]_0[G]_0 - [HG][H]_0 - [HG][G]_0 + [HG]^2\right)$$

$$\Leftrightarrow \quad [HG] = K_a[H]_0[G]_0 - K_a[HG][H]_0 - K_a[HG][G]_0 + K_a[HG]^2 \quad | -[HG]$$

$$\Leftrightarrow \quad 0 = K_a[HG]^2 - \left(K_a[HG][H]_0 + K_a[HG][G]_0 + [HG]\right) + K_a[H]_0[G]_0$$

$$\Leftrightarrow \quad 0 = K_a[HG]^2 - \left(K_a[H]_0 + K_a[G]_0 + 1\right)[HG] + K_a \times [H]_0[G]_0$$

$$\Leftrightarrow \quad 0 = [HG]^2 - \left([H]_0 + [G]_0 + 1/K_a\right)[HG] + [H]_0[G]_0 \tag{4}$$

The quadratic eqn. 4 can be solved in the usual way by comparison with

$0 = x^2 + p \cdot x + q$, for which the general solution $x = -\frac{p}{2} \pm \sqrt{\left(\frac{p}{2}\right)^2 - q}$ applies.

This yields the concentration of host-guest complex under equilibrium conditions:

$$[HG] = \left([H]_0 + [G]_0 + 1/K_a\right)/2 \pm \sqrt{\left([H]_0 + [G]_0 + 1/K_a\right)^2/4 - [H]_0[G]_0} \tag{5}$$

Now the concentration of free guest can be determined by combining eqs. 3 and 5.

$$[G] = ([G]_0 - [H]_0 - 1/K_a)/2 \pm \sqrt{([H]_0 + [G]_0 + 1/K_a)^2/4 - [H]_0[G]_0} \qquad (6)$$

Similarly, the concentration of free host by eqs. 2 and 5 is obtained:

$$[H] = ([H]_0 - [G]_0 - 1/K_a)/2 \pm \sqrt{([H]_0 + [G]_0 + 1/K_a)^2/4 - [H]_0[G]_0} \qquad \mathbf{(7)}$$

During the titration experiment we observe the fluorescence intensity of the fluorescent guest and the fluorescent host-guest complex, which is given by the molar fraction.

$$FI = x_g I_g + x_{gh} I_{gh} = \frac{[G]}{[G]_0} I_g + \frac{[HG]}{[G]_0} I_{gh}$$

Substituting the concentration of host-guest complex by eqn. 3 gives

$$FI = \frac{[G]}{[G]_0} I_g + I_{gh} - \frac{[G]}{[G]_0} I_{gh} = I_{gh} + (I_g - I_{gh}) \frac{[G]}{[G]_0} \qquad (8)$$

Combining eqs. 6 and 8 gives the equation, which can be implemented into fitting programs:

$$FI = I_{gh} + (I_g - I_{gh}) \frac{([G]_0 - [H]_0 - 1/K_a)/2 \pm \sqrt{([H]_0 + [G]_0 + 1/K_a)^2/4 - [H]_0[G]_0}}{[G]_0}$$

The respective Origin file is host1guest1.fdf, in which the following parameters are used:

Ig fluorescence intensity of an uncomplexed guest (fluorescent dye)
Ihg fluorescence intensity of the host-guest complex
Go total concentration of guest (fluorescent dye)
K association constant of the guest (fluorescent dye) with the host

```
void _nlsfhost1guest1
// Fit Parameter(s):
double Ig, double Ihg, double G0, double K,
// Independent Variable(s):
double H0,
// Dependent Variable(s):
double& Int)
{
        // Beginning of editable part
        Int=Ihg+(Ig-Ihg)*(((G0-H0-1/K)/2+sqrt(((H0+G0+1/K)^2)/4-H0*G0))/G0);
        // End of editable part
}
```

Commonly, Go, and Ig are known, such that these parameters can be fixed during the fitting procedure.

Competitive Titrations

The underlying binding model is as follows:

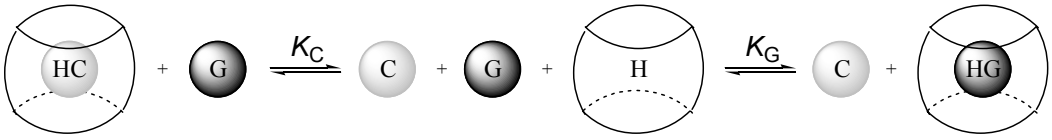

Therefore the following equations can be derived:

$$K_G = \frac{[HG][C]}{[H][G][C]} = \frac{[HG]}{[H][G]} \tag{1}$$

$$K_C = \frac{[HC][G]}{[H][G][C]} = \frac{[HC]}{[H][C]} \tag{2}$$

Law of mass conservation further requires that:

$$[G] = [G]_0 - [HG] \tag{3}$$

$$[C] = [C]_0 - [HC] \tag{4}$$

$$[H] = [H]_0 - [HC] - [HG] \tag{5}$$

From (1) follows with (3)

$$[HG] = K_G[H][G] = K_G[H][G]_0 - K_G[H][HG] \quad | + K_G[H][HG]$$
$$[HG] + K_G[H][HG] = K_G[H][G]_0$$
$$[HG](1 + K_G[H]) = K_G[H][G]_0 \quad | : (1 + K_G[H])$$
$$[HG] = \frac{K_G[H][G]_0}{1 + K_G[H]} \tag{6}$$

From (2) follows with (4)

$$[HC] = K_C[H][C] = K_C[H][C]_0 - K_C[H][HC] \quad | + K_C[H][HC]$$
$$[HC] + K_C[H][HC] = K_C[H][C]_0$$
$$[HC](1 + K_C[H]) = K_C[H][C]_0 \quad | : (1 + K_C[H])$$
$$[HC] = \frac{K_C[H][C]_0}{1 + K_C[H]} \tag{7}$$

From (5) with (6) and (7)

$$[H] = [H]_0 - \frac{K_C[H][C]_0}{1 + K_C[H]} - \frac{K_G[H][G]_0}{1 + K_G[H]}$$

$$= [H]_0 - \frac{K_C[H][C]_0 + K_G K_C[C]_0[H]^2}{(1 + K_C[H])(1 + K_G[H])} - \frac{K_G[H][G]_0 + K_C K_G[G]_0[H]^2}{(1 + K_G[H])(1 + K_C[H])}$$

$$
\begin{aligned}
\Leftrightarrow \quad & (1+K_C[H])(1+K_G[H])[H] = (1+K_C[H])(1+K_G[H])[H]_0 \\
& -K_C[H][C]_0 - K_GK_C[C]_0[H]^2 - K_G[H][G]_0 - K_CK_G[G]_0[H]^2 \\
\Leftrightarrow \quad & [H]+K_G[H]^2 + K_C[H]^2 + K_CK_G[H]^3 = [H]_0 + K_G[H]_0[H] \\
& +K_C[H]_0[H]+K_CK_G[H]_0[H]^2 - K_C[H][C]_0 - K_GK_C[C]_0[H]^2 \\
& -K_G[H][G]_0 - K_CK_G[G]_0[H]^2 \\
\Leftrightarrow \quad & K_CK_G[H]^3 + K_G[H]^2 + K_C[H]^2 - K_CK_G[H]_0[H]^2 \\
& +K_GK_C[C]_0[H]^2 + K_CK_G[G]_0[H]^2 + [H] - K_G[H]_0[H] - K_C[H]_0[H] \\
& +K_C[H][C]_0 + K_G[H][G]_0 - [H]_0 = 0 \\
\Leftrightarrow \quad & K_CK_G[H]^3 + \\
& (K_G + K_C - K_CK_G[H]_0 + K_GK_C[C]_0 + K_CK_G[G]_0)[H]^2 + \\
& (1 - K_G[H]_0 - K_C[H]_0 + K_C[C]_0 + K_G[G]_0)[H] \\
& -[H]_0 = 0 \\
\Leftrightarrow \quad & K_CK_G[H]^3 + \\
& (K_C + K_G + K_CK_G[G]_0 + K_CK_G[C]_0 - K_CK_G[H]_0)[H]^2 + \\
& (K_C[C]_0 - K_C[H]_0 + K_G[G]_0 - K_G[H]_0 + 1)[H] \\
& -[H]_0 = 0
\end{aligned}
\tag{8}
$$

Substitution with:

$$a = K_CK_G$$

$$b = K_C + K_G + K_CK_G[G]_0 + K_CK_G[C]_0 - K_CK_G[H]_0$$

$$c = K_C[C]_0 - K_C[H]_0 + K_G[G]_0 - K_G[H]_0 + 1$$

and $d = -[H]_0$

Yields the expected cubic equation:

$$0 = a[H]^3 + b[H]^2 + c[H] - d$$

The conversion into fluorescence intensity is carried by using the molar fractions:

$$FI = x_g I_g + x_{gh} I_{gh} = \frac{[G]}{[G]_0} I_g + \frac{[HG]}{[G]_0} I_{gh}$$

With (3) and (6) follows:

$$FI = \frac{[G]_0 - [HG]}{[G]_0} I_g + \frac{\frac{K_G[H][G]_0}{1+K_G[H]}}{[G]_0} I_{gh} = \frac{[G]_0 - [HG]}{[G]_0} I_g + \frac{K_G[H][G]_0}{[G]_0 + K_G[G]_0[H]} I_{gh}$$

Which can be simplified via:

$$
\begin{aligned}
FI &= \frac{[G]_0 - [HG]}{[G]_0} I_g + \frac{\frac{K_G[H][G]_0}{1+K_G[H]}}{[G]_0} I_{gh} = \frac{[G]_0 - [HG]}{[G]_0} I_g + \frac{K_G[H][G]_0}{[G]_0 + K_G[G]_0[H]} I_{gh} \\
&= \frac{[G]_0 - \frac{K_G[H][G]_0}{1+K_G[H]}}{[G]_0} I_g + \frac{K_G[H][G]_0}{[G]_0 + K_G[G]_0[H]} I_{gh} \\
&= \left(1 - \frac{K_G[H]}{1+K_G[H]}\right) I_g + \frac{K_G[H]}{1+K_G[H]} I_{gh} = I_g - \frac{K_G[H]}{1+K_G[H]} I_g + \frac{K_G[H]}{1+K_G[H]} I_{gh}
\end{aligned}
$$

To arrive at:

$$FI = I_g + (I_{gh} - I_g)\frac{K_G[H]}{1+K_G[H]}$$

The respective Origin file is competitive.fdf, in which the following parameters are used:

Go total concentration of guest (fluorescent dye)
Ho total concentration of host
Kg association constant of the guest (fluorescent dye) with the host
Kc association constant of the competitor
Ig fluorescence intensity of an uncomplexed guest (fluorescent dye)
Igh fluorescence intensity of the host-guest complex

```
// Add code here for other Origin C functions that you want to define in this file,
// and access in your fitting function.

static double rac(double Kg, double Kc, double Co, double Go, double Ho)
{
	double dx,r,a,b,c,d;

	r=1;
	dx=0.01;
	a=Kc*Kg;
	b=Kc+Kg+Kc*Kg*Go+Kc*Kg*Co-Kc*Kg*Ho;
	c=Kc*Co-Kc*Ho+Kg*Go-Kg*Ho+1;
	d=-Ho;
	while (fabs(dx)>1e-10)
	{
		//Newton-Raphson method f(x)/f'(x)
		dx=(a*r^3+b*r^2+c*r+d)/(3*a*r^2+2*b*r+c);
		r=r-dx;
	}
	return r;
}

void _nlsfcompetitiveIo(
// Fit Parameter(s):
double Go, double Ho, double Kg, double Kc, double Ig, double Igh
// Independent Variable(s):
double x,
// Dependent Variable(s):
double& y)
{
	// Beginning of editable part
	y= Ig+(Igh-Ig)*Kg*rac(Kg,Kc,x,Go,Ho)/(1+Kg*rac(Kg,Kc,x,Go,Ho));
	// End of editable part
}
```

Commonly, Kg, Go, and Ho are known (Kg from a preliminary 1:1 host-guest binding titration), such that these parameters can be fixed during the fitting procedure.

I_{gh} is however not the initial fluorescence intensity I_0 before adding the competitor, because the displacement titration could also be carried out with e.g. initial 70 % complexation. Therefore, I_0 is implemented by the equation for the 1:1 host-guest binding.

$$I_0 = I_{gh} + \left(I_g - I_{gh}\right)\frac{\left([G]_0 - [H]_0 - 1/K_a\right)/2 \pm \sqrt{\left([H]_0 + [G]_0 + 1/K_a\right)^2/4 - [H]_0[G]_0}}{[G]_0}$$

Substitution and rearrangement gives the term for I_{gh}

$$I_0 = I_{gh} + \left(I_g - I_{gh}\right)x = I_{gh} + I_g x - I_{gh} x = I_{gh} - I_{gh} x + I_g x \quad \left| -I_g x \right.$$

$$I_0 - I_g x = I_{gh} - I_{gh} x = I_{gh}(1 - x)$$

$$I_{gh} = \frac{I_0 - I_g x}{1 - x} = \frac{I_0 - I_g \dfrac{\left([G]_0 - [H]_0 - 1/K_a\right)/2 \pm \sqrt{\left([H]_0 + [G]_0 + 1/K_a\right)^2/4 - [H]_0[G]_0}}{[G]_0}}{1 - \dfrac{\left([G]_0 - [H]_0 - 1/K_a\right)/2 \pm \sqrt{\left([H]_0 + [G]_0 + 1/K_a\right)^2/4 - [H]_0[G]_0}}{[G]_0}}$$

The respective Origin file is competitiveIo.fdf, in which the following parameters are used:

Ig fluorescence intensity of an uncomplexed guest (fluorescent dye)
Io fluorescence intensity in the absence of competitor under the specified concentrations
Kg association constant of the guest (fluorescent dye) with the host
Kc association constant of the competitor
Go total concentration of guest (fluorescent dye)
Ho total concentration of host

```
// Add code here for other Origin C functions that you want to define in this file,
// and access in your fitting function.

static double rac(double Kg, double Kc, double Co, double Go, double Ho)
{
	double dx,r,a,b,c,d;

	r=1;
	dx=0.01;
	a=Kc*Kg;
	b=Kc+Kg+Kc*Kg*Go+Kc*Kg*Co-Kc*Kg*Ho;
	c=Kc*Co-Kc*Ho+Kg*Go-Kg*Ho+1;
	d=-Ho;
	while (fabs(dx)>1e-10)
	{
			//Newton-Raphson method f(x)/f'(x)
			dx=(a*r^3+b*r^2+c*r+d)/(3*a*r^2+2*b*r+c);
			r=r-dx;
	}
	return r;
}

static double Igh(double Io, double Ig, double Kg, double Go, double Ho)
{
	double I;

	I=(Io-Ig*((Go-Ho-1/Kg)/2+sqrt(((Ho+Go+1/Kg)^2)/4-Ho*Go))/Go)
	/(1-((Go-Ho-1/Kg)/2+sqrt(((Ho+Go+1/Kg)^2)/4-Ho*Go))/Go);
	return I;
}

void _nlsfcompetitiveIo(
// Fit Parameter(s):
double Ig, double Io, double Kg, double Kc, double Go, double Ho,
// Independent Variable(s):
double x,
// Dependent Variable(s):
double& y)
{
	// Beginning of editable part
```

```
        y=Ig+(Igh(Io,Ig,Kg,Go,Ho)-
        Ig)*Kg*rac(Kg,Kc,x,Go,Ho)/(1+Kg*rac(Kg,Kc,x,Go,Ho));
        // End of editable part
}
```

Commonly, Io, Kg, Go, and Ho are known (Kg from a preliminary 1:1 host-guest binding titration), such that these parameters can be fixed during the fitting procedure.

Both fitting procedures can be used complementarily in the following manner. First, the latter fitting program (competitiveIo.fdf) is used to obtain the unknown parameters (Ig and Kc), because it can be more intuitively used owing to the implementation of the initial fluorescence intensity (Io), which is experimentally given.

As an independent proof, the obtained parameters are used as starting values for the former fitting program (competitive.fdf), in which now all parameters except the fluorescence intensity of the host-guest complex (Igh) are fixed. The fitting should progress quickly and should perfectly match the fitting with the latter program (competitiveIo.fdf), in particular when afterwards also the unknown parameters (Ig and Kc) are allowed to vary.

In both fitting procedures, care should be taken that the extrapolated fluorescence intensities (Igh and Ig) are positive. If this is not the case the fitting should be repeated by applying a lower boundary condition in the Options → Constraints section of the Origin Advanced Fitting Tool. Particularly alarming is, when the extrapolated Igh (with the latter fitting procedure) becomes negative in a fluorescence regeneration experiment, although the fitted curves with both procedures perfectly match the experimental data. If the latter applies, it should be judged on a rational basis, which parameters should be allowed to vary, and the whole fitting should be repeated with more flexibility in the parameters, but with the boundary conditions, i.e. Igh > 0 and Ig > 0.

Titrations for 2:1 Host-Guest Binding

The underlying binding model is as follows:

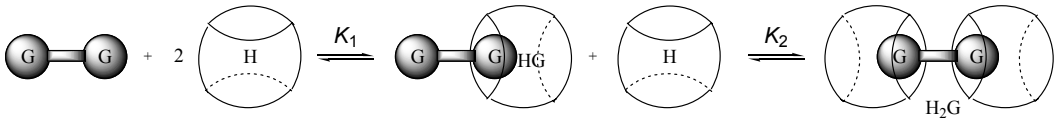

The 2:1 formation of host-guest complexes can be described by the sequential binding model, in which the stepwise formation of the 2:1 complex is accounted for by the law of mass action of two different equilibria.

$$K_1 = \frac{[HG][H]}{[H]^2[G]} = \frac{[HG]}{[H][G]} \tag{1}$$

$$K_2 = \frac{[H_2G]}{[HG][H]} \tag{2}$$

The law of mass conservation requires that

$$[G] = [G]_0 - [HG] - [H_2G] \tag{3}$$

$$[H] = [H]_0 - [HG] - 2[H_2G] \tag{4}$$

Substituting $[HG]$ by eq. 1 and $[H_2G]$ by eq. 2 into eq. 3 followed by simplifications, yields

$$[G] = [G]_0 - K_1[H][G] - K_2[HG][H] = [G]_0 - K_1[H][G] - K_1K_2[H]^2[G]$$

which can be simplified via

$$1 = {[G]_0}/{[G]} - K_1[H] - K_1K_2[H]^2 \qquad \left| \; + K_1[H] + K_1K_2[H]^2 \right.$$

$${[G]_0}/{[G]} = 1 + K_1[H] + K_1K_2[H]^2 \qquad \left| \; \times [G] \; \right| : \; 1 + K_1[H] + K_1K_2[H]^2$$

to afford the concentration of free guest dependent on the concentration of free host (eq. 5)

$$[G] = \frac{[G]_0}{1 + K_1[H] + K_1K_2[H]^2} \tag{5}$$

Rearrangement of eq. 3 and substitution of $[G]$ by eq. 5 and $[H_2G]$ by eq. 2, 1 and 5 affords

$$[HG] = [G]_0 - \frac{[G]_0}{1 + K_1[H] + K_1K_2[H]^2} - \frac{K_1K_2[G]_0[H]^2}{1 + K_1[H] + K_1K_2[H]^2}$$

which is simplified by

$$[HG] = \frac{\left(1 + K_1[H] + K_1K_2[H]^2\right)[G]_0 - [G]_0 - K_1K_2[G]_0[H]^2}{1 + K_1[H] + K_1K_2[H]^2}$$

$$[HG] = \frac{\left(1 + K_1[H] + K_1K_2[H]^2 - 1 - K_1K_2[H]^2\right)[G]_0}{1 + K_1[H] + K_1K_2[H]^2}$$

until one obtains eq. 6:

$$[HG] = \frac{K_1[H][G]_0}{1 + K_1[H] + K_1K_2[H]^2} \tag{6}$$

Now we can substitute equations 5 and 6 into eq. 3 to get the concentration of the host-guest 2:1 complex dependent on the concentration of free host (eq. 7)

$$\begin{aligned}
[H_2G] &= [G]_0 - [HG] - [G] \\
&= [G]_0 - \frac{K_1[H][G]_0}{1 + K_1[H] + K_1K_2[H]^2} - \frac{[G]_0}{1 + K_1[H] + K_1K_2[H]^2} \\
&= \frac{\left(1 + K_1[H] + K_1K_2[H]^2\right)[G]_0 - K_1[H][G]_0 - [G]_0}{1 + K_1[H] + K_1K_2[H]^2} \\
&= \frac{\left(1 + K_1[H] + K_1K_2[H]^2 - K_1[H] - 1\right)[G]_0}{1 + K_1[H] + K_1K_2[H]^2} \\
&= \frac{K_1K_2[H]^2[G]_0}{1 + K_1[H] + K_1K_2[H]^2} \qquad \textbf{(7)}
\end{aligned}$$

Now, with the concentrations of host-guest 1:1 complex (eq. 6), and host-guest 2:1 complex (eq. 7) at hand, one can substitute these formerly unknowns into eq. 4 to arrive at an equation, which contains the concentration of the free host as the only unknown (eq. 8)

$$0 = [H]_0 - [HG] - 2[H_2G] - [H]$$

With (6) and (7) one obtains:

$$0 = [H]_0 - \frac{K_1[H][G]_0}{1 + K_1[H] + K_1K_2[H]^2} - \frac{2K_1K_2[H]^2[G]_0}{1 + K_1[H] + K_1K_2[H]^2} - [H]$$

Multiplication of both sides with $\left(1 + K_1[H] + K_1K_2[H]^2\right)$ yields:

$$\begin{aligned}
0 = \quad & [H]_0 + K_1[H][H]_0 + K_1K_2[H]^2[H]_0 - K_1[H][G]_0 \\
& -2K_1K_2[H]^2[G]_0 - [H] - K_1[H]^2 - K_1K_2[H]^3
\end{aligned}$$

Multiplication of both sides with − 1 and rearrangement yields:

$$\begin{aligned} 0 = \quad & K_1K_2[H]^3 + K_1[H]^2 + 2K_1K_2[G]_0[H]^2 - K_1K_2[H]_0[H]^2 \\ & +[H] + K_1[H][G]_0 - K_1[H][H]_0 - [H]_0 \\ 0 = \quad & K_1K_2[H]^3 + (K_1 + 2K_1K_2[G]_0 - K_1K_2[H]_0)[H]^2 \\ & +(1 + K_1[G]_0 - K_1[H]_0)[H] - [H]_0 \end{aligned} \tag{8}$$

Substitution with

$$a = K_1K_2$$

$$b = K_1 + 2K_1K_2[G]_0 - K_1K_2[H]_0$$

$$c = 1 + K_1[G]_0 - K_1[H]_0$$

and $d = -[H]_0$

yields the expected cubic equation, which can be numerically solved by the Newton-Raphson method

$$0 = a[H]^3 + b[H]^2 + c[H] - d$$

The conversion into fluorescence intensity is achieved in the usual way via the molar fractions

$$FI = x_g I_g + x_{gh} I_{gh} + x_{ghh} I_{ghh} = \frac{[G]}{[G]_0} I_g + \frac{[HG]}{[G]_0} I_{gh} + \frac{[H_2G]}{[G]_0} I_{ghh}$$

in which the unknowns can be substituted with the equations 5, 6, and 7, which yields

$$\begin{aligned} FI = \quad & \frac{1}{1 + K_1[H] + K_1K_2[H]^2} I_g \\ & + \frac{K_1[H]}{1 + K_1[H] + K_1K_2[H]^2} I_{gh} \\ & + \frac{K_1K_2[H]^2}{1 + K_1[H] + K_1K_2[H]^2} I_{ghh} \end{aligned}$$

The respective Origin file is host2guest1.fdf, in which the following parameters are used:

Go total concentration of guest (fluorescent dye)
K1 association constant of the guest (fluorescent dye) with the host
K2 association constant of the host-guest complex with a second host
Ig fluorescence intensity of an uncomplexed guest (fluorescent dye)
Igh fluorescence intensity of the host-guest 1:1 complex
Ighh fluorescence intensity of the host-guest 2:1 complex

```
// Add code here for other Origin C functions that you want to define in this file,
// and access in your fitting function.

static double rac(double K1, double K2, double Ho, double Go)
{
        double dx,r,a,b,c,d;

        r=1;
        dx=0.01;
        a=K1*K2;
        b=K1+2*K1*K2*Go-K1*K2*Ho;
        c=1+K1*Go-K1*Ho;
        d=-Ho;
        while (fabs(dx)>1e-10)
        {
                dx=(a*r^3+b*r^2+c*r+d)/(3*a*r^2+2*b*r+c);
                r=r-dx;
        }
        return r;
}

void _nlsfhost2guest1 (
// Fit Parameter(s):
double Go, double K1, double K2, double Ig, double Igh, double Ighh,
// Independent Variable(s):
double x,
// Dependent Variable(s):
double& y)
{
        // Beginning of editable part
        y = Ig/(1+K1*rac(K1,K2,x,Go)+K1*K2*(rac(K1,K2,x,Go))^2)
        +
        (Igh*K1*rac(K1,K2,x,Go))/(1+K1*rac(K1,K2,x,Go)+K1*K2*(rac(K1,K2,x,G
        o))^2)
        +
        (Ighh*K1*K2*(rac(K1,K2,x,Go))^2)/(1+K1*rac(K1,K2,x,Go)+K1*K2*(rac(K
        1,K2,x,Go))^2);
        // End of editable part
}
```

Commonly, Go, and Ig are known, such that these parameters can be fixed during the fitting procedure.

Enzyme Kinetics

Suitable for [S] << K_M

The equation for the enzymatic reaction is described in ref. 170. For convenience, the initial constant fluorescence intensity before addition of the enzyme (*cf*. Figure 2.2) has been implemented into the fitting program. The respective Origin file is enzyme_c.fdf, in which the following parameters are used:

Io	initial (constant) fluorescence intensity before addition of enzyme
Imax	final fluorescence intensity
Enz	enzyme concentration
to	time of enzyme addition

```
void _nlsfenzyme_c(
// Fit Parameter(s):
double I0, double Imax, double Enz, double k, double t0,
// Independent Variable(s):
double t,
// Dependent Variable(s):
double& y)
{
        // Beginning of editable part
        if (t<=t0)
                y = I0;
        if (t>=t0)
                y = I0+(Imax+I0)*(1-exp(-Enz*k*(t-t0)));
        // End of editable part
}
```

Knowledge of the enzyme concentration and fixing of that parameter is essential.

Appendix 2: Curriculum Vitae

Gender:	male
Nationality:	German
Date of birth:	01.05.1978

Education

08/1990 - 06/1997	Gymnasium Groß Ilsede, Germany
10/1997 - 10/1998	Civilian service in the „Alten- und Pflegeheim des Landkreises Peine“
10/1998 - 02/2004	TU Braunschweig, Germany
	Completed with diploma degree in chemistry: „very good“
	Thesis in the research group of Prof. S. Schulz:
	„Analyse und Synthese von quorum-sensing aktiven *N*-Acylhomoserinlactonen“
03/2004 - to date	Jacobs University Bremen, Germany
	PhD studies in the research group of Prof. W. M. Nau

Fellowships and Awards

1993	Dr.-Mya-Tha Memorial Award
2001	Faculty Prize of the „Freunde des Instituts für Organische Chemie“
05/2001 - 02/2004	Fellow of the „Studienstiftung des deutschen Volkes“
03/2004 - 03/2007	PhD-stipend of Hoffmann-La Roche for the Nano-TRF project

Practical Experience

04/2002 - 08/2002	Research visit at Universität Basel, Switzerland
02/2004 - to date	Responsible for NMR maintenance, service and repair
09/2004 - 12/2004	NMR service for lab course „Advanced Organic Chemistry“
01/2005 - 02/2005	Research visit at Hoffmann-La Roche, Switzerland

Teaching Experience

2000 - 2003	Lab assistant for undergraduate course in Organic Chemistry
2003	Lab assistant for undergraduate course in Inorganic Chemistry for Biologists
02/2004 - 12/2006	Teaching assistant for undergraduate course in Organic Chemistry
03/2004- to date	Supervised in total three undergraduate and two graduate students

09/2006 - 12/2006 Tutorial „From Spectra to Structure“ covering 1D- and 2D-NMR, IR, MS for advanced Bachelor and Master students (16 lectures, 75 min each)

Publications

1. A. Hennig, Analyse und Synthese von quorum-sensing aktiven *N*-Acylhomoserinlactonen, Diplomarbeit, **2004**, TU Carolo-Wilhelmina zu Braunschweig, Deutschland.
2. Wagner-Döbler, V. Thiel, L. Eberl, M. Allgaier, A. Bodor, S. Meyer, S. Ebner, A. Hennig, R. Pukall, S. Schulz, Discovery of Complex Mixtures of Novel Long-Chain Quorum Sensing Signals in Free-Living and Host-Associated Marine Alphaproteobacteria, *ChemBioChem*, **2005**, *6*, 2195-2206.
3. A. Hennig, D. Roth, T. Enderle, W. M. Nau, Nanosecond Time-Resolved Fluorescence Protease Assays, *ChemBioChem*, **2006**, *7*, 733-737.
4. H. Sahoo, A. Hennig, W. M. Nau, Temperature-Dependent Loop Formation Kinetics in Flexible Peptides Studied by Time-Resolved Fluorescence Spectroscopy, *Int. J. Photoenergy*, **2006**, Article ID 89638, 9 pages.
5. A. Hennig, M. Florea, D. Roth, T. Enderle, W. M. Nau, Design of Peptide Substrates for Nanosecond Time-Resolved Fluorescence Assays of Proteases: 2,3-Diazabicyclo[2.2.2]oct-2-ene as a Noninvasive Fluorophore, *Anal. Biochem.*, **2007**, *360*, 255-265.
6. A. Hennig, G. Ghale, W. M. Nau, Effects of Cucurbit[7]uril on Enyzme Activity, *Chem. Comm.*, **2007**, 1614-1616.
7. A. Hennig, T. Schwarzlose, W. M. Nau, Bridgehead Carboxy-Substituted 2,3-Diazabicyclo[2.2.2]oct-2-enes: Synthesis, Fluorescent Properties and Host-Guest Complexation Behavior, *Arkivoc*, **2007**, *8*, 341-357.
8. A. Hennig, H. Bakirci, W. M. Nau, Label-free Continuous Enzyme Assays with Macrocycle-Fluorescent Dye Complexes, *Nature Methods*, **2007**, *4*, 629-632.
9. H. Sahoo, D. Roccatano, A. Hennig, W. M. Nau, A 10-Å Spectroscopic Ruler Applied to Short Polyprolines, *J. Am. Chem. Soc.*, **2007**, *129*, 9762-9772.
10. W. M. Nau, A. Hennig, A. L. Koner, Squeezing Fluorescent Dyes into Nanoscale Containers - The Supramolecular Approach to Radiative Decay Engineering, *Springer Series On Fluorescence*, Vol. 4, **2007**, 185-211.
11. H. Sahoo, A. Hennig, M. Florea, D. Roth, T. Enderle, W. M. Nau, Single-Label Kinase and Phosphatase Assays for Tyrosine Phosphorylation Using Nanosecond Time-Resolved Fluorescence Detection, *J. Am. Chem. Soc.*, **2007**, *51*, 15927-15934.

Manuscripts in Preparation

1. A. Hennig, D. Roth, T. Enderle, W. M. Nau, Interaction of Cucurbit[7]uril with Protease Substrates: Application to Nanosecond Time-Resolved Fluorescence Assays, *in preparation*.
2. A. Hennig, H. Bakirci, W. M. Nau, A Supramolecular Sensor System for Nanosecond Time-Resolved Fluorescent Detection, *in preparation*.
3. A. Hennig, R. D'Souza, W. M. Nau, Supramolecular Tandem Assays, *in preparation*.
4. A. Hennig, W. M. Nau, Determination of Arginase Inhibition by a Substrate-Coupled Supramolecular Tandem Assay, *in preparation*.

Patents

1. W. M. Nau, A. Hennig, H. Bakirci, Bestimmung von Konzentrationsänderungen mit Hilfe von supra-biomolekularen Tandem-Assays, PCT Patent Application.

Attended Conferences

1. NRP Meeting: “Intellectual Property and Technology Transfer from the Viewpoint of Science and Research“, 12.06.2002, Bern (CH)
2. 37th Discussion Meeting of the DGMS (German Society for Mass Spectrometry), 07.03.-10.03.2004, Leipzig (D), Poster: “Mass Spectrometric Investigation of derivatized *N*-acyl-homoserinelactones“
3. 2nd European Short Course on Principles & Applications of Time-Resolved Fluorescence Spectroscopy, 01.11.-05.11.2004, Berlin (D)
4. Meeting of the photochemistry branch of the GDCh, 29.03.-31.05.2005, Jena (D), Poster: “Fast Time-Resolved Fluorescent (Fast-TRF) Protease Assays“
5. NRP Spring School: Supramolecular Functional Materials, 11.04.-15.04.2005, Murten (CH), Poster: “Supramolecular Radiative Decay Engineering (SRDE) with Cucurbituril“
6. NRP Final Symposium: Supramolecular Functional Materials, 16.06.-18.06.2005, Murten (CH), Short presentation: “Enhancement on time-resolved energy transfer assays by supramolecular complex formation“
7. Central European Conference on Photochemistry (CECP), 05.03.-09.03.2006, Bad Hofgastein (A), Poster: “Fluorescence Lifetime-Based Sensor Applications: Nano-TRF Assays & Lifetime Enhancers“, Poster: “Nanosecond Time-Resolved Fluorescence (Nano-TRF) Assays – Application to Proteases“
8. Joint International Symposium on Macrocyclic & Supramolecular Supramolecular Chemistry, 25.06.-30.06.2006, Victoria, BC (CDN), Poster: “Interactions of Cucurbituril with Peptide Substrates in Enzyme Assays: Potential Applications“
9. ChemieContact – Innovation sucht Partner des VCI (Verband der Chemischen Industrie e.V.), 10.10.2006, Hamburg (D), Poster: “Enzym- und Katalysatorscreening mit Hilfe von suprabiomolekularen Tandem-Assays“
10. Bremen Molecular and Marine Biology (BMMB) meeting, 26.01.-27.01.2007, Etelsen (D), Poster: “Supra-Biomolecular Tandem Assays“
11. II. International Symposium on Macrocyclic & Supramolecular Supramolecular Chemistry, 24.06.-28.06.2007, Salice Terme (IT), Poster: “Supramolecular Tandem Assays – Application Examples”.

Other Skills

Languages	*German:* mother tongue *English:* fluent
Computer	*Operating Systems:* MS Windows, Mac OS, Linux
	Software (general): MS Office (Word, Powerpoint, Excel), Adobe Acrobat/Photoshop/Illustrator, Net Objects Fusion, Ulead GIF Animator
	Software (scientific): Proficiency in: Microcal Origin, EndNote, SciFinder, MDL Crossfire Commander, JEOL Delta NMR software, CS Chem Office. *Basic knowledge in:* ProFit, Swiss PDB Viewer, Maple, SpinWorks, Hyperchem
	Programming Languages: Basic Knowledge in: Origin C, LabTalk, Turbo Pascal, C#
Scientific Techniques	*Proficiency in:* UV- and fluorescence spectroscopy, time-resolved fluorescence spectroscopy, 1H and 13C NMR spectroscopy. *Basic knowledge in:* Organic synthesis, CD spectroscopy, mass spectrometry (EI, ESI, CI) & chromatographic techniques (HPLC, GC), transient absorption spectroscopy

Appendix 3: Enzyme Assay Protocols

Protocol: Steady-State Carboxypeptidase A Assay with Dbo-labeled Peptides

Materials

Reagents

LiCl (Fluka)

Tris-HCl (Fluka)

NaCl (Fluka)

Carboxypeptidase A (suspension in 10 % toluene, Fluka)

H-Dbo-Gly-Trp-OH

Equipment

Varian Eclipse spectrofluorometer (λ_{exc} = 365 nm, λ_{em} = 450 nm) with temperature controller (25 °C). 500-µl cuvette.

Time Taken

40 min for steps 4-6.

Procedure

1. Prepare the following solutions: 10 % LiCl in H_2O and 1 M NaCl, 0.05 M Tris, pH 7.5 (reaction buffer).
2. Prepare the following stock solutions: ca. 1 mM H-Dbo-Trp-OH in H_2O (which facilitates further use in assays, which require other buffers), and ca. 6 µM carboxypeptidase A (CPA) in 10 % LiCl.
3. Determine the accurate concentrations by absorption spectroscopy using ε_{278} = 64200 $M^{-1}cm^{-1}$ for carboxypeptidase A and ε_{278} = 5500 $M^{-1}cm^{-1}$ for the peptide. Dilute the CPA stock solution with 10 % LiCl to 3 µM and the peptide stock solution to 200 µM with reaction buffer.
4. Add 250 µl peptide stock (200 µM) and 200 µl reaction buffer to the cuvette and place the cuvette into the fluorometer and wait until the temperature has equilibrated.

5. Start recording in the kinetic mode (λ_{exc} = 365 nm, λ_{em} = 450 nm). For convenience in the data analysis at least five minutes of constant fluorescence intensity should be recorded.
6. Add 50 µl of CPA stock (3 µM) to the solution to initiate the reaction and record fluorescence until no change in fluorescence intensity is registered.
7. Total assay volume is 500 µl. Final concentrations are: 300 nM CPA, 100 µM H-Dbo-Gly-Trp-OH. Steps 4-6 can be repeated with varying enzyme or substrate concentrations.

Troubleshooting

If the fluorescence intensity in the cuvette increases already in the absence of CPA, a more thorough cleaning of the cuvette by washing with a detergent (e.g. SODOSIL® RM 02) is required. This efficiently removes proteins from the quartz glass surfaces.

If the increase in fluorescence intensity is much smaller than 30fold, the peptide should be checked for decomposition, e.g. by time-resolved fluorescence measurements or by HPLC.

Critical Steps

None.

Anticipated Results

The fluorescence should be constant before addition of the enzyme and should afterwards increase in a time-dependent manner (in ca. 10-20 minutes by a factor of ca. 30).

References

Hennig, A.; Roth, D.; Enderle, T.; Nau, W. M., *ChemBioChem* **2006,** *7*, 733-737.

Protocol: Nano-TRF Carboxypeptidase A Assay with Dbo-labeled Peptides

Materials

Reagents

LiCl (Fluka)

Tris-HCl (Fluka)

NaCl (Fluka)

Carboxypeptidase A (suspension in 10 % toluene, Fluka)

H-Dbo-Gly-Trp-OH

Equipment

IOM Nano-TRF reader (λ_{exc} = 365 nm, λ_{em} = 450/40 nm in the microsecond channel, i.e. Channel 1).

Black 384-well microplates (Corning NBS).

Electronic Eppendorf pipette with Dispensing Mode.

Time Taken

60 min for steps 4-8.

Procedure

8. Prepare the following solutions: 10 % LiCl in H_2O and 1 M NaCl, 0.05 M Tris, pH 7.5 (reaction buffer).
9. Prepare the following stock solutions: ca. 1 mM H-Dbo-Trp-OH in H_2O (which facilitates further use in assays, which require other buffers), and ca. 6 µM carboxypeptidase A (CPA) in 10 % LiCl.
10. Determine the accurate concentrations by absorption spectroscopy using ε_{278} = 64200 $M^{-1}cm^{-1}$ for carboxypeptidase A and ε_{278} = 5500 $M^{-1}cm^{-1}$ for the peptide. Dilute the CPA stock solution with 10 % LiCl to 300 nM and the peptide stock solution to 60 µM with reaction buffer.
11. Add 0, 5, 10, 15, 20, and 25 µl peptide stock (60 µM) in triplicates into the wells of the microplate and fill up with reaction buffer to a volume of 45 µl.

12. For reference purposes, the fluorescence intensity is recorded once before addition of the enzyme.
    a. Therefore the "WinLac" program is started, and the "MikroWin" program is started.
    b. In the WinLac, allow the laser to warm up, and turn the laser on and set it to ext. trigger mode.
    c. In the MikroWin, choose File→Open and specify the *.par file. Open the "1ch_singlegate-384_DBO_Assay" parameter file.
    d. Choose Options→Read and press "Options" in the dialog box.
    e. Specify the wells to be recorded, set the Gateposition to 0.150 and the sensitivity to "Medium".
    f. Close both dialog boxes by pressing "OK".
    g. Press the green "Start button", do NOT save changes and insert the plate after the plate carrier has opened. Press "OK" to start the measurement.
    h. Your data is in the Result→ChG1 window and can be copied into Excel.
13. Now, prepare everything for the kinetic measurement.
    a. Enter the plate setup and specify the wells, which will be recorded in the kinetic mode (peptide and blank). Set the number of measurements to 100 and the interval time to 1min. Set the shake time to 5 s and the shake mode to "High". Make sure that the sensitivity is set to "Medium" and the gate position is at 0.150. Confirm with "OK" Close the "Options Read" dialog with "OK".
    b. Press the green "Start" button. Do NOT save changes, but do not press ok, when the "Insert plate" dialog appears!
14. Now be prepared to perform the following steps quickly. Carry out these steps in front of the plate reader to save time.

15. Add 5 µl of CPA stock (300 nM) to the every well to initiate the reaction. Use for this purpose the "Dispensing Mode" of an electronic Eppendorf pipette to save time. After adding enzyme to the last well immediately place the microplate into the plate reader and confirm the "Insert plate" dialog.
16. After the measurement has finished, your data is in the Graphics→Kinetics window and can be copied into Excel. Therefore, the traces are highlighted by clicking onto them, Strg-C is pressed and the data is pasted into an Excel sheet.
17. Total assay volume is 50 µl. Final concentrations are: 30 nM CPA, 6,12,18,24,30 µM H-Dbo-Gly-Trp-OH. Steps 4-6 can be repeated with varying enzyme or substrate concentrations.

Troubleshooting

Troubleshooting should be performed with the steady-state assay. No complications were found in case of working steady-state assays.

Critical Steps

None.

Anticipated Results

The fluorescence should increase in a time-dependent manner (in ca. 120 minutes to a value of ca. 4000 arbitrary units for the highest concentration).

References

Hennig, A.; Roth, D.; Enderle, T.; Nau, W. M., *ChemBioChem* **2006,** *7*, 733-737.

Protocol: Lysine Decarboxylase Assay with Cucurbit[7]uril

Refers to A. Hennig, H. Bakirci, and W. M. Nau, Lysine Decarboxylase Assay with Cucurbit[7]uril, *Nature Protocols*, doi:10.1038/nprot.2007.281.

Materials

Reagents

Cucurbit[7]uril (Sigma-Aldrich)

Dapoxyl (Molecular Probes, Eugene, Oregon)

Lysine decarboxylase (partially purified 1.6 U/mg, Sigma-Aldrich)

10 mM NH_4OAc, adjusted to pH 6.0 with HCl and NaOH

L-lysine

Equipment

Varian Eclipse spectrofluorometer (λ_{exc} = 336 nm, λ_{em} = 380 nm) with temperature controller (25 °C). 1-ml cuvette.

Time Taken

10 min for steps 2-5. The reaction should be finished under the specified conditions in < 20 min.

Procedure

18. Prepare the following stock solutions in 10 mM NH_4OAc, pH 6.0: 500 µM cucurbit[7]uril, 25 µM dapoxyl, 1 mM lysine, 800 µg/ml lysine decarboxylase.
19. Add 100 µl Dapoxyl stock (25 µM) and 780 µl buffer to the cuvette and place the cuvette into the fluorometer. Start recording in the kinetic mode (λ_{exc} = 336 nm, λ_{em} = 380 nm).
20. Add 20 µl of cucurbit[7]uril stock (500 µM) to the solution and wait ca. 2 min until the fluorescence intensity has equilibrated.
21. Add 50 µl of lysine stock (1 mM) to the solution.
22. Add 50 µl of lysine decarboxylase (800 µg/ml) to initiate the reaction and record fluorescence until no change in fluorescence intensity is registered.

23. Total assay volume is 1 ml. Final concentrations are: 2.5 µM Dapoxyl, 10 µM cucurbit[7]uril, 50 µM lysine, 40 µg/ml lysine decarboxylase. Steps 2-5 can be repeated with varying enzyme, substrate, or cucurbit[7]uril concentrations.

Troubleshooting

The sequential addition steps specified under "Procedure" provide an internal control. The following observations were made:

After step (2), one should observe a very low fluorescence. If the fluorescence is too high readjust the settings of the fluorometer.

After step (3), the fluorescence intensity should immediately increase ca. 10-20-fold. If the fluorescence increase is very different, check the pH of the buffer.

After step (4), the fluorescence should not change by more than 10%. If it changes by a larger amount, check the lysine sample for impurities.

After step (5), the fluorescence should decrease first stepwise (immediately) and then more slowly with time. If the latter time-resolved fluorescence decay is not observed after 5 min, the enzyme may be inactive.

If the stepwise (immediate) decrease in fluorescence intensity in step (5) is very pronounced (we relate this to varying degrees of salts and impurities in the enzyme sample), the sequence of steps (4) and (5) can be exchanged to obtain visually improved enzyme kinetic traces. In this case the time-resolved fluorescence decay is only observed after the addition of substrate in step (5), while upon addition of enzyme in step (4) only an immediate stepwise decrease in fluorescence intensity is observed.

Critical Steps

The pH of the buffer needs to be thoroughly adjusted, since the fluorescence intensity before addition of enzyme varies strongly upon slight changes in pH.

Anticipated Results

The fluorescence should decrease in a time-dependent manner (in ca. 10-20 minutes by a factor of ca. 3).

References

A. Hennig, H. Bakirci, W. M. Nau, Label-Free Continuous Enzyme Assays with Macrocycle-Fluorescent Dye Complexes, *Nature Methods*, **2007**, doi:10.1038/nmeth1064.

– APPENDIX 4 –
SELECTED PUBLICATIONS